Effects of periodic temperature changes on crystal shape

McCarthy, C. J.

Award date:
1986

Awarding institution:
University of Bath

EFFECTS OF PERIODIC TEMPERATURE CHANGES ON CRYSTAL SHAPE

Submitted by C.J.McCarthy B.Pharm.,M.P.S.

for the degree of Doctor of Philosophy

of the University of Bath

1986

This research has been carried out in the School of Pharmacy and Pharmacology of the University of Bath under the supervision of Mr.G.S.Riley M.Pharm.,M.Sc.,F.P.S. and Professor J.E.Rees B.Pharm.,Ph.D.,M.P.S.

COPYRIGHT

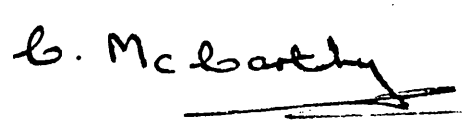

ProQuest LLC
789 East Eisenhower Parkway
P.O. Box 1346
Ann Arbor, MI 48106-1346

ACKNOWLEDGEMENTS

The author wishes to express her thanks for the encouragement and advice received from Mr.G.S.Riley, Professor J.E.Rees and Dr.J.N.Staniforth throughout all stages of this work. Her thanks are due to the School of Pharmacy and Pharmacology and the University for providing the facilities for research and to various members of the school for their participation in many useful discussions. Her sincere thanks are also due to Mrs.J.Hart for writing the computer programs used in conjunction with the Microsight 1 Image Analysis System; to Mr.S.Bryan for writing the computer program used in conjunction with the Magiscan and his assistance in all aspects of its use; to the Central Electricity Generating Board for allowing the author the use of the Magiscan at Berkeley Nuclear Power Station; and Mr.B. Chapman of the School of Physics for his assistance with the X-ray diffraction work. This work was carried out with the aid of a grant from the Science and Engineering Research Council to whom the author also wishes to express her gratitude.

The author's sincere thanks are also due to her mother, Mrs.J.M.Williams, for the typing of the manuscript, and to her father, Mr.R.F.Williams for the figures and proof reading. Finally the author wishes to thank her husband for his help, financial and moral support and encouragement during all stages of this work.

SUMMARY

Periodic temperature cycling of soluble crystalline compounds has been reported to produce crystals with a rounded habit. The objective of this study was to evaluate the potential application of such a technique to relatively insoluble pharmaceutical crystalline solids. A quantitative measure of the overall shape change was needed to establish whether or not the products were significantly different from the starting materials.

A laboratory temperature cycling apparatus was devised. The effect of periodic temperature cycling on the crystal shape of three sulphonamides - sulphadimidine, sulphamethizole and sulphathiazole, was investigated. Aqueous crystal suspensions were cycled for differing numbers of thirty-minute temperature cycles consisting of fifteen minutes successive heating to 40°C and cooling to 30°C. Further studies on sulphamethizole investigated the effect of altering the temperature cycling conditions and the use of an alternative solvent system in which the compound was more soluble - 95% ethanol. Initially quantitative shape assessment on limited data was obtained on the Magiscan. These results were compared with those obtained using the Digithurst Microsight 1 Image Analysis System. The latter image analysis system was used in the present study to determine the ratios of the radii of the inscribed and circumscribed circles, I_i / I_c, and the fractal

dimensions of the crystal images.

Analysis of these experiments indicated that the most marked rounding effect occurred after thirty-minute temperature cycles consisting of fifteen minutes successive heating to 40°C and cooling to 30°C. The results indicated that the deposition period may have more effect on the rounding process than the dissolution period. There is also evidence of a shape reversion occurring under certain cycling conditions, which may be due to the amount of deposition exceeding the amount of dissolution. Various mechanisms of crystal growth and dissolution are reviewed. In the case of sulphamethizole, the observed rounding effect was not significantly improved by altering the temperature cycling conditions. However the use of a more efficient solvent did significantly improve the rounding effect.

It was concluded that although temperature cycling is unlikely to prove commercially viable, it may prove a useful technique in developmental studies for evaluating physico-mechanical effects on powder properties such as flow. Fractal dimension in conjunction with the circle ratio, I_i / I_c, gave valuable information about crystal shape and surface texture. The microcomputer based image analysis system, although simple and inexpensive, proved a very useful research tool.

CONTENTS

ORIGIN AND SCOPE OF THE WORK

The shape of a crystal can assist in its identification and analysis, influence the physico-mechanical properties of the bulk powder and affect its behaviour. Bulk densities, flow and friction conditions within the powder bed, all depend on the size, shape and surface characteristics of the constituent particles. Certain crystal habits are undesirable in commercial crystalline solids because they may result in a poor product appearance or they may make the bulk powder prone to caking or impart poor flow properties. The latter is especially important in the pharmaceutical industry as it may create problems in the handling, processing or packaging of the material.

In nearly every industrial crystallisation process some form of habit modification is used to control the type of crystal produced. The present work originated from a paper by Nyvlt (1973) in which he described a method for producing rounded crystals by periodic temperature cycling. He suggested that this rounding effect was produced by successive dissolution of the corners and edges of the crystal and deposition on the slower growing faces. Nyvlt used very soluble crystalline materials, but if this method could be applied to less soluble

crystalline compounds it might be useful pharmaceutically for improving their handling and processing characteristics.

A laboratory scale temperature cycling apparatus was designed and three sulphonamides were studied - sulphadimidine, sulphamethizole and sulphathiazole. The aqueous solubility profiles of these compounds were determined and the effects of periodic temperature cycling investigated. These effects were assessed in terms of a change in shape factor with reference to the starting material. The ratio of the radii of the inscribed and circumscribed circles was used to study this change together with fractal dimension. A relatively simple image analysis system was set up to assess these changes.

The effect of varying the periodic temperature cycle was investigated for sulphamethizole in order to study the effects of prolonging the period of dissolution or deposition. Sulphamethizole was also temperature cycled in 95% ethanol to compare the effects of periodic temperature cycling in a solvent system in which the same compound is more soluble. The products obtained were all examined by T.L.C., I.R.spectroscopy and X-ray diffraction to ensure that no physical or chemical changes had occurred as a result of the process.

INTRODUCTION

1.1 THE CRYSTALLINE STATE

The term crystal was originally used to describe ice. It is now applied to solids exhibiting flat faces and symmetry closely related to their internal structure. Crystalline solids have a precise geometrical internal structure and are characterised by the regular arrangement of the constituent molecules, atoms or ions in a fixed pattern or lattice.

Crystallisation is an important unit operation in the pharmaceutical industry. It usually produces a pure, stable, solid material. By controlling the crystallisation process, a material with specific desired properties can be obtained. It is therefore important to understand the mechanisms involved in growth and dissolution of crystals as well as the effects of external environmental factors on these processes.

1.2 MECHANISMS OF CRYSTAL GROWTH AND DISSOLUTION

Crystals can be formed from a solution, melt or vapour. The former is probably the most important in a pharmaceutical context and will be considered here. Crystallisation from solution involves three basic stages:- the achievement of supersaturation or supercooling, formation of crystal nuclei and finally, crystal growth. Supersaturation is an essential condition for crystallisation to occur,

but it is not sufficient alone to cause crystallisation. This has given rise to the hypothesis that a metastable zone exists below the saturation temperature, enabling the formation of nuclei. However the presence of impurities may also contribute to the formation of nuclei. This is followed by enlargement of the nuclei and subsequent crystal growth.

1.2.1. Early Theories

1.2.1.1. Surface Energy Theories. The surface energy theories are based on the postulation by Gibbs (1929) that the shape assumed by a growing crystal is that which has a minimum surface free energy. Curie (1885) adapted this theory in an attempt to explain crystal growth using the concept of interfacial tension. Many researchers have since tried to modify these theories but have not been able to apply them successfully to all crystalline substances.

1.2.1.2. Diffusion Theories. Noyes and Whitney (1897) were the first workers to consider growth and dissolution of crystals on the basis of diffusion. They assumed that crystallisation was the reverse of dissolution, and that the rates of both processes were governed by the difference between the concentration at the solid surface and in the bulk solution. They proposed the following relationship:-

$$\frac{dm}{dt} = K_m A (c - c_o) \quad \text{.....(1)}$$

where m = mass deposited in time t

A = surface area of crystal

c = solute concentration in the solution (supersaturated)

c_o = equilibrium saturation concentration

K_m = coefficient of mass transfer

Nernst (1904) later modified this relationship to:-

$$\frac{dm}{dt} = \frac{D}{x} A (c - c_o) \quad \text{.....(2)}$$

where D = coefficient of diffusion of the solute

x = length of the diffusion path

This assumed the existence of a thin laminar film of liquid adjacent to the growing crystal face through which molecules of the solute must diffuse.

However the rates of growth and dissolution of crystal faces are not equal as these relationships would imply. Substances generally dissolve faster than they crystallise, under the same conditions of temperature and pressure. Generally crystals are anisotropic with the exception of those of the cubic system. Although many modifications have been made to these relationships, it is impossible using the diffusion theory, to explain the mechanism by which material is incorporated into the crystalline

surface. While this theory does not explain crystal growth adequately, an explanation has been offered by Berthoud (1912) and Valeton (1923,1924) based on interfacial theories.

1.2.2 Recent Theories Also Concerning Mechanisms of Growth.

Volmer (1929) proposed a mechanism of crystal growth based on the existence of an adsorbed layer of solute atoms or molecules on a crystal face. This has since been extended by other researchers. Kossel (1934) considered the mechanism of growth in detail using a simplified crystal model (Fig. 1.2.2.1.). The vertical wall, AB, limiting the layer of growth units is called a step. Along the length of the step, growth units are missing, the cavities thus formed are called kinks. It can be seen that the top flat face of the crystal is incomplete and that there are many possible positions at which an individual building unit could be incorporated. The position requiring the greatest work of separation from the crystal will be the most stable. The most favoured position will be that of III and growth will proceed by successive addition in such positions until the row is completed. Successive strips will then be laid down until the layer is completed. Continuation of growth will require the formation of a secondary nucleus on this surface to start the formation of a new flat surface. Although the supersaturation necessary to effect this secondary nucleation is theoretically of the order of 25% - 40% (Fox et al, 1963), this condition is rarely

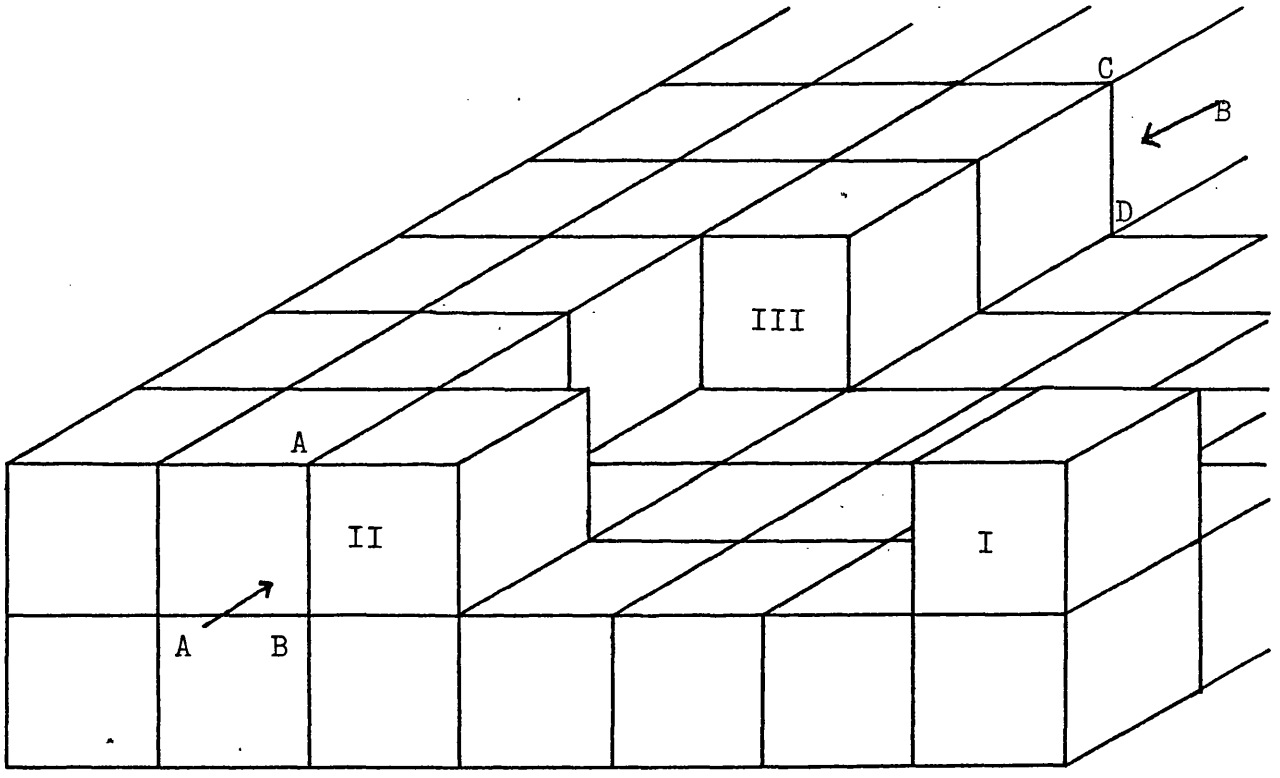

Fig.1.2.2.1. Kossel Crystal Representing the Three Types of Possible Positions of Attachment of Growth Units.

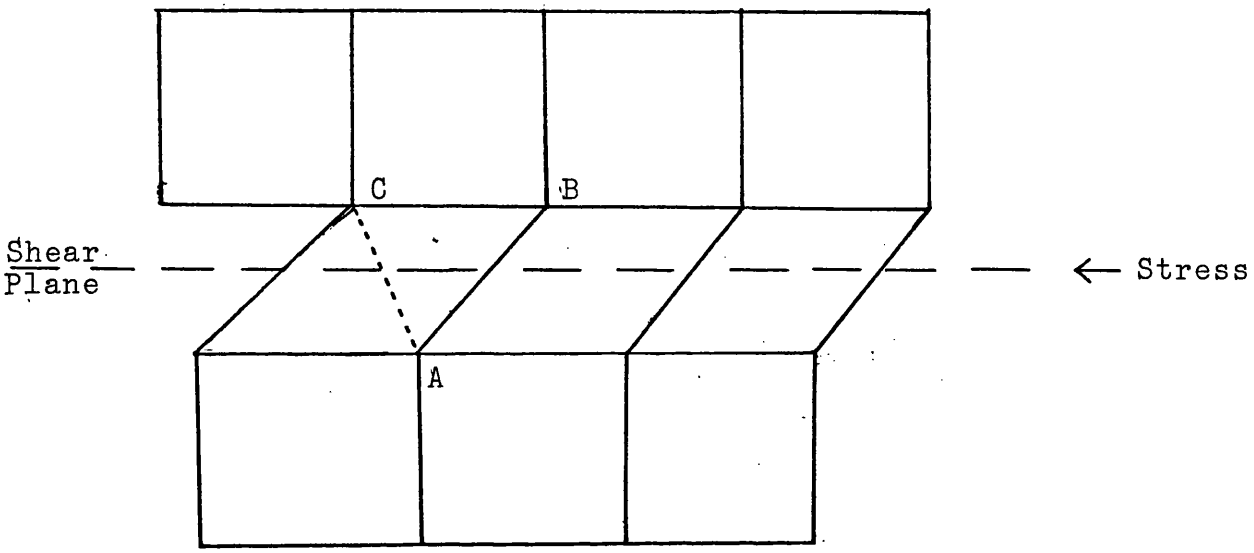

Fig.1.2.2.2 Formation of an Edge Dislocation

achieved; in practice growth occurs with supersaturations of 1% or less.

Frank (1949) explained this anomaly by considering the dislocations present in most crystals. Few crystals grow without some imperfection occurring which will render the surface heterogeneous in an energy sense. The imperfections may be lattice or point defects. However these are confined to the interior of the crystal and they can only affect growth during the addition of one molecular layer. Dislocations may also be created. They may occur during the growth of a crystal under the influence of shear stress either at the surface or internally. The stress may originate from external forces applied to the crystal, or from internal thermal stress, or growth irregularities. Dislocations tend to emerge at the surface of a growing crystal and therefore play an important part in the growth process of a crystal. The two types of dislocation are:-

(i) Edge dislocations. The atoms are displaced along a slipway at right angles to the dislocation line. (Fig. 1.2.2.2.). The application of stress causes A to move away from B and closer to C. Eventually the bond AB will break and a new bond AC will form. This will move along until it appears on the surface of the crystal as a step. This is often referred to as a Taylor-Orowan dislocation.

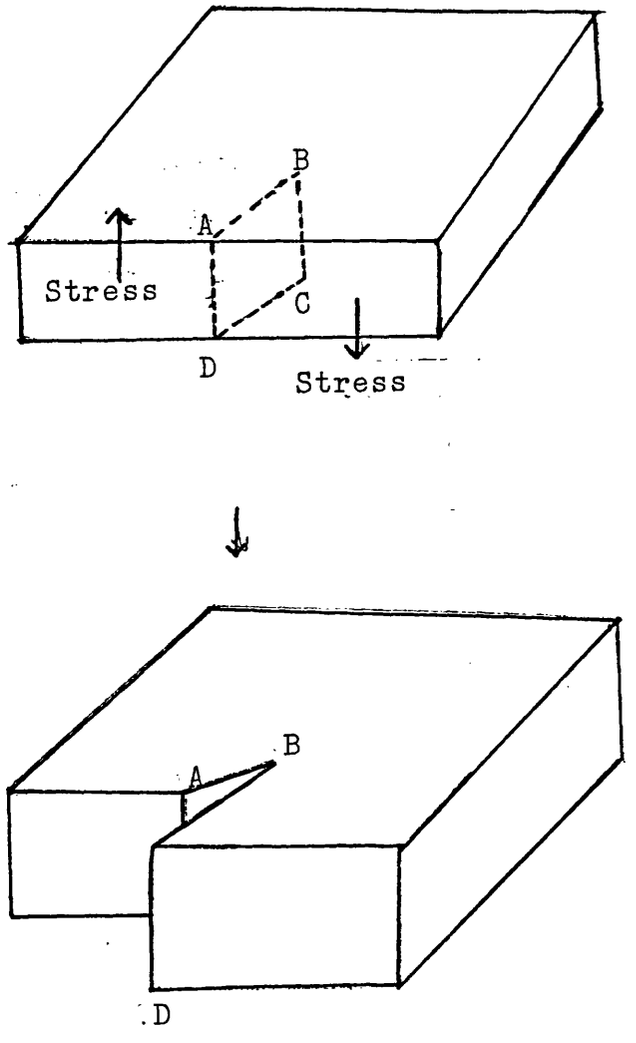

Fig. 1.2.2.3 Formation of a Screw Dislocation

(ii) Screw dislocations (or Burgers dislocations). These occur if the displacement occurs along the dislocation line. The correct number of atoms are present but there is a distortion of configuration. (Fig. 1.2.2.3).

Frank (1949) proposed that these dislocations would form the basis of a growth nucleus, eliminating the need for a secondary nucleus, and hence allowing for the growth of a crystal in a weakly supersaturated solution. Growth can occur on a step on the crystal surface formed as a result of an edge dislocation even if the supersaturation is weak. However as soon as a sufficient number of growth units are attached to the step so that the crystal surface becomes planar, growth ceases until other dislocations are created at the crystal surface.

If a screw dislocation occurs, growth units attach themselves to cavities formed by missing units along the length of the step exposed by the dislocation. The point of emergence of this dislocation is fixed so that after completion of one layer the dislocation will still be present but one layer higher. As the outside edge of the step moves at a constant rate, the step unrolls in a spiral. The form of the spiral remains constant and growth continues by rotation of the entire spiral around the point of emergence of the dislocation. As the step continually renews itself there is no need for two dimensional nucleation and

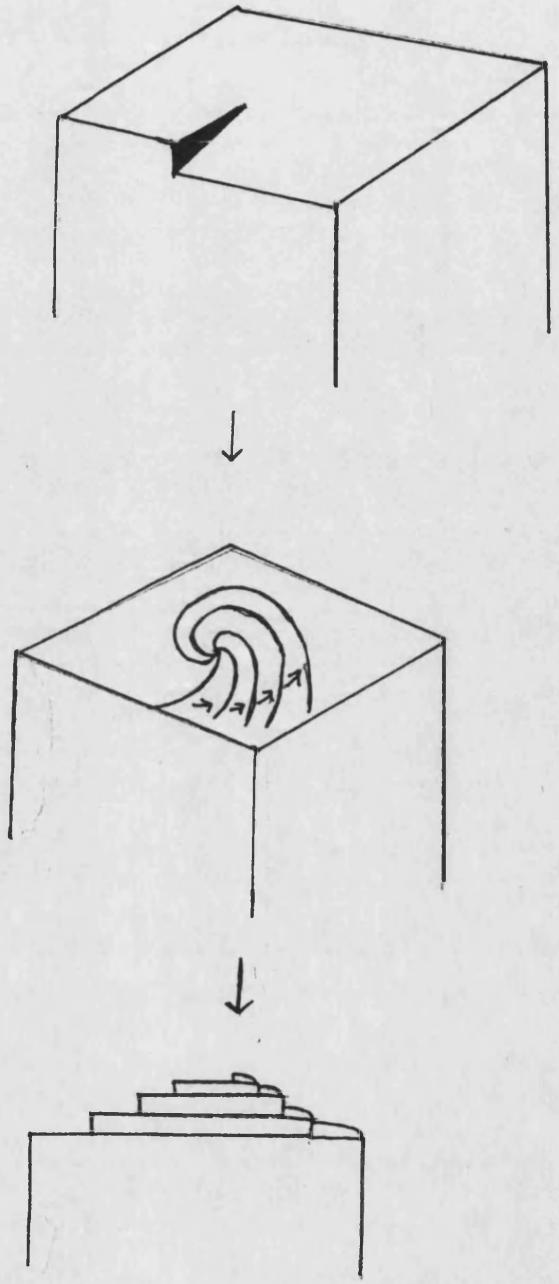

Fig.1.2.2.4 Development of a Growth Spiral Starting From a Screw Dislocation.

the crystal continues to grow at levels of supersaturation below those otherwise required (Fig. 1.2.2.4.).

1.2.3 Mechanisms of Dissolution Based on Dislocations

Growth and dissolution of crystals are produced respectively by addition or removal of monomolecular steps on the crystal surface. When the surface of an ideal crystal is exposed to a solvent, dissolution commences by the formation of cavities or 'unit pits'. If the crystal initially was perfect it would be hard to explain how these cavities occur, however in practice dislocations act as preferential sites for the formation of pits. If a pit formed at a dislocation is repeated it results in the formation of a polymolecular cavity or 'etch pit'. Gilman and co-workers (1957, 1958) have shown that the formation of these etch pits depends on two factors: the rate of formation of the pits, and the rate of displacement of the steps. However this mechanism does not exclude the possibility of a surface reaction occurring in dissolution and it has been shown that some dissolution processes can also involve a slow chemical reaction at the surface of the crystal lattice (Bennett and Lewis, 1958).

1.3 CRYSTAL HABIT

Crystal habit may be defined as the type of external shape which results from the differing rates of growth

of the various crystallographic faces. Depending on the conditions of crystallisation, one or more faces may grow faster than others, or alternatively, the growth of one or more faces may be retarded. Therefore it follows that crystals of the same substance which have been crystallised by different methods may have completely different crystal habits, even though their internal structure is the same. Certain crystal habits are undesirable in commercial materials for a number of reasons. For example, they may give the crystalline mass a poor appearance, they may make the product prone to caking, or they may give rise to poor flow characteristics and create difficulties in the handling or the packaging of the material. Flow characteristics are of especial interest in the pharmaceutical industry because of their influence on tabletting and capsule filling operations. In nearly every industrial crystallisation process some technique of habit modification is used to control the type of crystal produced. A large number of factors can affect crystal habit and various methods are used in practice in order to achieve the most favourable crystal habit for that particular purpose.

1.3.1. Equilibrium Habit

The equilibrium habit of a crystal depends on thermodynamic conditions. Gibbs (1929) postulated that the equilibrium shape of a crystal is that which has the minimum surface free energy for a given volume.

According to this theory, if any crystal is kept in a saturated solution for a sufficiently long period of time, it should eventually attain its equilibrium shape. However in practice this is hard to achieve. Gibbs suggested that this was due to the different degrees of internal atomic or molecular order in crystals and liquids. Also as crystals grow by deposition of new layers of material, this layer formation is governed by certain activation energies which may be independent of the surface area of the crystal face. As the crystals grow larger the deposition of new layers on the different faces will be determined more by their orientation and less by their size and the surrounding faces.

Wulff (1901) showed that the equilibrium shape of a crystal depends on the relative surface free energies of the crystal faces. He suggested that the crystal faces would grow at rates proportional to their surface free energies. Von Laue (1943) modified Wulff's theory. He considered all the possible combinations of faces in order to determine which of the surface free energies was the actual minimum. Wells (1946) demonstrated that there was a definite equilibrium shape for crystals of a given solute crystallised from a particular solvent. When a crystal of a given substance was grown slowly in one solvent and then transferred to a different solvent, the crystal developed the characteristic habit of a crystal grown in the original solvent.

This shows that the equilibrium shape not only depends on interactions of the atoms or molecules in the various crystal faces with the solvent and other molecules in solution, but is also a function of the internal structure of the crystal.

1.3.2 Determination of the Equilibrium Habit

Several qualitative methods of predicting the most stable crystal habit have been proposed. These include those proposed by Bravais (1866), Donnay and Harker (1937), and Hartman and Perdok (1955). However it should be noted that crystal growth nearly always occurs under non-equilibrium conditions, and therefore the concept of an equilibrium habit relates to an ideal situation and is not likely to be realised in practice.

Bravais (1866) recognised that the structural units of a crystal were arranged in one of fourteen different lattices. These are defined by Mullin (1972). Bravais suggested that the development of a crystal face was related to its fundamental lattice and that the most stable faces of a crystal corresponded to those that had a high lattice plane density. This has become known as the Law of Bravais which states that the stability of a face is proportional to the reticular density or the concentration of lattice points on that face and inversely proportional to the reticular area. It is thus directly proportional

to the interplanar spacing, (d), where d is the distance between parallel planes of atoms in the crystal and is defined in the Bragg equation (see page 68).

Donnay and Harker (1937) proposed modifications that took into consideration the space group symmetry, so that not only the type of lattice, but also the presence of screw axes and glide planes were taken into account when correlating face development with internal atomic structure. However these modifications did not consider the influence of atomic bonding or arrangement and also did not distinguish between growth morphology and cleavage. They also could not predict surface structure.

A more recent theory is that of Hartman and Perdok (1955) who considered the bond energies involved in the incorporation of growth units into the lattice. This is based on the assumption that the surface energy of a crystal depends mainly on chemical bond energies. Uninterrupted chains of strong bonds are referred to as periodic bond chains (PBC's). The attachment energy of a growth unit is related to the direction (with respect to the surface) of these PBC's. The greater the attachment energy, the greater the displacement velocity of a crystal face and the lower its morphological importance. Important zones are parallel to PBC vectors and correspond to chains containing only strong bonds. Prominent faces are parallel to at least two high energy coplanar bond

chains and are termed F or flat faces. These grow by the lateral extension of steps. The S or stepped faces are those which contain only one PBC vector. The K or kinked faces do not contain any PBC vectors. The K faces grow faster than S faces, which in turn grow faster than F faces and hence in order of morphological importance:

$$K < S < F$$

One disadvantage of this theory is that it is sometimes difficult to identify the slowest growing faces. None of the current methods of predicting the equilibrium habit of a crystal can be applied universally.

1.4 CRYSTAL HABIT MODIFICATION

It is very difficult to predict the effect of any crystal habit modifying operation on a particular crystalline substance due to a lack of information about the mechanisms of crystal habit modification. The factors which may affect the habit of a crystal can be divided into two categories: those affecting growth conditions and those acting as impurities in the crystallising solution.

1.4.1 Influence of Growth Conditions

There are many environmental factors known to affect crystal habit, such as the degree of supersaturation or supercooling, the rate of cooling,

the temperature of crystallisation, the degree of agitation, the p H. of the solution and the choice of solvent.

(i) Supersaturation

The growth kinetics of individual crystal faces usually depend to differing extents on the supersaturation, therefore it is often possible to exert considerable control over the crystal habit by raising or lowering the supersaturation. Kern (1953) found that when potassium iodide was crystallised from aqueous solution, at low supersaturations the majority of faces had Miller indices of {100} but at higher supersaturations the {111} faces predominated. A similar effect was observed by Aslanian and Kostov (1972) on crystallising oxalic acid from aqueous solution. Increasing the supersaturation decreased the development of {011} and {110} faces and increased the development of {10$\bar{1}$} and {101} faces. For a definition of Miller indices and a description of their use in crystal face terminology the reader is referred to Mullin (1972).

(ii) Rate of Cooling.

Rapid cooling of a solution or melt often causes preferential growth of a crystal in one particular direction giving rise to the formation of needles. This is due to the necessity to dissipate the heat generated by the exothermic crystallisation process

as rapidly as possible and this is the crystal habit most suited for that purpose because of its favourable surface/volume ratio. The crystallisation of naphthalene from cyclohexane demonstrates this (Wells, 1949). On rapid cooling needles of naphthalene are formed, but on slow evaporation compact tablets result. Rapid cooling may also result in the formation of a new crystal habit. Wells (1949) showed that when anthranilic acid crystals were grown slowly in ethanol, rhombic bipyramids predominated, whereas rapid growth resulted in diamond-shaped plates.

(iii) Choice of Solvent

Different solvents will often produce different habits of the same solute. Aspirin crystallises as needles from aqueous solution and as plates from certain other solvents (Buckley, 1951); iodoform crystallises as hexagonal prisms from cyclohexane and as hexagonal pyramids from aniline (Wells, 1949). Changing the solvent may also change the solubility of the solute. Increased solubility will increase the availability of growth sites, whilst a decreased solubility will decrease the number of available growth sites and hence retard growth. Bourne and Davey (1976) showed that hexamethylene tetramine crystals grown in aqueous solution have a growth rate an order of magnitude larger than the same crystals grown in ethanolic solution. The solubility of

hexamethylene tetramine is ten times greater in water than in ethanol.

As well as studying these general effects, attempts have been made to study the effect of solvents quantitatively and to relate a particular change of habit to the highly specific influence of that solvent. It is possible that crystal growth rates may be controlled by the rate at which desolvation occurs. Bliznakov et.al.(1971) showed that the {100} faces of potassium iodide grow faster than those of potassium bromide and potassium chloride. They attributed this to the differing desolvation energies of the anions:

$$I^- < Br^- < Cl^-$$

Since desolvation energy depends on particular solute - solvent interaction, a change of solvent may induce a change in crystal habit.

There is also evidence to suggest that solute and solvent can interact with each other in a very specific manner. If solvent associates strongly with a particular crystal face, the molecules may become incorporated into the lattice. Watson (1954) attributed the different habits of n- pentacontanol -1 in polar and non-polar solvents to the incorporation of polar solvent molecules into the crystal lattice by hydrogen bonding with the hydroxyl groups. Choice of solvent is therefore important in controlling

crystal habit and usually has a very specific effect.

(iv) p H. of the Solution

Occasionally the p H of an aqueous solution will influence crystal habit. The p H modifies the nature and concentration of ions in solution, especially when there are salts of weak acids or bases present. Byteva (1966) showed that the growth kinetics of adenosine diphosphate crystals are affected by p H. The growth kinetics of the {011} faces are related to the hydration of NH_4^+ ions and therefore growth decreases when p H is increased. The {010} faces have kinetics related to the hydration of $H_2PO_4^-$ ions and are less affected by p H. Therefore habit changes may occur if the p H is varied, but in general this is not a major factor affecting crystal habit.

1.4.2 Impurities.

There are many examples of habit modification due to impurities. Very often only traces of an impurity are needed to produce a change of crystal habit, apparently by enhancing or retarding the relative growth rates of different crystal faces. An impurity may be selective in its effect and only modify the growth kinetics of one or two crystallographic faces. Comprehensive reviews of this topic have been written by Buckley (1951), Khamskii (1969), Mullin (1972) and Boistelle (1975). Impurities used in controlling

crystal habit can be divided into three categories:

(i) Certain inorganic compounds which are active mainly in ionic systems.

(ii) Surface active agents, dyestuffs and polymeric materials which may be active in both ionic and non-ionic systems.

(iii) Substances similar in structure to the crystallising solute but having additional functional groups, mainly in organic systems.

Many mechanisms have been proposed to explain these habit changes. The introduction of impurities may change the physico-chemical properties of the solution leading to a change in the structure of the solution or its equilibrium saturation concentration. Alternatively the impurity may alter the composition of the adsorption layer at the crystal-solution interface and thereby interfere with the integration of growth units into the crystal lattice; if the impurity is similar in size to the growth units, it may even be incorporated into the crystal lattice.

1.5 TEMPERATURE CYCLING

Temperature cycling can be used as a means of modifying crystal habit. The crystal suspension is subjected to alternate periods of heating and cooling around the equilibrium saturation temperature, during which it undergoes alternate periods of dissolution and growth, respectively. Nyvlt (1973) produced rounded crystals of sodium nitrate, sodium thiosulphate, urea and ammonium sulphate using this

method. He concluded that this rounding effect was due to dissolution of the corners of the crystals, followed by the edges and growth of the slower growing faces. The advantage of this method of crystal habit modification is that it is not necessary to introduce impurities into the system. This is of particular importance in the pharmaceutical industry where the presence of impurities in any pharmaceutical formulation may be undesirable. A number of temperature cycling apparatus have been described in the literature for various purposes.

Barnes (1956) described a temperature cycle controller with a simple cam design, easily modified to deal with processes of varied time-temperature requirements. Scott et al (1964) devised a simple programmed controller based on a standard slide-wire thermoregulator placed directly into the reaction vessel which was held in a water bath. An immersion heater in the bath was operated through the thermoregulator. For the cooling cycle, it was necessary to add a cooling cell to the bath to oppose the action of the heating element. A similar device based on a specially designed thermoregulator has also been described by Eriksen and Bird (1965). Other examples are an automatic control for a temperature cycling furnace (Lovell,1967), and a temperature programmed controller for an environmental chamber (Skerrett, 1968). These

would not, however, be applicable to the temperature cycling of crystal suspensions.

Temperature cycling devices designed specifically for studying crystal growth have been used by a number of workers. Varney (1967) described a mechanical device for transferring samples between two thermostatted water baths to study crystal growth in aqueous suspension. It was capable of continuous operation for several days. However no mention is made of any form of temperature monitoring during the process. Carless and Foster (1966) devised a temperature cycling apparatus to study accelerated crystal growth. Suspensions were alternately heated and cooled in a jacketed stainless steel reaction vessel. The suspension was stirred with a stainless steel paddle at 680 r.p.m. The temperature of the suspension was recorded using a conventional thermometer. Hot water was circulated from a thermostatically controlled bath through the vessel jacket for a period of eight minutes, then "cold" water from a second thermostatically controlled bath was allowed to flow for a further eight minutes. This sixteen minute cycle was repeated for the desired number of temperature cycles. The manually operated process was later automated using a "cyclothermostat" (Carless, Foster and Jolliffe, 1966).

Nyvlt (1973) reported the production of rounded crystals using periodic temperature cycling. He

carried out his initial experiments on single crystals placed in a thermostatted solution. Photographs of the crystals showed that dissolution started at the corners of the crystal. When deposition was allowed to occur, the corners and edges were reformed followed by growth of the faces in the usual manner. A second series of laboratory-scale experiments was carried out using a 300ml Erlenmayer flask containing the crystal suspension, a magnetic stirrer and a thermistor. The flask was immersed in a water bath equipped with two contact thermometers which controlled the upper and lower temperatures. The number of cycles was recorded by the thermistor in the crystallisation chamber. Nyvlt then scaled-up, first to a laboratory twinned crystalliser and finally to a corresponding pilot plant crystalliser of 750 litres capacity. The two interconnected stirred vessels were each operated at different temperatures and the crystal suspension was circulated between the two vessels in order to achieve the desired temperature-time cycles. For initial studies on the effect of temperature cycling and other factors on crystal habit, there is nevertheless a need for laboratory scale apparatus, that is preferably simple and inexpensive.

1.6 SHAPE

It is important to consider what is meant by the term "shape". The Oxford Dictionary (1961) defines shape

as "that quantity of a material object or a geometrical figure which depends upon constant relation of position and proportionate distance amongst all the points comprising its outline or external surface". The size of a solid particle gives an indication of the quantity of matter within it; its shape gives information about the pattern in which that quantity is fitted together. The concept of shape is really a process of pattern recognition and differences in shape are observed by noting the differences in these patterns.

Particle shape affects the properties and the handling of powders, in addition to the effects of particle size.The following are examples of processes and properties influenced by particle shape:

(i) the flow properties of a bulk powder
(ii) the rate of mixing of powders
(iii) the passage of powder through sieves
(iv) sedimentation and fluidization behaviour
(v) compaction behaviour
(vi) the abrasiveness of a powder
(vii) crystal growth and dissolution rates
(viii) the way in which the particles pack together and hence the permeability of a powder bed.

Shape is a property of both two-dimensional and three-dimensional objects but, for simplicity, it is often represented as a two-dimensional outline. Shape is concerned solely with the outline of the external

Table 1.6.1. Definition of Particle Shape (extracted from B.S.2955: Glossary of Terms Relating to Powders and Allen, 1975)

Acicular	needle-shaped
Angular	sharp edged or having roughly polyhedral shape
Crystalline	of geometric shape freely developed in a fluid medium
Dendritic	having a branched crystalline shape
Fibrous	regularly or irregularly thread like
Flaky	plate like
Granular	having approximately an equidimensional irregular shape
Irregular	lacking any symmetry
Nodular	having rounded, irregular shape
Spherical	global shape

surface and therefore shape factors will not provide any information about internal pores. Shape is composed of every point on the particle surface. In principle it would therefore be necessary to carry out an infinite series of measurements on a surface in order to define its shape. This is often unrealistic so one must consider how much information is needed in practice to define a particle adequately in terms of its shape.

Qualitative expressions have been used to classify powders (Table 1.6.1.) using descriptive terms for the shapes most commonly encountered.

Whilst these terms may give a general idea of particle shape, they do not give any quantitative information about the shape characteristics of a powder.

The quantitative assessment of shape has been approached in three main ways:

(i) measurement of individual particles to obtain ratios of various selected diameters. A mean value may be assigned to the bulk powder after the measurement of a large number of particles.

(ii) adoption of some standard geometrical shape with which the actual particle shape can be compared.

(iii) measurement of a physical property of the bulk powder and then categorizing the shape of the constituent particles according to their bulk behaviour.

Many attempts have been made to quantify shape and various shape factors have been devised. However all have been subject to criticism because of ambiguity, difficulty in measurement or a dependence on viewing particles in a particular direction. Ideally a shape factor should be readily calculable from easily measurable parameters, and there should be only one value associated with each geometrical shape.

1.6.1. Early Shape Assessment Methods

Attempts to quantify shape were made as early as 1897. Mackie (1897) examined a number of sands from north-east Scotland and counted the number of rounded, sub-angular and angular grains in samples of two hundred grains. He assigned numerical values to each qualitative parameter and calculated a mean value for each sample to give a crude index of roundness. Wentworth (1919) studied the rounding of pebbles by water. He based his assessment of roundness on the surface area-to-volume ratio, the average deviation of diameters from a mean diameter and the average deviation of convexities from a mean convexity. He obtained values ranging from 1.0 for a perfect sphere

to virtually zero for a sharp corner. Tester (1931) improved upon this by extrapolating the plane sides of a particle to give its assumed initial shape. He then took the ratio,

$$\frac{\text{(original length) - (abraded length)}}{\text{original length}} \times 100 \quad \ldots\ldots (3)$$

to give an index where zero represented a newly fractured particle and 100 represented a completely rounded one.

The use of an area-to-perimeter ratio as an index of circularity was suggested by Cox (1927). He realised that the surface-to-volume ratio was a useful measure of how closely the shape of a particle approximated to the spherical. However because of the difficulty involved in measuring surface area he suggested measuring the cross-sectional area of sections of the particle and determining the roundness of these sections. He proposed that since for any image shape,

$$\frac{\text{area}}{(\text{perimeter})^2} = \text{constant} \quad \ldots\ldots\ldots\ldots (4)$$

and the value of that constant for a circle is equal to $1/4\pi$, it could be said that,

$$\frac{4\pi \times \text{area}}{(\text{perimeter})^2} = K \quad \ldots\ldots\ldots\ldots\ldots\ldots (5)$$

where K = 1 for a circle and lies between 0 and 1 for other shapes. The factor K is known as Cox's Index of Circularity.

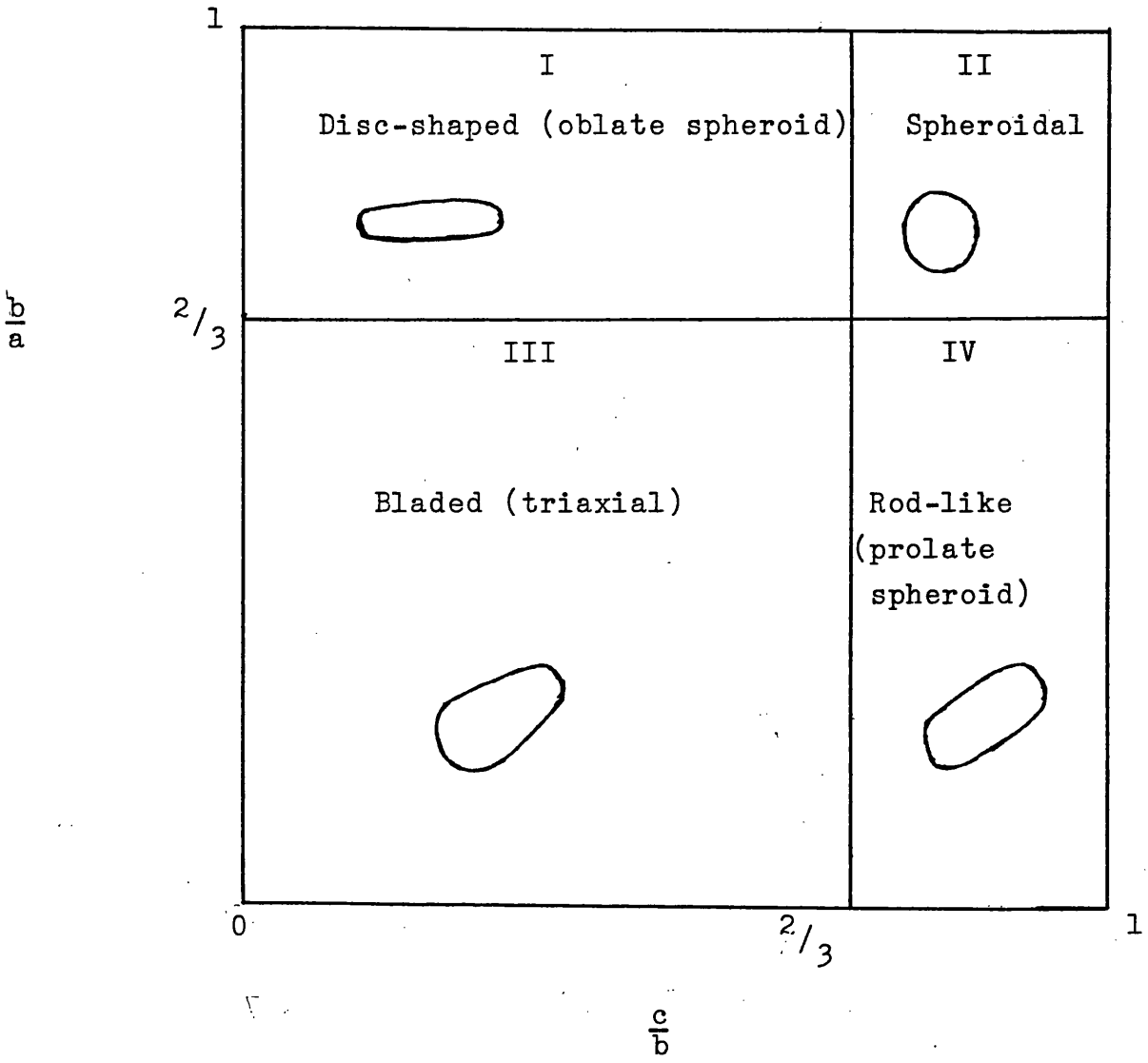

Fig.1.6.1.1 Zingg Diagram

Wadell (1932) distinguished between the terms "roundness" and "sphericity". Sphericity was taken to be the ratio of the surface area of a sphere having the same volume as a particular particle to the actual surface area of that particle. This ratio is 1 for a spherical particle and between 0 and 1 for other shapes. Roundness was measured as the ratio of the radius of curvature of the corner,(r), to the radius of the maximum inscribed circle, (R). This ratio is 1 for a circular particle and between 0 and 1 for other shapes. The methods of Cox and Wadell proved to be very time consuming so Riley (1941) introduced a projection sphericity method which involved only the calculation of the square root of the ratio of the diameters of the inscribed, (D_i), to circumscribed, (D_c), circles. He called this ratio, $(D_i/D_c)^{\frac{1}{2}}$, sphericity.

Zingg (1935) and Krumbein (1941) both introduced new concepts of sphericity based on volume rather than surface area. Zingg measured the three principal diameters, at right angles to one another, a, b and c of a pebble; by plotting b/a against c/b he established four shape classes and drew a shape classification diagram known as a Zingg diagram (Fig.1.6.1.1.). Depending on the point represented by a particle on the Zingg diagram, a rough estimate of shape can be made; however this does not give a numerical shape factor. Krumbein used an ellipsoid

as a standard reference shape, instead of a sphere. This allowed differentiation between different kinds of ellipsoids. A sphere has commonly been chosen as the standard reference shape because it is easily characterised by one dimension, but the orthotetrakaidecahedron has also been used as a standard reference shape by Aschenbrenner (1956) because its surface area and volume can be easily expressed. It is a regular solid shape composed of squares and hexagons, with all its edges being equal in length. It can be packed to zero porosity. Aschenbrenner used its three mutually perpendicular dimensions and its geometric characteristics to define the shape of particles both in terms of Wadell's sphericity and also Zingg's shape factor.

From this early work Lees (1964) observed that particles of a given roundness could vary greatly in angularity. He developed a method for measuring the angularity of particles that took into account the degree of acuteness of the angles of the corners, the number of angular corners and the degree of projection of the corners from the body of the particle. He gave values of angularity for various geometric shapes and devised a chart for visual estimation of the angularity of actual particles. Hausner (1966) attempted to characterise the shape of individual particles by comparing their features with those of a rectangle of minimum area drawn around the projected image of the particle. He

defined three ratios, elongation, bulkiness and a surface factor, which in combination characterised the shape of a particle independently of its size.

All the methods mentioned above require large numbers of measurements of individual particles. For practical considerations individual particles are of less importance than the properties and behaviour of the bulk material. A logical alternative therefore is to use a shape factor based on a function of the entire assembly of particles. Heywood (1933) defined shape numerically using two coefficients, a surface coefficient and a volume coefficient. Both coefficients are related to the mean projected area diameter, (d_a), of the particle viewed in the plane of greatest stability, and are represented by the following equations:

$$\text{Volume of a particle} = k\, d_a^{3} \qquad \ldots\ldots\ldots (6)$$

$$\text{Surface area of a particle} = f\, d_a^{2} \qquad \ldots\ldots (7)$$

where k is a volume shape factor and f is a surface shape factor. The specific surface, S_c, is determined from:

$$S_c = \frac{f}{\rho k} \cdot \frac{1}{d_s} \qquad \ldots\ldots\ldots\ldots\ldots (8)$$

where ρ = density of material

d_s = mean surface area diameter of the particles in the sample

The ratio f/k is a measurement of particle shape and has a value of 6 for spheres. This value increases as particles increase in irregularity. Later Heywood

(1954) showed how these surface and volume factors could be calculated from three orthogonal dimensions of a particle, length, (L), Breadth, (B) and thickness, (T). He used these values to define the two following ratios:

$$m = \frac{B}{T} = \text{flatness ratio} \quad \ldots\ldots\ldots\ldots\ldots (9)$$

$$n = \frac{L}{B} = \text{elongation ratio} \quad \ldots\ldots\ldots\ldots (10)$$

He derived an equation for numerical values of f and k and related these values to shape classes. The equation he proposed is given below:

$$f = 1.57 + c\left(\frac{k_e}{m}\right)^{4/3} \cdot \left(\frac{n+1}{n}\right) \quad \ldots\ldots (11)$$

$$k_e = km\sqrt{n} = k \text{ for equidimensional particles}$$

$$\therefore f = 1.57 + ck^{4/3} \cdot \left(\frac{n+1}{n^{1/3}}\right) \quad \ldots\ldots\ldots\ldots (12)$$

where c = a coefficient that can be assigned to a specific shape group.

In order to use the above equation (12) the following three experimental measurements must be made. Firstly the mean solid volume, (V), must be determined and secondly the mean projected area diameter must be determined, for example from microscopical measurements. From these two measurements k may be calculated from:

$$k = \frac{V}{d_a^3} \quad \ldots\ldots\ldots\ldots\ldots\ldots\ldots\ldots (13)$$

Thirdly the elongation ratio, n, can be determined by microscopy. Using Heywood's tables to find the value, c, for the relevant shape category identified by microscopic examination, the value of f may be calculated.

Hausner (1967) showed that the ratio of the consolidated ("tapped") bulk density to the poured bulk density of a powder sample is an indication of frictional conditions within the powder bed and varies with particle shape. Kostelnik and Beddow (1970) and Riley and Mann (1972) both attempted to use Hausner's ratio of densities as a shape index. Whilst both observed that this ratio varies with shape, Kostelnik and Beddow reported that this ratio also varied with particle size. Riley and Mann showed that the ratios for two extremes of shape, spheres and flakes, differed by only 0.1 and therefore could not be used to discriminate between intermediate shapes. Other workers (Ridgway et al, 1969, 1970) have studied the relationship between particle shape and bulk properties such as flow through an orifice and tablet compression.

1.6.2. More Recent Methods of Shape Assessment

Schwarcz and Shane (1969) were among the first workers to publish a paper on particle shape measurement making use of a mathematical model. They analysed beach sand silhouettes and derived quantities from the Fourier coefficients of a two-dimensional closed curve forming the perimeter of the projection of the particle image. These quantities corresponded to the conventional characteristics of roundness and sphericity. The curves were plotted in polar co-ordinates, r and θ, and a harmonic analysis of

the function r (θ) was made by numerical analysis of the measurements at equally spaced sample points along the curve. The equation they derived predicted the "rollability" of individual particles.

Meloy (1969, 1971) used fast Fourier transforms to process signals representing particle silhouettes. The (x,y) co-ordinates of the particle silhouette were identified and then converted into a polar co-ordinate system based on a radius vector from the centre of gravity of the particle outline to the particle outline. From the original (x,y) data points the centres of gravity were calculated by a standard technique. The number of original data points were then counted and a number, N, chosen such that $N = 2^x$ where x was an integer and N was equal to or less than the number of data points. In order to use the fast Fourier transform the sample points had to be equally spaced. The interval was taken as $2\pi/N$ and for each of the N values of θ, a value of R, the radius vector from the centre of gravity to the particle surface was computed. This is called the Nyquist set and once computed can be fed into the fast Fourier transform to obtain the Fourier coefficients. If $R(\theta)$ is the radius vector from the centre of gravity to the particle outline, then:

$$|R(\theta)| = A_o + \sum A_n \cos(n\theta + \theta_n) \quad \ldots\ldots\ldots (14)$$

where A_n is the n^{th} Fourier coefficient and represents the amplitude of the component wave of frequency n,

and θ_n is the phase angle. Meloy derived a particle "signature" by plotting $\log_n (A_n)$ versus $\log_n n$. A straight line relationship was found with values of the slope ranging from 2.5 to 1.34. Particles with high aspect ratios were found to have higher slope values and rounded particles had lower slope values.

Beddow and Philip (1975) showed how a number of particle silhouette shapes could be analysed and reproduced by Fourier transforms. Gotoh and Finney (1975) used a three-dimensional Fourier approach to fit a particle to an equivalent ellipsoid. Meloy (1977) also pointed out that as well as a Fourier series, other mathematical functions might be used to characterise particle shape. These complex mathematical methods of shape analysis have been reviewed by Kaye (1978) and Clark (1981).

Sutton (1976) noted that the Fourier series could not be applied directly to particles with re-entrant shapes. This problem was considered by Staniforth and Rees (1981), who proposed a shape factor, ﷺ (shah), to quantify the shape of re-entrant particles in different batches of habit-modified lactose powders. This shape factor was calculated from the number of downward pointing projections, e, in a sample set of particles and the total number of particles, n, in the sample according to the formula ﷺ = e/n. The two variables, e and n, were

measured on an image analysing computer. Re-entrant particles were distinguished from non-re-entrant particles, the latter having a Ψ value of unity. This shape factor was not able to characterise geometric form alone but, when combined with the Heywood factor, f/k, was capable of describing re-entrant, non-re-entrant, simple and complex geometric forms from measurement of bulk powder properties as well as individual particle measurements.

Another method of particle shape assessment was suggested by Medalia (1970/71). He considered the profile of a fine particle as a thin lamina and calculated the dimensions of an ellipse having the same radius of gyration about the principal axes. He went on to define two dimensionless shape factors which described the particle profile, using the dimensions of an ellipse having equivalent properties. The first of these factors was the anisometry, defined as the ratio of the major to minor axes of the ellipse; this describes elongation and flatness. The second factor was the bulkiness defined as the ratio of the area of the ellipse to that of the particle profile. These shape factors are often called dynamic shape factors but they have not been widely used due to a lack of information about their physical significance for fine particle systems.

1.7 IMAGE ANALYSIS

The advent of fully automatic image analysers has

Fig.1.7.1. Total Area

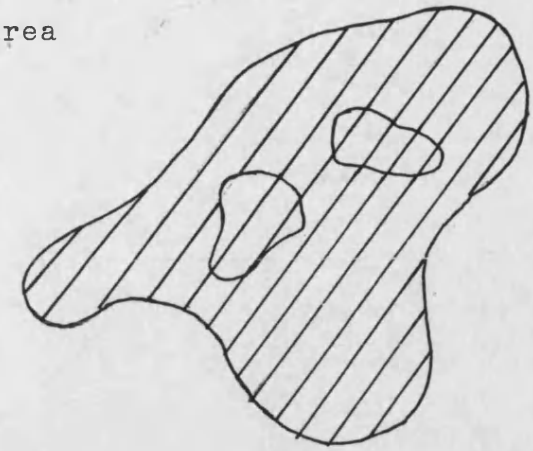

Fig.1.7.2. Exclusive Area

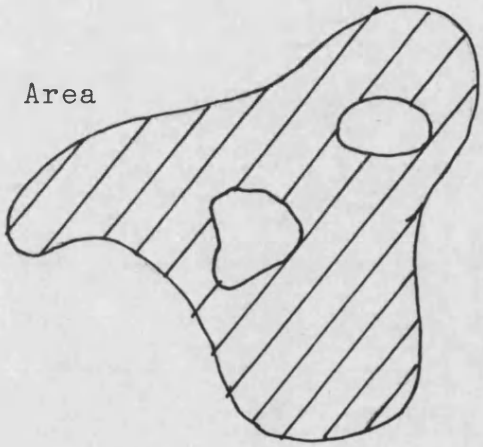

Fig.1.7.3. Total Perimeter

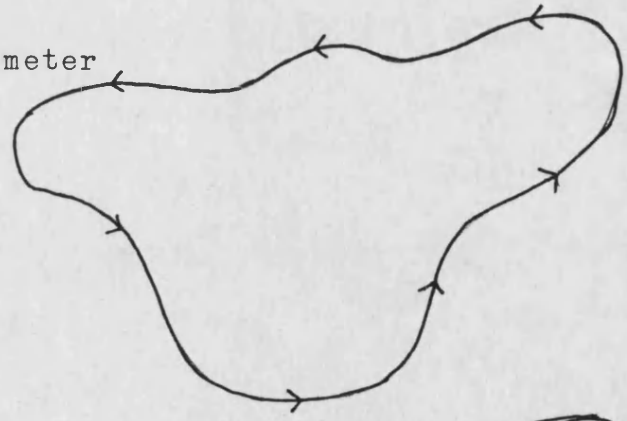

Fig.1.7.4. Convex Perimeter

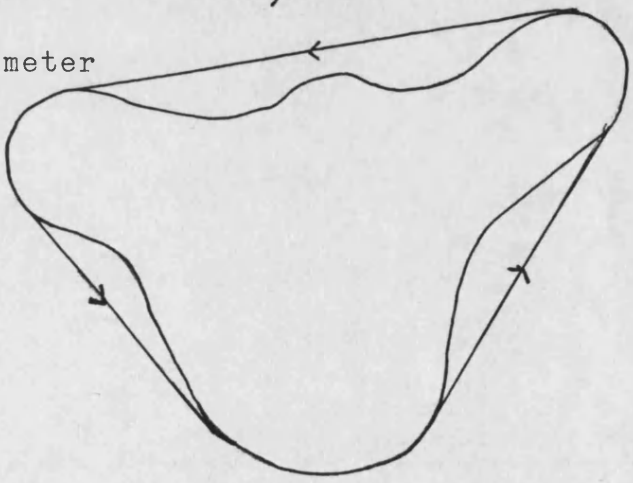

enabled many basic shape parameters to be measured easily and rapidly. In general the following basic measurements are possible on most instruments:

(i) Area - either the total area inside the boundary of the feature regardless of any different phase regions contained within the feature (Fig.1.7.1.) or the exclusive area i.e. the area within a feature boundary excluding holes (Fig.1.7.2.).

(ii) Perimeter length - either the total path length around the boundary of a feature (Fig.1.7.3) or the perimeter of smallest convex region containing the feature (Fig.1.7.4)

(iii) Projected lengths - both horizontal and vertical

(iv) Particle dimensions - including maximum and minimum lengths

(v) Tangent or Feret diameters

(vi) Number of features

These parameters and mathematical combinations of them may be used to obtain the numerical shape factors described in section 1.6.1, and hence routine methods of shape assessment based on the measurement of a large number of individual particles has become a more practical proposition.

The most commonly used image analysers are the fully automatic systems with a T.V.interface. These instruments convert optical information from a television camera into an electrical signal. The

feature is then detected by signal modulation using a signal discriminator to measure the grey level of the image. Grey level thresholding is the simplest form of image analysis. Two grey level values are used to define a band of grey values or an image phase. A binary image is created in which all the image points with a density within the defined band are assigned to the one state and the remaining points to the zero state. The image of the feature thus obtained, can then be processed to calculate the desired shape factor.

However it should be noted that the scope and flexibility of these instruments depends upon the computer software. Most instruments have software inputs for data handling, processing and statistical calculations. This facility enables very specific computer programs to be used in conjunction with the image analyser in order to determine exact information about the image required by the operator. Many instruments can also be used in conjunction with a light pen which allows the operator to interact with the machine. In this mode the image analyser becomes only semi-automatic and subjective judgement may tend to be introduced; some time saving advantage is also lost. There is a wide range of image analysers commercially available and these have been reviewed by Hougardy (1974, 1976).

The advantages of using automatic image analysis to assess shape include:

(i) Elimination of subjective judgement

(ii) Time saving - more particles can be measured in much less time than when using an optical microscope.

(iii) Images can be stored in digital form and processed further, possibly at a later date, using software.

(iv) Image information e.g. percentage area, aspect ratios can readily be reduced to numbers.

(v) Image data handling is simplified and fast.

The main disadvantage of automatic image analysis to date, has been the prohibitive cost of instrumentation. However recent advances in electronics and computing have made a low cost image analyser a practical proposition. Such a system has been used by Beresford (1984) to obtain particle shape information. The hardware used is essentially the same as that used in this work. However the software used in both systems is very different, both having been developed totally independently.

1.8 ASSESSMENT OF SURFACE TEXTURE USING FRACTAL DIMENSIONS

The majority of shape assessment methods mentioned above have considered the profiles of relatively smooth fine particles. Mandelbrot(1977) pointed out

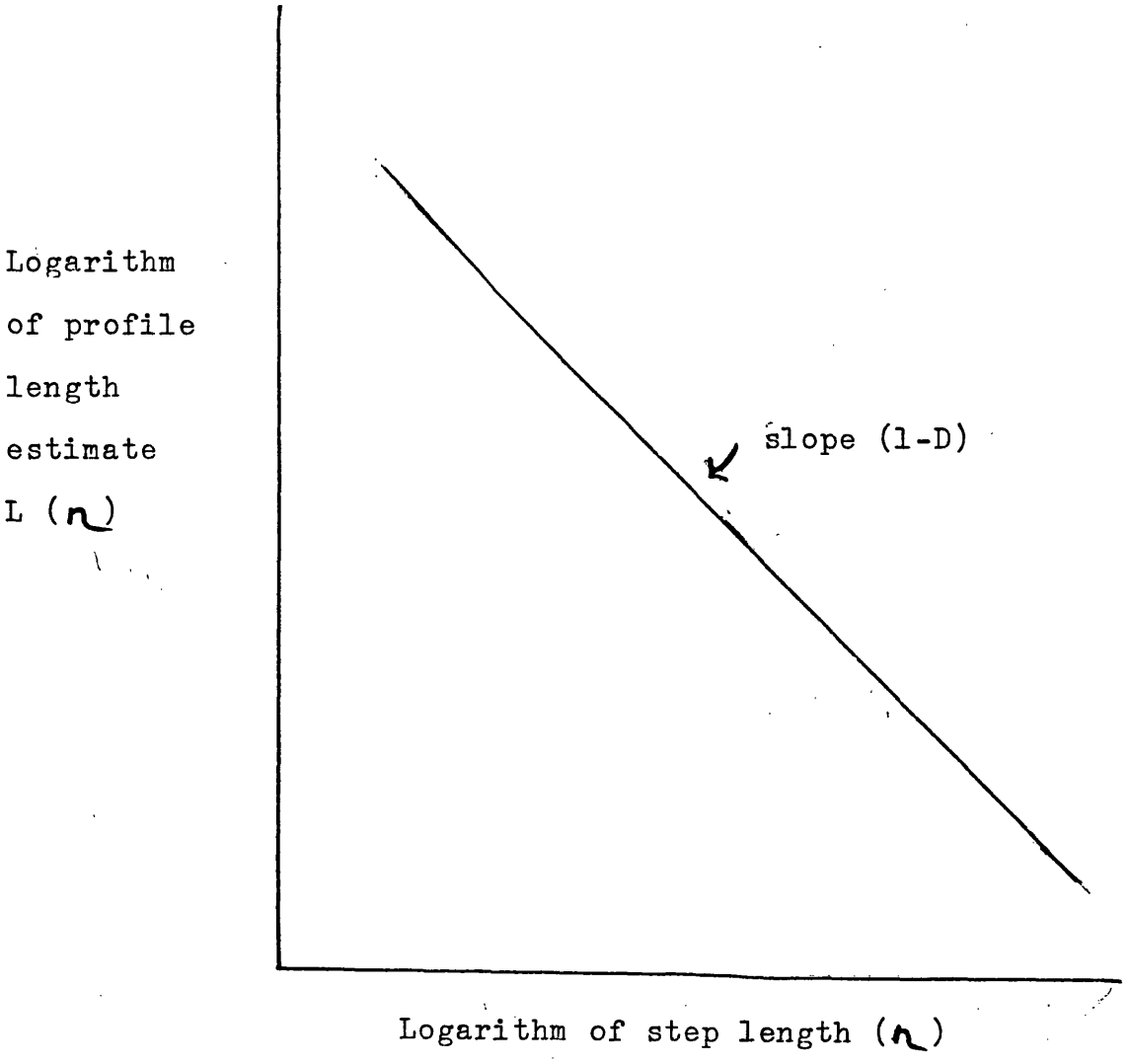

Fig.1.8.1. Richardson Plot for Evaluating Fractal Dimension

that many of the naturally occurring boundaries in the physical world could not be described by continuous curve mathematics, such as those used in calculus and traditional euclidean geometry. He reviewed the unpublished work of L.F.Richardson, who had estimated the length of the coastlines of various countries by stepping along a map of that coastline with a pair of dividers. Richardson found that the estimated length of a coastline, $L(\eta)$, tended to increase towards infinity as the step size, η, decreased. He concluded that there were two constants, λ and D, such that a polygon of side η, approximating the coastline, would have $\lambda\eta^{-D}$ sides. The estimate of perimeter would be approximately $\lambda\eta^{(1-D)}$. A plot of $\log_n L(\eta)$ versus $\log_n \eta$ yields a straight line with a slope of (1-D), and hence D can be evaluated. This plot is known as a Richardson plot (see Fig.1.8.1.). The parameter D was found to be fractional and characteristic of that particular coastline. It also measured dimension. Mandelbrot applied the term "fractal" to this parameter, D, and defined it as a number between 1 and 2, which represents a rugged line in one to two dimensional space. Kaye (1984) extended the concept of fractal dimensions. He described three-dimensional fine particle systems having a fractal dimension of between 2 and 3, and "fractal dusts" having a fractal dimension of less than 1. Hence a fractal dimension can range from 0 to 3.

Kaye (1978) reviewed the work of Mandelbrot on fractals, and showed that they could be used as an alternative mathematical model to obtain an index of ruggedness or texture of fineparticles. Flook (1978) described a method for evaluating fractal dimension using a Quantimet 720 image analyser fitted with a 2D Amender module. He measured geometrically constructed particles of known fractal dimension, and also carbonblack agglomerates. The manual method of Richardson for estimating fractal dimension was found to be not readily adaptable for use with a computer; Flook (1978) therefore used a method which considered a curve to be made of a series of closely spaced equidistant points. A series of overlapping circles of radius r was drawn with their centres on each of the points of the curve. This described a path of width $2r$ covering the curve. The area of this path divided by its width gave an estimate of the length of the curve. As r increased, the circles had a greater degree of overlap and obscured more fine detail of the curve, and the length estimate, $L(r)$, decreased. The fractal dimension was calculated from a plot of $\log_n L(r)$ versus $\log_n r$ as previously described. Flook found that for carbonblack agglomerates this plot showed departure from linearity at large and small step sizes; he suggested that this was due to the structure of the sub-unit of the agglomerate predominating at small step sizes, whilst at large step sizes the fractal dimension was due to the coarse structure of the agglomerate. Flook concluded

that this method overcame the problems in terms of time and effort involved in manual calculation of fractal dimension and thus made characterisation of surface texture of particles a practical possibility.

However Flook's method requires an automatic image analyser with a dilation unit. Dilation is the process of adding structuring elements to each point in a given array of points and is performed by the 2D Amender module on the Quantimet 720. Flook's method cannot be applied to automatic image analysers without this facility because the extensive computer time and space it would require, is not usually available. Schwarcz and Exner (1980) suggested a method suitable for calculating fractal dimension on a semi-automatic analyser. They developed a new algorithm which can be used if a string of co-ordinates along the particle profile is available. The constant spacing between these points is adjusted to the maximum dimension of the feature to be characterised. Firstly the profile length, P, is estimated using all the co-ordinate points as described by Mandelbrot (1977). In the next step every second pair of co-ordinates are used to obtain a length estimate. In the following step every third pair of co-ordinates are used and so on up to fifty steps. The mean side length, $\bar{S}$, is taken as the ratio of the profile length estimate and the number of distances counted. The plot of $\log_n P$ versus $\log_n \bar{S}$ gives the fractal dimension of the particle.

Whalley and Orford (1982, 1983) applied fractal dimensions to describe sand grains. They concluded that basic particle shapes are not readily distinguishable by fractal analysis, Fourier analysis being much more efficient. Fractals were found to be best suited to highly indented outlines and, in contrast to Fourier methods, were not very sensitive to small changes in outline variation. They suggested fractal and Fourier techniques are complementary in providing an overall picture of particle shape and texture.

MATERIALS AND METHODS

2.1 MATERIALS

Sulphadimidine, mol.wt. 278.3, was supplied by Imperial Chemical Industries, Macclesfield. A single batch was used (ICI PM241). It is a white crystalline powder of Ph.Eur. grade containing not less than 99% w/w sulphadimidine.

Sulphamethizole, mol.wt. 270.3, was supplied by Sigma Chemical Company, Poole. A single batch was used (89C 0613). It is a white crystalline powder of laboratory grade containing 99 - 101% w/w anhydrous sulphamethizole.

Sulphathiazole, mol.wt. 255.3, was supplied by Sigma Chemical Company, Poole. A single batch was used (50F 0341). It is a white crystalline powder of laboratory grade containing 99 - 101% w/w anhydrous sulphathiazole.

Chemicals and reagents used throughout were of Analar grade unless otherwise stated.

Distilled water was obtained from a double all-glass still.

Glassware. Volumetric glassware was of grade B. All glassware was cleaned by complete immersion in freshly prepared chromic acid, rinsed several times in tap water and five times with distilled water.

2.2 INSTRUMENTATION

Spectrophotometers. Visible scanning spectrophotometry was employed for the identification of absorbance maxima using a Unicam SP1800 recording spectrophotometer in conjunction with a Unicam AR25 linear recorder. Single point fixed - wavelength absorbance determinations were obtained with a Unicam SP1800. Matched 1 cm glass cuvettes were used.

Infra-red spectrophotometry was carried out using a Unicam SP1025 recording IR spectrophotometer.

Balances. An Oertling (model R41) single pan analytical balance was used for all weighings.

Temperature Cycling. This was achieved by use of a Grant SE20 programmed dual temperature water bath, fitted with a sixty minute timer. This enabled the bath to be set to cycle between any two pre-set temperatures for any cycle time between one minute and one hour and maintain that temperature to $\pm$ 0.5°C. A copper cooling coil (length 100 cm, bore 1 cm diameter) was placed in the bath and connected to the mains cold water supply, to promote more rapid cooling. A three necked round bottomed flask containing the solvent was clamped in the bath and allowed to equilibrate. This flask was then removed from the bath and a weighed amount of crystals introduced to the solvent through one of the necks. The flask was shaken to wet and disperse the crystals and then returned to the bath and clamped. Agitation was provided by a glass paddle attached to a Gallenkamp variable speed stirrer set at 2000 r.p.m. A schematic diagram of the temperature cycling apparatus is shown in Fig.2.2.1. The temperature cycles were recorded using a Servoscript Servogor 120 chart recorder which recorded the change in e.m.f. of a thermocouple placed in the crystal suspension

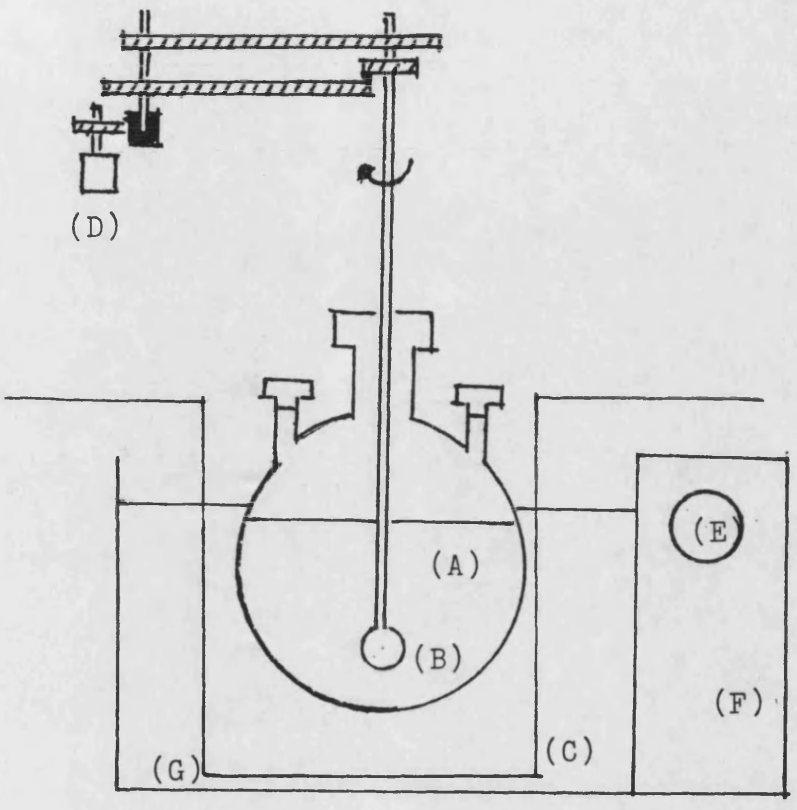

(A) Crystal Suspension

(B) Agitator

(C) Water Bath

(D) Motor

(E) Timer

(F) Dual Temperature Control

(G) Cooling Coil

Fig.2.2.1 Apparatus for Periodic Temperature Cycling

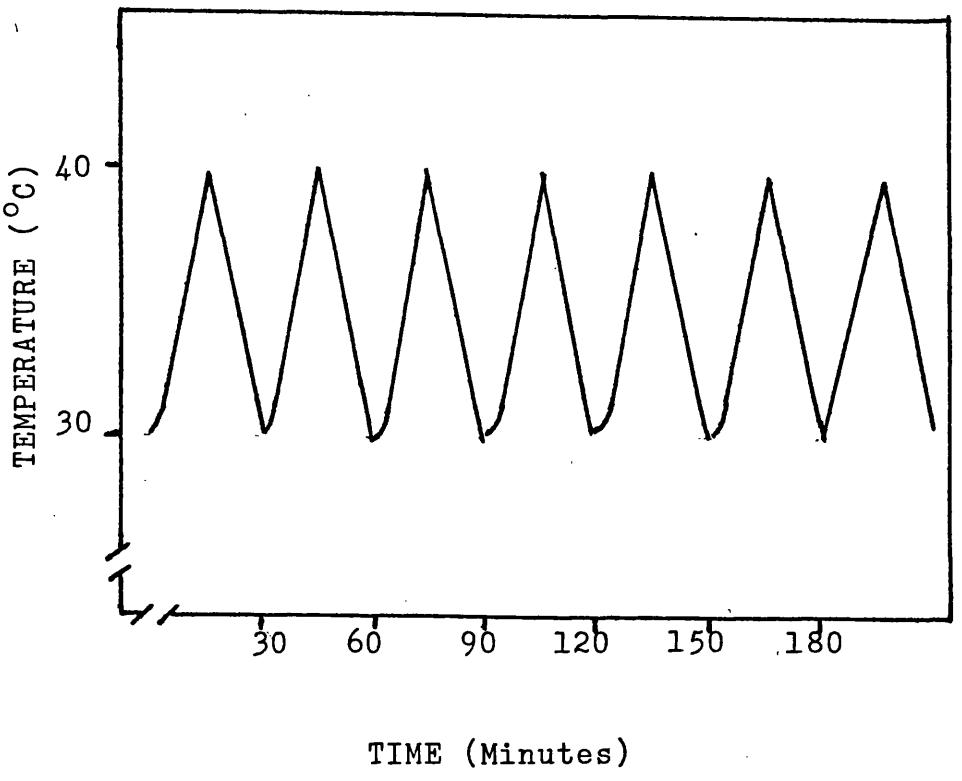

Fig.2.2.2 Temperature-Time Trace of the Suspension.

with reference to a thermocouple placed in ice in a Dilvac Dewar flask (inside a container). The temperature change was calculated using the International Standard Thermocouple Tables. The calibration was checked with reference to ice and boiling water. A typical temperature-time trace is shown in Fig.2.2.2.

Temperature Control. This was achieved in the solubility studies by use of a Grant SE water bath fitted with a Grant SU6 thermostat capable of maintaining the temperature to $\pm$ 0.10°C. Plastic spheres were placed on the surface of the water to minimise heat loss.

Solubility Apparatus. The apparatus consisted of three glass jacketed cells through which water was circulated from a constant temperature bath ($\pm$ 0.1°C), at a pre-determined temperature. The solute and solvent were placed in 50 ml stoppered conical flasks, which were placed inside the jacketed cells. Water was placed between the cells and the conical flasks to provide good heat transfer. The cells were then placed on magnetic stirrers (Rodwell Monotherm) and a magnetic bar was placed in each of the conical flasks to provide stirring.

X-Ray Diffraction. A Philips 'PW 1730' 2 kW X-ray generator in conjunction with a Philips 'PW 1050' vertical diffractometer goniometer with a 'PW 4620'

rate meter/channel analyser and a flat bed recorder was used. Diffracted Copper Kα X-rays (wavelength 1.5418×10^{-10}m) were detected by means of a Xenon probe counter with an appropriate pulse height discriminating facility to reduce background interference.

2.3 METHODS

2.3.1 MAGISCAN IMAGE ANALYSIS SYSTEM

Automatic image analysis was necessary for quantitative evaluation of the effect of temperature cycling on crystal habit. Initially the Joyce-Loebl Magiscan (Joyce-Loebl Ltd., Gateshead.) was used. This consists of a 625 line television camera fitted with a silicon diode tube to give linearity and a low signal to noise ratio. This was mounted on to a Leitz Ortholux II microsc ope. The signal from the television camera is digitised by a high speed analogue/digital converter with a 6 Bit resolution. A system clock controls the sampling rate and scanning pattern of the television camera to ensure precise registration of image points. The digitised signal is fed to the image processor where it is reconverted and displayed on a video screen so that the operator sees exactly the same image as the computer. This may be compared with the original image by pressing the appropriate button on the keyboard. It is at this stage that the operator may interact with the instrument using the high resolution lightpen to edit or select features of interest. A schematic diagram of the Magiscan is shown in Fig.2.3.1.1.

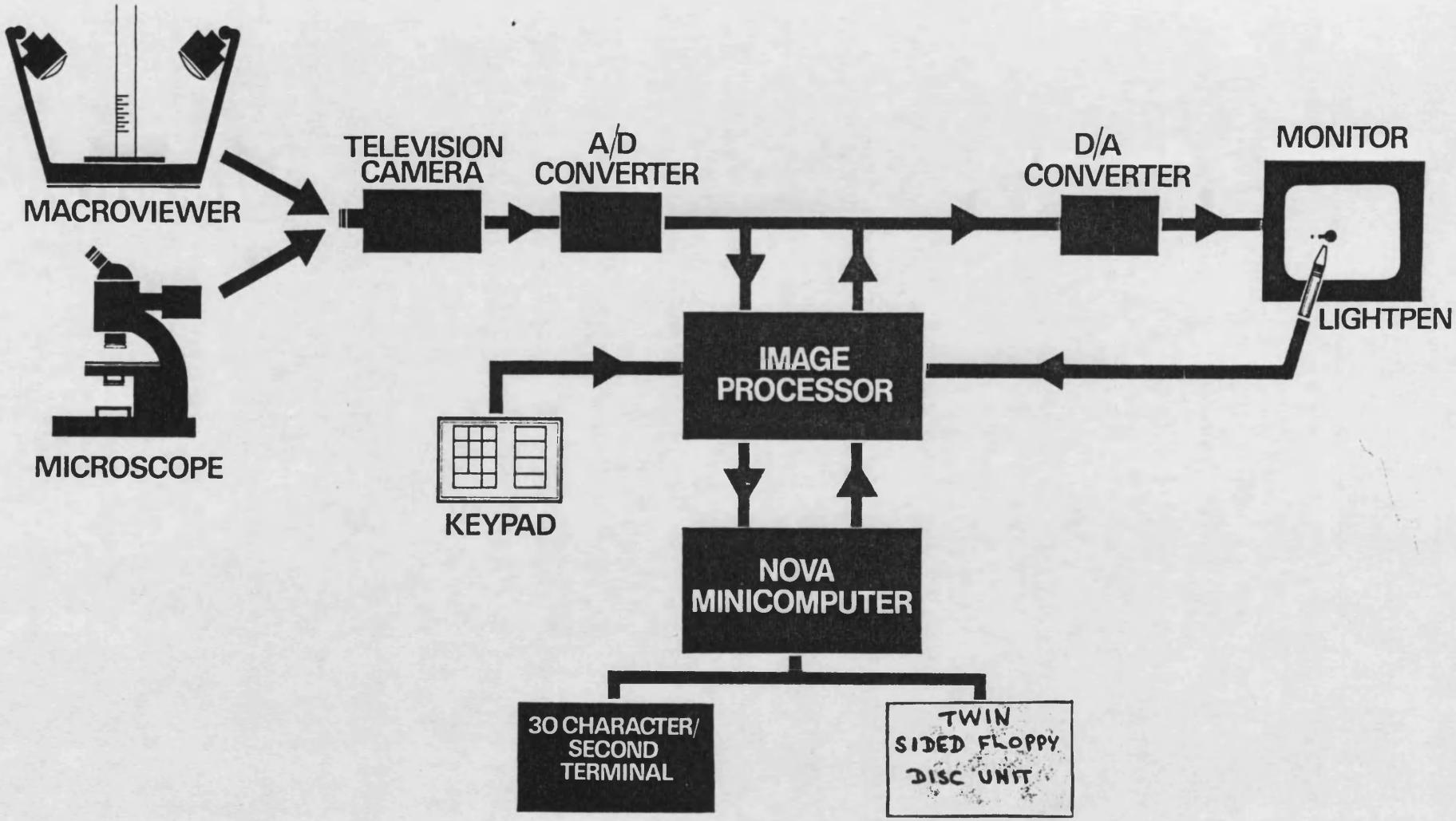

Fig.2.3.1.1 A Schematic Diagram of the Magiscan Image Analysis System.

Quantitative analysis of the selected structural features was carried out by the Nova minicomputer. This can perform analyses ranging from simple operations such as counting and sizing to more complex operations involving geometric and stereological problems. The software package SPEL (Simple Picture Evaluation Language) provides all the fundamental measurements such as area, count, perimeter, maximum chord length, etc. Logical and arithmetic combinations of these operations may be defined by the operator. The image processor is also fully programmable in MAGIC (an extension of BASIC) or FORTRAN, at the terminal. It is not possible to interface with SPEL.

All routine operations of the Magiscan are controlled by a simple keypad and lightpen. Structural analyses and measurement routines are called up by the operator using the lightpen on a 'video keyboard' displayed on the screen. Instructions accepted are confirmed on the display. The machine is programmed to reject illogical instructions .

The Magiscan can be calibrated to make measurements in any system of absolute units, using a graduated scale. Before structural representation of any image is made the Magiscan must be informed as to which parts of the image correspond to the features of interest. The basic method of separating a feature from the background is by difference in grey level. Two grey level values are

used to define a band of grey values or an image phase. A binary image is created in which all the image points with a density within the band are assigned to one state and all the remaining points to the zero state. This method of structural analysis is simple and fast, but is not suitable for images which have a non-uniform background, or if the grey level of the background in one part of the image is similar to that of a feature in a different region. In addition, sizing errors may occur on features which do not have sharp boundaries, due to the difficulty in setting the correct level for each feature.

The Magiscan is an interactive machine, i.e. it has an image editor which allows the operator to change any detected feature using a lightpen and thereby modify the structural representation before measurement. The editor options are:

Line: Material is added to the structural representation. Boundary lines can be 'touched up', imperfectly detected features filled in, or undetected features outlined.

Erase: Material is removed from the structural representation. Touching features can be separated, spurious detail removed, and editing mistakes corrected.

Clear: This removes all material within a closed region. Unwanted detail or features can be completely removed from the structural representation of the image.

The altered image can be compared with the stored image before structural analysis. Results are presented on the video screen or printed out.

Initially Cox's Index of Circularity (Cox,1927) was used as a shape factor to monitor any change in crystal habit that occurred as a result of temperature cycling.

$$\frac{\text{Area of crystal. } 4\pi}{(\text{Perimeter of crystal})^2} \quad \ldots\ldots \text{ Cox's Index of Circularity}$$

This index could be readily obtained using SPEL.,but it proved to be insensitive to the observed shape change. The ratio of the radius of the smallest circle that would enclose the whole crystal, (the circumscribed circle) to the largest circle that could be drawn completely within the crystal, (the inscribed circle) appeared to be a more sensitive shape factor. A program in Fortran was used to calculate these dimensions for an individual crystal and to calculate the resulting ratio. The mean and standard deviation were calculated for 100 crystals.

The Magiscan is obviously a very sophisticated image analysis system, but in the present work it was not practical for use as a routine monitoring method, since the equipment was not on site, and access to it was very limited by distance and availability by courtesy of the C.E.G.B. As a result it was decided to set up a simple image analysis system using a microcomputer. This could then be used in the laboratory

to look at the batch of crystals immediately after temperature cycling.

2.3.2 MICROSIGHT 1 IMAGE ANALYSIS SYSTEM

A Microsight 1 image analysis system from Digithurst (Royston, Herts.) was used in conjunction with a BBC model B microcomputer with Acorn disc interface and a Cumana 40/80 track switchable double disc drive. A Zeiss Standard Fluorescence microscope was fitted with a 40/0.75 Neofluor universal objective through which slides of the crystals were viewed. The microscope was also fitted with a trinocular head, to which was attached an ITC/Kegami A.1.Lens model television camera fitted with a Cosmicar television lens 16mm 1:1.4 to transmit the image from the microscope to a C.A.& G CD12G video screen. The video screen image was processed by the 'Micro Eye' interface which sent the data back to the microcomputer as an 8 bit digitised video image, displayed on a second video screen. An Epson FX - 80 printer was also connected to the set up to enable digitised images and data to be printed. The system is shown in Fig.2.3.2.1.

The Microscale basic software package was also supplied by Digithurst. Images of the crystals on the microscope slide were digitised and a small digitised image displayed on the video screen to allow for any interactive adjustment of the camera when necessary. A larger digitised image was then displayed on the screen to enable adjustment of the grey scale to

Fig.2.3.2.1 The author using the Microsight Image Analysis System.

achieve a definite outline of the crystal. When a satisfactory digitised picture was obtained it could then be stored on disc for further processing and/or printed out.

A problem was encountered with the basic software package. A certain amount of light from the microscope was transmitted by the crystals so that their digitised image appeared as a solid outline with the centre portion the same colour as the background. Hence, even when the grey level was adjusted, it proved impossible for the digitiser to distinguish between the central portion and the background, and therefore the processed image appeared as a crystal outline, rather than a solid image. To overcome this an additional command was written into the Microscale package, - a 'remove' command. This enabled the lighter centre portion of the crystal to be 'removed' and replaced with the same colour as that of the solid outline thus resulting in a solid image.

The digitised crystal images were stored on disc and then processed further. Two types of shape factor were used in order to try and characterise the crystal habit before and after temperature cycling. The ratio of the radii of the inscribed circle and the circumscribed circle was chosen to try and monitor any rounding that occurred. The program to calculate this also calculates the area and perimeter of the crystal. The second shape indicator chosen was the fractal dimension of the crystal

(Mandelbrot, 1977) to monitor the effect on the ruggedness or texture of the crystal as a result of temperature cycling. One hundred crystals from each batch were studied.

2.3.3 CALIBRATION OF THE MICROSIGHT 1 IMAGE ANALYSIS SYSTEM

A square was drawn on graph paper and viewed through the television camera on the videoscreen. This image was processed and a digitised image was displayed on the second videoscreen. The digitised image was rectangular, rather than square because the aspect ratio of the videoscreen used was different from the one used by the manufacturers to set up the system.

The width potentiometer in the 'Micro Eye' was adjusted until a square digitised image was obtained. This was checked by measuring the length, width, area and perimeter of the digitised square using the Microscale software package. Calibration was then carried out using a stage micrometer in the usual manner.

Results

A x 40 objective was used throughout.

Horizontal Calibration.

77 pixels = 150 μm

1 pixel = 1.9 μm

Vertical Calibration.

53 pixels = 100 μm

1 pixel = 1.9 μm

The accuracy of this calibration was limited by the instrumentation, and is therefore quoted to only one decimal place, taking 1 pixel ≡ 1.9μm as the calibration figure to be used in all programs involving the calculation of length and area.

2.3.4 X-RAY DIFFRACTION ANALYSIS

The wavelength of an X-ray beam is of the same order of magnitude as the distance between atoms in a crystal (about 10^{-10}m), and the crystal lattice can act as a diffraction grating for X-rays. When X-rays fall on a single plane of atoms in a crystal, each atom scatters a small fraction of the incident beam, producing a weak secondary wavelet of X-rays. In most directions destructive interference of the wavelets occurs and wavelets of the same frequency, when superimposed, will be out of phase, and the maximum and minimum amplitudes of the waves will cancel each other out. However, in the direction for which the angle of incidence equals the angle of 'reflection' (or diffraction) there is reinforcement and constructive interference occurs so that wavelets of the same frequency will be in phase when superimposed resulting in a summation of amplitudes.

All planes of atoms to which the X-rays penetrate behave similarly. The reflected beams from all the planes involved interfere, but the resultant reflected beam is only strong if the path distance between

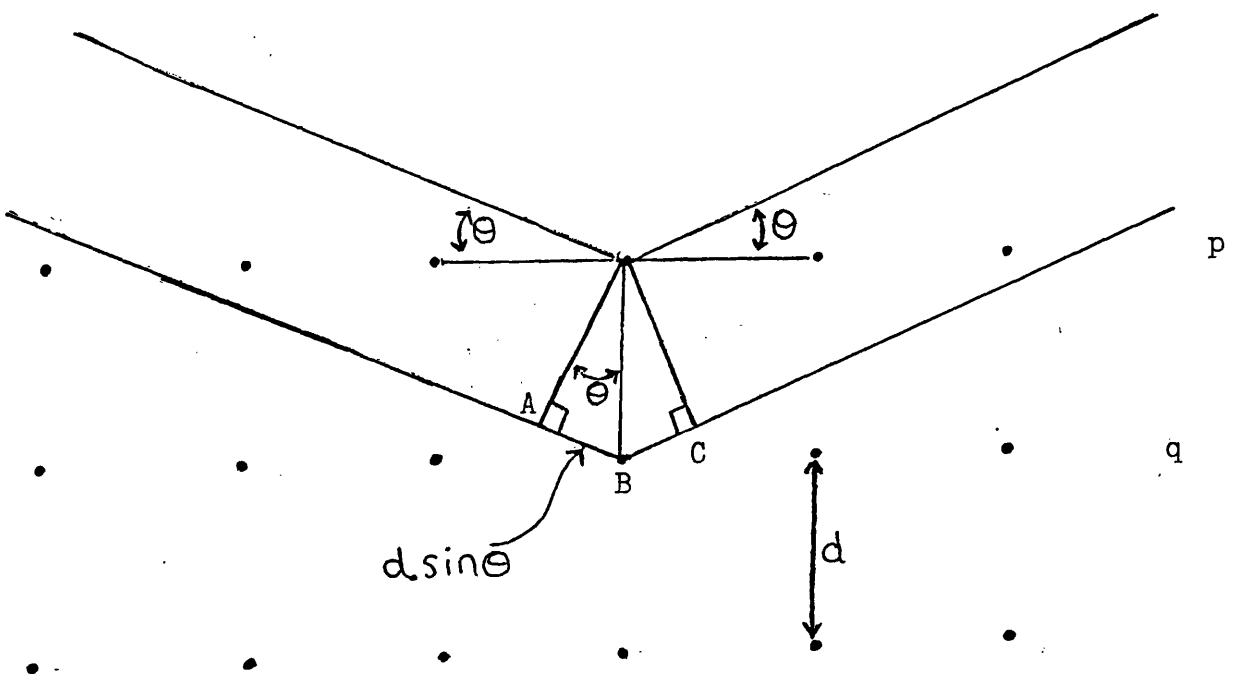

Fig.2.3.4.1 Diffraction From Successive Parallel Planes of Atoms.

successive planes is an integral number of wavelengths of the incident X-radiation. Under these conditions the diffracted waves will arrive at the detector in phase.

From Fig.2.3.4.1 it can be seen that reinforcement only occurs for planes p and q when

$$AB + BC = n\lambda \quad \ldots\ldots\ldots\ldots\ldots\ldots (15)$$

where n is an integer and indicates the order of diffraction, and λ is the wavelength of the X-rays (nm). If d is the distance between the parallel planes of atoms and θ is the angle between the X-ray beam and the crystal surface (the 'glancing' angle) i.e. half the angle between the incident and diffracted beams, then

$$AB + BC = 2\, d \sin\theta \quad \ldots\ldots\ldots\ldots\ldots\ldots (16)$$

When the angles of the incident and diffracted beams are the same, there is a maximum intensity at the detector. For parallel planes of atoms (or molecules) the reflected (or diffracted) beams must reach the detector in phase in order for summation of intensities to occur. Therefore for parallel planes of atoms

$$2\, d \sin\theta = n\lambda \quad \ldots\ldots\ldots\ldots\ldots\ldots (17)$$

The above equation (17) is an expression of Braggs Law and has two important applications. Firstly, if the 'd' spacings of the planes of the crystal lattice are known, then the wavelength of the X-rays can be calculated from the measured angle of diffraction, θ. This procedure has been used to investigate elements and determine their atomic number. Secondly, if the wavelength of the incident beam is known, the characteristic interplanar spacings

('d' spacings) can be computed from the measurements of the diffraction angle θ. It should be noted that the derivation of Braggs Law depends on the lattice planes being regularly spaced. If the arrangement of atoms (or molecules) in any one plane is irregular, sharp X-ray diffraction patterns are not observed.

Studies in theoretical physics, and internal crystal structure determinations, are usually carried out on single crystals of a substance. Phase identification work is usually done with a powdered sample of crystals, in which case the technique is called X-ray powder diffraction. The advantage of this technique is that the sample can be examined as presented (apart from any necessary particle size reduction). There is no need to treat the sample chemically.

Crystal structure determines the intensity and position of the diffracted beam due to the fact that different atoms have different numbers of electrons, and therefore their relative scattering power varies. Even when two crystals have identical lattices, the kinds of atoms comprising them may be different; hence each crystal species diffracts X-rays in a characteristically different way.

The effect of impurities varies depending on the type of impurity involved. Simple admixtures of differing crystallinity, which show no interaction, are revealed as a superposition of the X-ray patterns of the constituent materials. Solid solutions of

impurities can lead to changes in lattice parameters, and, therefore, a change in the position of lines within a diffraction pattern. Polymorphic forms of the same substance will have different interplanar spacings, whereas isomorphous forms of different compounds will have similar spacings, but vary in relative intensities. The resulting X-ray pattern will be characteristically different from that of the parent crystal and can therefore be used as a means of identification.

2.3.5 POWDER PLATE STUDIES

The sample, after being finely ground in a glass mortar, was packed into a flat holder. This was then inserted into the X-ray diffractometer. The monochromatic light source was focused on the centrally positioned flat sample holder. The X-ray detector (or counter) was placed on the circumference of a circle centred on the sample. The schematic features of the X-ray diffractometer are shown in Fig.2.3.5.1.

The supports for the detector and specimen holder are mechanically coupled so that the rotation of the detector through 2θ degrees is accompanied by rotation of the specimen through θ degrees. This is necessary in order to maintain correct focusing conditions. The detector is linked to a flat bed recorder synchronised to the movement of the detector through increasing values of 2θ producing a chart recording of X-ray diffraction intensities in a position proportional to 2θ.

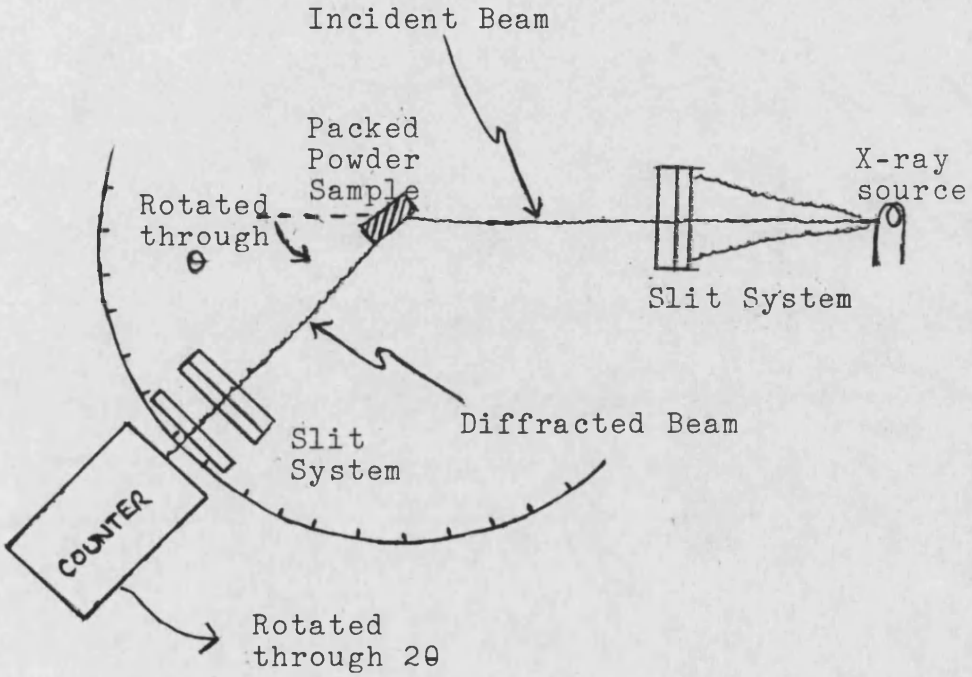

Fig.2.3.5.1 Schematic Diagram of A Powder Plate Diffractometer.

Consequently the 'd' spacings can be calculated by use of the Bragg equation.

Intensities of the X-ray maxima are represented as a ratio I/I_{ℓ} where I is the intensity of the maximum corresponding to its indicated 'd' value, and I_{ℓ} is the intensity of the strongest maxima of the pattern. If confirmation of the identity of a powder sample is required, then the 'd' values calculated from the diffraction diagram can be compared with the published 'd' value of a standard listed in the Powder Diffraction File (1975).

2.3.6 CRYSTALLINITY AND POLYMORPHISM

X-ray diffraction patterns for sulphadimidine, sulphamethizole and sulphathiazole, as supplied and after undergoing temperature cycling, were obtained by the powder plate method. All three sulphonamides were subjected to 30 minute cycles of 15 minutes alternate heating and cooling between 30°C and 40°C in distilled water. Results are quoted for 200 cycles, this being the maximum number of cycles each 5 litre batch underwent. In addition sulphamethizole was used to investigate the effect of altering cycle times, as initial studies showed that sulphamethizole exhibited the most marked degree of rounding after all three sulphonamides had been subjected to the same temperature cycling conditions. Results are quoted for a 5 litre batch that underwent the longest period

of heating for the greatest number of cycles - in this case a 60 minute cycle of 50 minutes heating and 10 minutes cooling between 30°C and 40°C for 75 cycles. The effect of altering the solvent was also investigated and results are quoted for a 5 litre batch of sulphamethizole that was subjected to 200 30 minute cycles of 15 minutes alternate heating and cooling between 30°C and 40°C in 95% ethanol.

The 'd' spacings and relative peak intensities calculated from the recordings by use of the Bragg equation are given in Tables 2.3.6.1, 2.3.6.2, and 2.3.6.3, and are compared with the values given by the Powder Diffraction File of the American Society for Testing Materials (1975).

It can be seen that temperature cycling under the stated conditions did not result in any polymorphic changes or any alteration in the crystalline nature of the three sulphonamides. It can therefore be inferred that when less severe conditions are used in temperature cycling, i.e. shorter heating periods and/or fewer cycles, then the crystalline nature of the three sulphonamides will not be altered, nor will there be any polymorphic changes. This will also apply to temperature cycling of sulphamethizole in 95% ethanol.

Sulphadimidine Standard		Sulphadimidine starting material		Sulphadimidine 5L 15/15 200 cycles	
'd' spacing (Å)	Relative Intensity (% max)	'd' spacing (Å)	Relative Intensity (% max)	'd' spacing (Å)	Relative Intensity (% max)
9.45	100	9.31	100	9.31	100
5.82	60	5.79	13	5.81	25
4.80	60	4.78	16	4.80	23
4.44	100	4.46	75	4.47	76
3.60	100	3.58	48	3.59	54
3.32	20	3.38	9	3.38	11
3.19	16	3.19	8	3.19	10
3.11	16	3.06	37	3.13	7

Table 2.3.6.1

'd' Spacings and Relative Peak Intensities of the Major Peaks of Sulphadimidine For the Reference and Experimental X-Ray Diffraction Patterns.

Sulphathiazole Standard		Sulphathiazole starting material		Sulphathiazole 5L 15/15 200 cycles	
'd' spacing (Å)	Relative Intensity (% max)	'd' spacing (Å)	Relative Intensity (% max)	'd' spacing (Å)	Relative Intensity (% max)
5.81	100	5.79	21	5.83	15
5.47	13	5.44	8	5.47	8
4.80	27	4.82	6	4.82	5
4.61	27	4.60	17	4.62	11
4.44	34	4.44	11	4.44	7
4.32	27	4.31	11	4.33	6
4.12	100	4.11	51	4.11	40
4.02	100	4.04	100	4.06	100
3.76	20	3.76	5	3.76	4
3.53	67	3.51	69	3.52	64
3.31	34	3.34	13	3.33	6
2.95	13	2.94	4	2.94	3
2.76	20	2.75	4	2.75	7
2.69	27	2.70	6	2.71	9
2.47	20	2.48	4	2.49	6

Table 2.3.6.2

'd' Spacings and Relative Peak Intensities of the Major Peaks of Sulphathiazole For The Reference and Experimental X-Ray Diffraction Patterns.

Sulphamethizole standard		Sulphamethizole starting material		Sulphamethizole 5L 15/15 200 cycles		Sulphamethizole 5L 50H/10C 75 cycles		Sulphamethizole in 95% Ethanol 2L 15/15 200 cycles	
'd' spacing (Å)	Relative Intensity (% max)	'd' spacing (Å)	Relative Intensity (% max)	'd' spacing (Å)	Relative Intensity (% max)	'd' spacing (Å)	Relative Intensity (% max)	'd' spacing (Å)	Relative Intensity (% max)
10.5	85	10.6	100	10.6	100	10.5	100	10.6	100
7.3	35	7.3	56	7.3	49	7.3	48	7.3	72
5.6	13	5.5	20	5.6	28	5.5	16	5.5	60
5.1	10	5.1	19	5.1	12	5.1	13	5.1	37
4.5	100	4.5	75	4.5	73	4.5	68	4.5	87
4.05	20	4.0	43	4.0	39	4.0	38	4.0	29
3.6	8	3.6	15	3.6	9	3.6	11	3.6	18
3.4	25	3.4	22	3.4	14	3.4	30	3.4	55
3.3	30	3.3	41	3.3	54	3.3	30	3.3	56
3.2	25	3.2	40	3.2	68	3.2	56	3.2	53
2.95	9	2.9	12	2.9	14	2.9	10	2.9	14
2.6	9	2.6	16	2.6	12	2.6	21	2.6	20
2.3	5	2.3	6	2.3	5	2.3	7	2.3	8

Table 2.3.6.3

'd' Spacings and Relative Peak Intensities of the Major Peaks of Sulphmethizole for the Reference and Experimental X-Ray Diffraction Patterns.

2.3.7 INFRA-RED SPECTRA

A potassium bromide/sulphonamide disc was prepared from oven dried potassium bromide and air dried and desiccated sulphonamide. The I.R spectra obtained were qualitatively identical to that of the reference spectra (Sadtler, 1962). The wavelengths of the peaks numbered in Figs.2.3.7.1, 2.3.7.2, and 2.3.7.3 are compared with those of the reference spectra in Tables 2.3.7.1, 2.3.7.2, and 2.3.7.3.

2.3.8 THIN LAYER CHROMATOGRAPHY

TLC identification of sulphonamides and impurities present in the corresponding samples has been previously reported (Tansey, 1969). This method was used for the qualitative identification of sulphanilamide as a potential degradation product of the sulphonamides as a result of temperature cycling.

A silica gel G: water (1:2) slurry was prepared and spread to a depth of 0.25mm on 10cm x 20cm glass plates. The plates were air dried overnight, activated at 105° for one hour in a hot air oven, and then stored in a desiccator over silica gel until cool. Solutions of each of the sulphonamide starting materials, the sulphonamide products and sulphanilamide were prepared in 95% ethanol to give a final concentration of 5mg ml^{-1}. Five 5μl aliquots of each were spotted 4cm from the base of the plates using an Agla micrometer syringe

Fig. 2.3.7.1 Infra-Red Spectrum of Sulphadimidine (Starting Material)

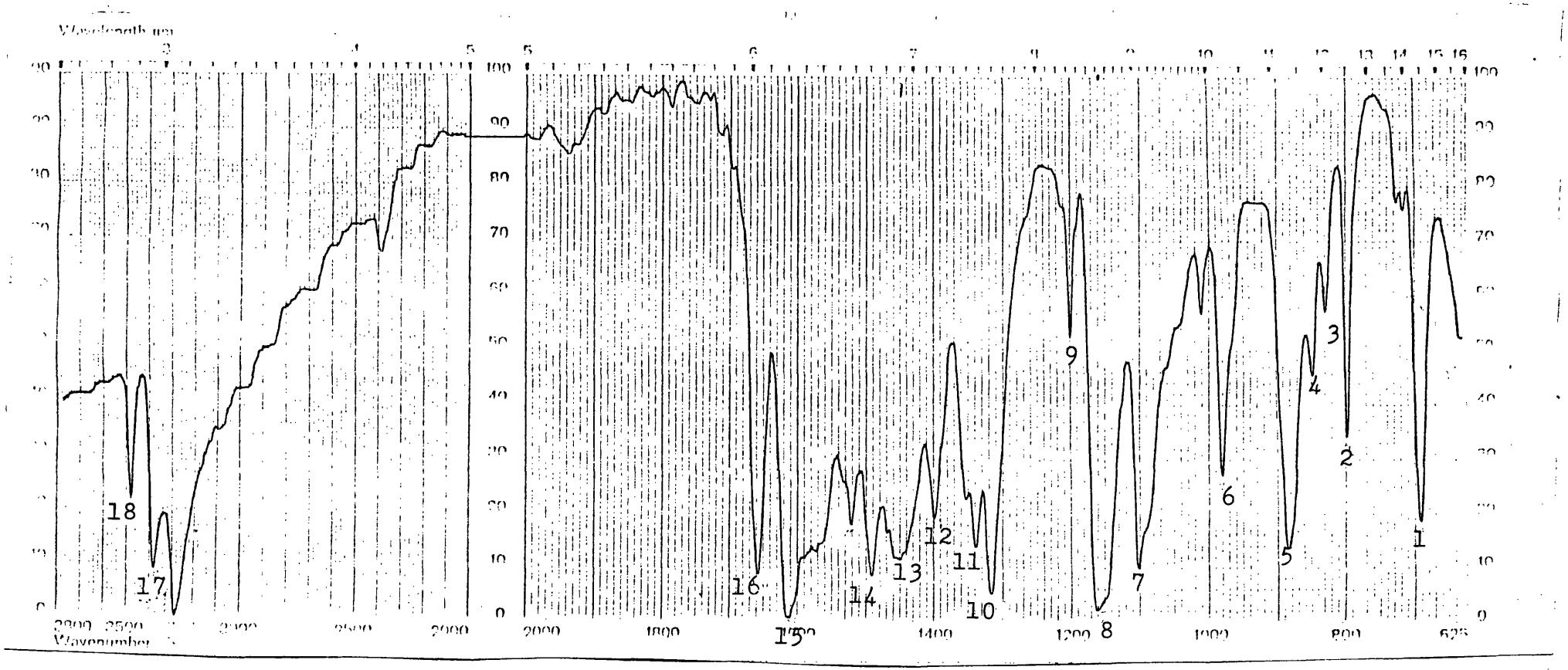

	Wavelength (μm) for peaks No.																	
Peak No.	1	2	3	4	5	6	7	8	9	10	11	12	13	14	15	16	17	18
Reference	14.8	12.7	12.2	12.0	11.5	10.3	9.2	8.8	8.4	7.7	7.6	7.2	7.0	6.8	6.3	6.1	3.1	3.0
Sulphadimidine starting material	14.5	12.5	12.0	11.8	11.3	10.2	9.1	8.7	8.3	7.6	7.5	7.2	6.9	6.7	6.2	6.0	3.05	2.95
Sulphadimidine 5L 15/15 200 cycles	14.5	12.5	12.0	11.8	11.3	10.2	9.1	8.6	8.3	7.6	7.5	7.2	6.9	6.7	6.2	6.0	3.05	2.95

Table 2.3.7.1 Comparison of Infra-Red Spectra Peaks of Sulphadimidine For the Reference and Experimental Spectra.

Fig. 2.3.7.2 Infra-Red Spectrum of Sulphathiazole Starting Material

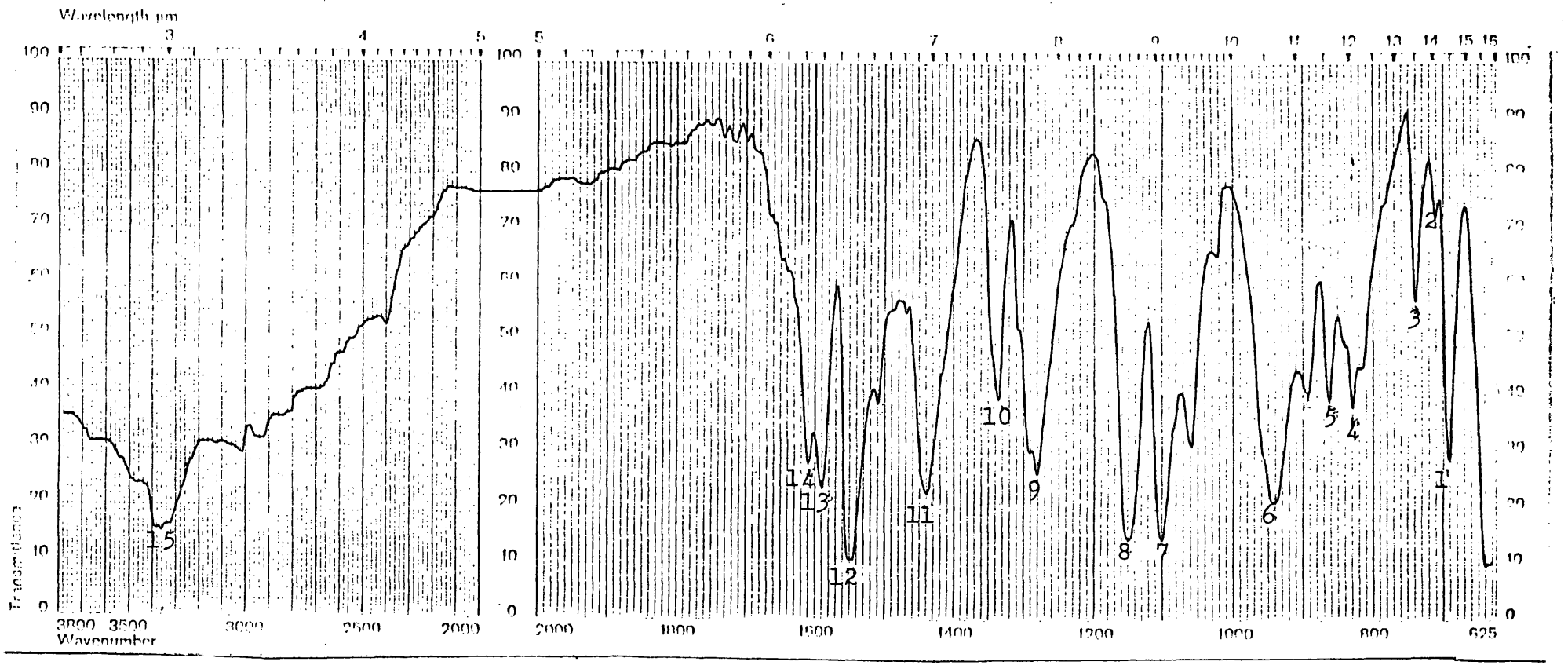

	Wavelength (μm) for peaks No.														
Peak No.	1	2	3	4	5	6	7	8	9	10	11	12	13	14	15
Reference	14.7	14.3	13.7	12.2	11.7	10.7	9.2	8.8	7.9	7.6	7.0	6.5	6.35	6.25	3.0
Sulphathiazole starting material	14.5	14.1	13.5	12.1	11.6	10.6	9.1	8.7	7.8	7.45	6.95	6.45	6.3	6.2	3.0
Sulphathiazole 5L 15/15 200 cycles	14.5	14.1	13.5	12.1	11.6	10.6	9.1	8.7	7.8	7.5	6.95	6.45	6.3	6.2	3.0

Table 2.3.7.2 Comparison of Infra-Red Spectra Peaks of Sulphathiazole For the Reference and Experimental Spectra.

Fig. 2.3.7.3 Infra-Red Spectrum of Sulphamethizole Starting Material

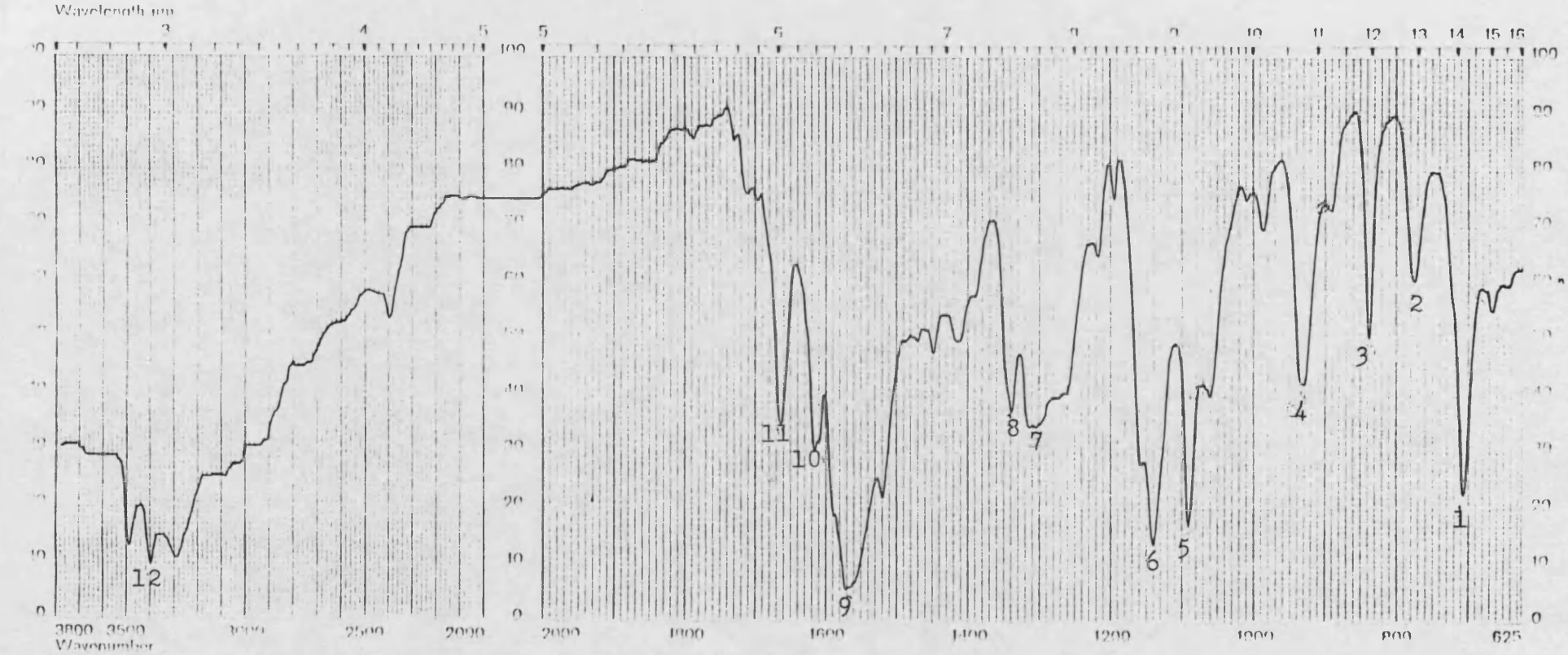

	Wavelength (μm) for peaks No.											
Peak No.	1	2	3	4	5	6	7	8	9	10	11	12
Reference	14.4	13.1	12.1	10.9	9.3	8.9	7.8	7.5	6.45	6.25	6.1	3.0
Sulphamethizole starting material	14.3	13.0	12.0	10.8	9.2	8.8	7.7	7.45	6.4	6.2	6.0	2.95
Sulphamethizole 5L 15/15 200 cycles	14.2	13.0	12.0	10.8	9.2	8.8	7.7	7.45	6.4	6.2	6.0	2.95
Sulphamethizole 5L 50H/10C 75 cycles	14.3	13.0	12.0	10.8	9.2	8.8	7.7	7.45	6.4	6.2	6.0	2.95
Sulphamethizole in 95% Ethanol 15/15 200 cycles	14.3	13.0	12.0	10.8	9.2	8.8	7.7	7.45	6.4	6.2	6.0	2.95

Table 2.3.7.3 Comparison of Infra-Red Spectra Peaks of Sulphamethizole For the Reference and Experimental Spectra.

(Burroughs Wellcome) fitted with a flat needle, and dried for thirty seconds with a hairdryer. Each spot therefore contained 125$\sim$g of material.

The plates were placed vertically in a developing tank lined with Whatman No.1 chromatography paper. The plates were developed using acetone : methanol : diethylamine (9:1:1). The tanks were allowed to stand for two hours before use to ensure equilibration of the solvents with their vapours. They were kept in a dark cupboard to minimise temperature gradient effects on exposure to direct sunlight resulting in R_f value gradients across the plates. When the solvent front reached 10cm from the base line the plates were removed, the solvent front marked and then air dried for one hour in a fume cupboard. The spots were visualised as yellow chromophores by spraying the plate with a solution of 1% w/v 4-dimethylaminobenzaldehyde solution in equal volumes of concentrated hydrochloric acid and absolute ethanol.

Result. From the TLC analysis no degradation of any of the sulphonamides to sulphanilamide was found after undergoing temperature cycling. Reproducible R_f values of 0.40, 0.47, 0.66 and 0.86 were obtained for sulphamethizole, sulphathiazole, sulphadimidine and sulphanilamide respectively.

2.3.9 ASSAY OF SULPHONAMIDES IN AQUEOUS SOLUTION

The analytical methods currently recommended by the B.P., U.S.P. and E.P. use an amperometric titration, or alternatively, the B.P. recommends a non-aqueous potentiometric titration. These methods of analysis are all time consuming and hence, many authors have employed methods involving the Bratton-Marshall reaction, which enables the sulphonamides to be assayed relatively rapidly using visible spectrophotometry (Bican-Fister and Kajganovic, 1964, Brunner, 1972, 1973).

The Bratton-Marshall reaction involves conversion of the sulphonamide to a diazonium salt which reacts with N-1 naphthylethylenediamine to form a coloured azo complex. (See Fig.2.3.9.1). It should be noted that the Bratton-Marshall reaction is only reliable for the determination of unacylated sulphonamides as it requires a free aromatic amine function (Banes and Riggleman, 1971).

In this case an analytical method involving a modified Bratton-Marshall reaction was adopted (Tansey, 1969). The colour produced by the Bratton-Marshall reaction has been found to be stable for several hours, except at high concentration (50 - 70 μg ml^{-1}) where the colour tended to fade slowly owing to the precipitation of the azo dye, at a rate which may be influenced by acidity. At lower concentrations this effect is negligible (Dux and Rosenblun, 1949). This effect occurred when sulphathiazole was used in the concentration range of 1 - 10 μg ml^{-1}. A ten-fold increase in dilution was found to eliminate this phenomenon.

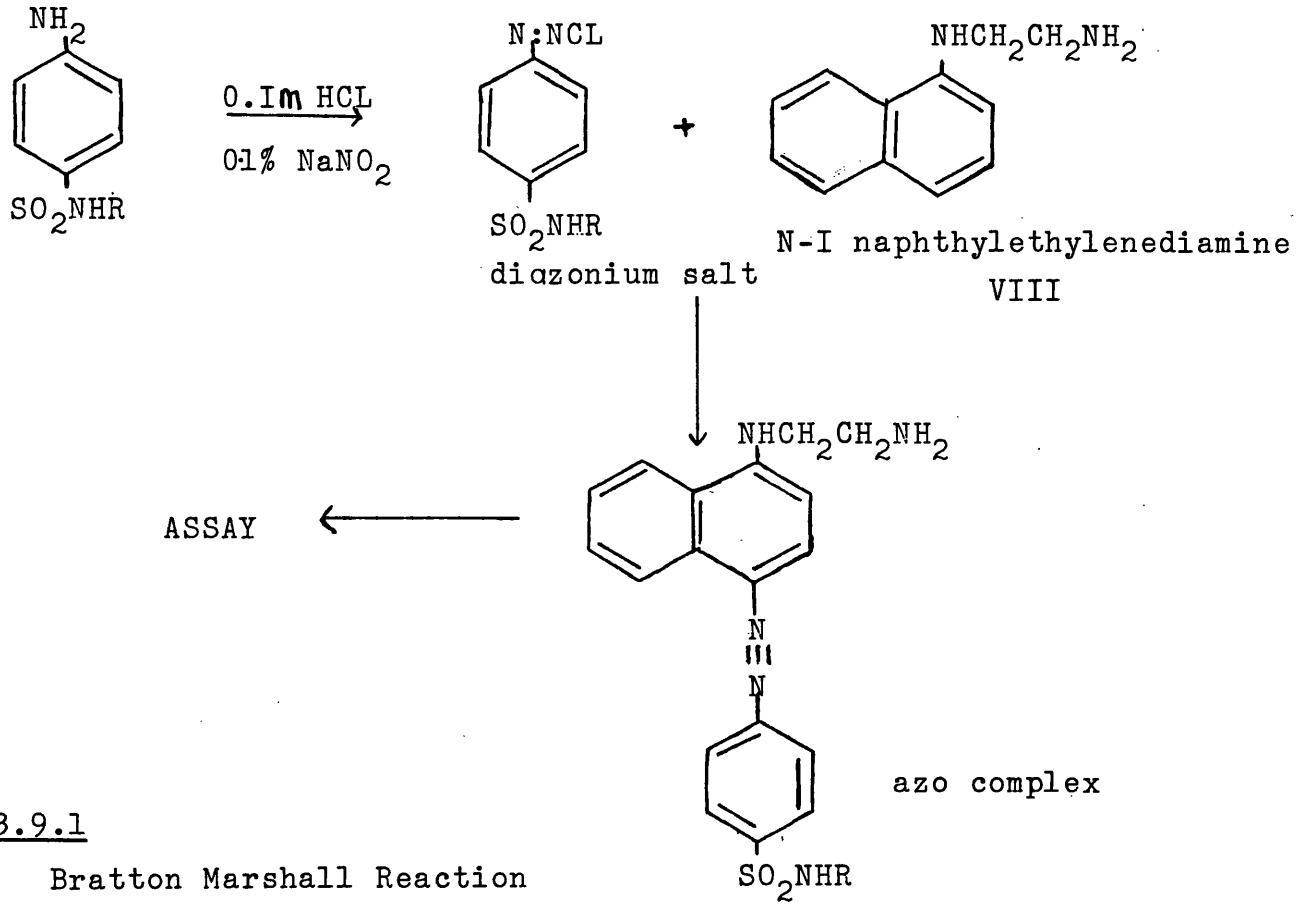

Fig.2.3.9.1

Bratton Marshall Reaction

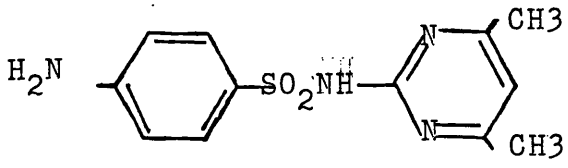

Sulphadimidine
M.Wt 278.3
$C_{12}H_{14}O_2N_4S$

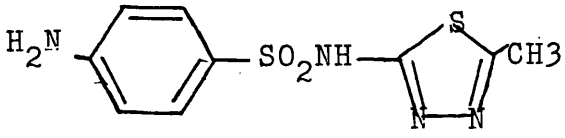

Sulphamethizole
M.Wt 270.3
$C_9H_{10}N_4O_2S_2$

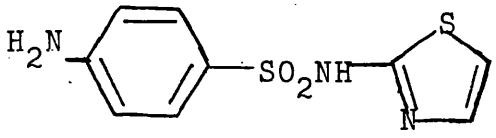

Sulphathiazole
M.Wt 255
$C_9H_{10}N_4O_2S_2$

Fig.2.3.9.2

Chemical Structures of Sulphadimidine, Sulphamethizole and Sulphathiazole.

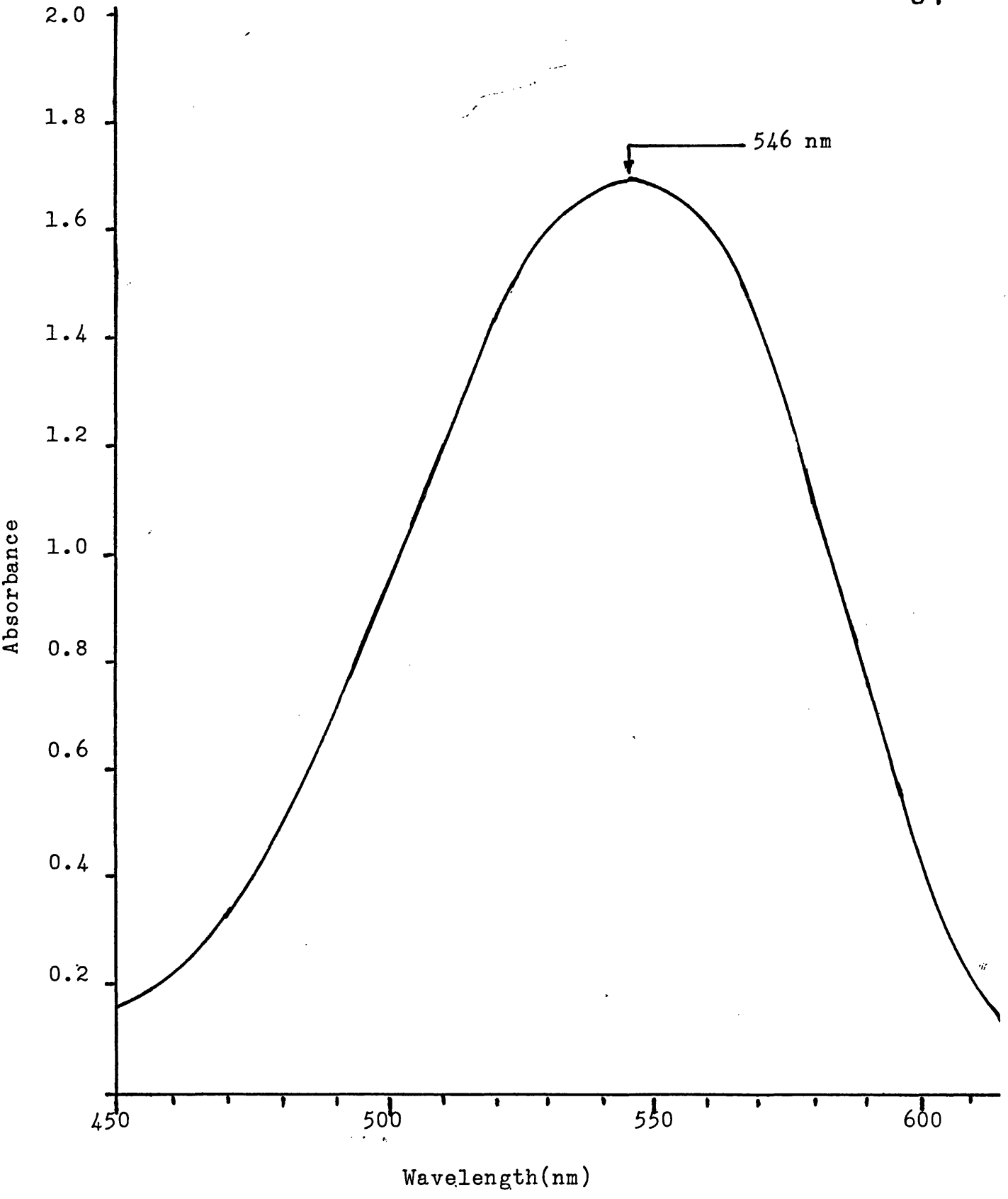

Fig.2.3.9.3. Ultraviolet Absorption Spectrum for the Azo Complex of Sulphadimidine in Distilled Water

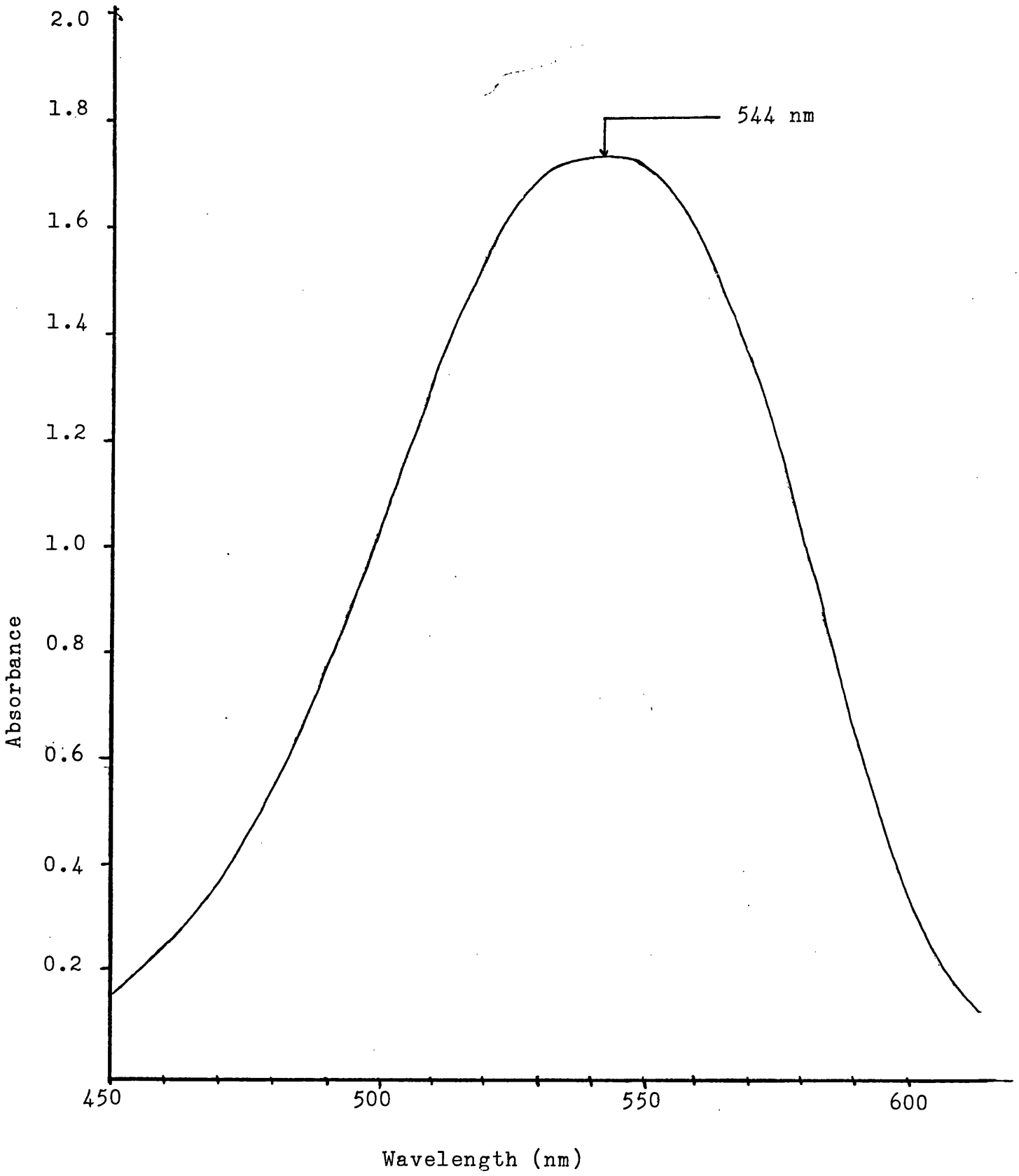

Fig.2.3.9.4 Ultraviolet Absorption Spectrum for the Azo Complex of Sulphamethizole in Distilled Water.

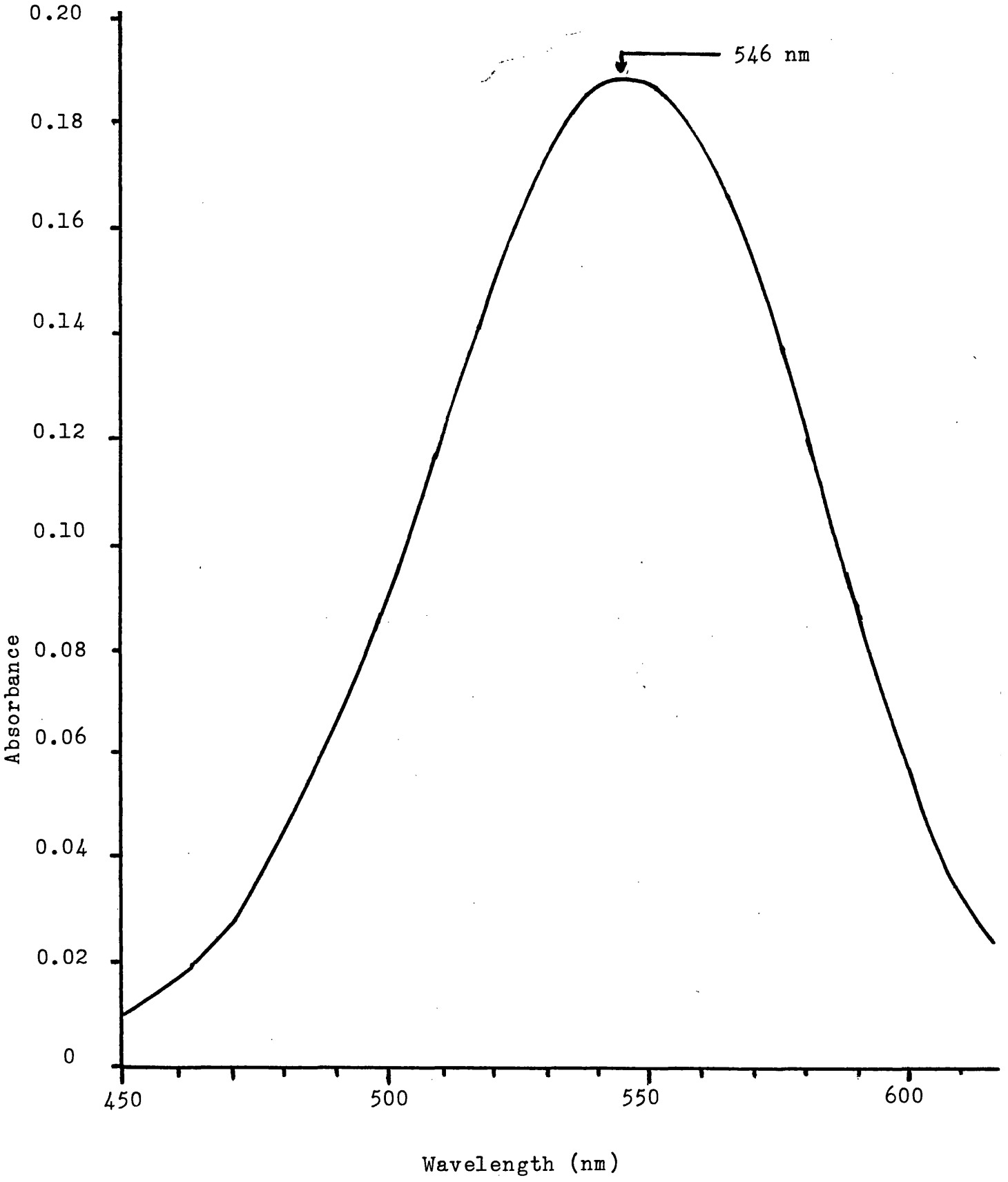

Fig.2.3.9.5 Ultraviolet Absorption Spectrum for the Azo Complex of Sulphathiazole in Distilled Water

Visible absorption spectra were obtained by derivatising 100μg ml^{-1} standard solutions of sulphadimidine and sulphamethizole and a 10μg ml^{-1} standard solution of sulphathiazole. Each of these solutions were subjected to the modified Bratton-Marshall reaction, as described in the following paragraph, and thus a 1 in 10 dilution was scanned over the range 450-610 nm to determine the wavelength of maximum absorption (λmax). The spectra (Figs.2.3.9.3, 2.3.9.4 and 2.3.9.5) showed an absorbance maxima of 544nm for sulphamethizole and 546nm for sulphathiazole and sulphadimidine. The calibration curve and quantitative determinations for each sulphonamide were carried out at their respective λmax values.

Adherence to the Beer-Lambert Law. A stock solution of each sulphonamide was prepared by dissolving 100 mg of sulphonamide in about 750 mls of distilled water and making up to one litre in a volumetric flask. From this stock solution a series of aqueous dilutions were performed to give standard solutions of 10 - 100μg ml^{-1} for sulphadimidine and sulphamethizole, and 1 - 10μg ml^{-1} for sulphathiazole. One ml of each of these solutions was pipetted into a 10 ml volumetric flask, covered with aluminium foil to protect the solution from light. To each was added 1 ml of 0.1M hydrochloric acid and 1 ml of 0.1% w/v aqueous sodium nitrite solution. Each flask was then shaken. Five minutes later 1 ml of 2% w/v aqueous ammonium sulphamate solution was added, followed after a further seven minutes by 1 ml of 0.1% w/v aqueous N-1-naphthylethylenediamine solution. Each solution was made

Sulphadimidine Concentration ($\mu g\ ml^{-1}$)	Absorbance of Azo Complex of Sulphadimidine at 546 nm	
	A	B
10	1.69	1.65
9	1.55	1.54
8	1.38	1.38
7	1.21	1.20
6	1.06	1.04
5	0.89	0.88
4	0.73	0.71
3	0.56	0.55
2	0.37	0.36
1	0.22	0.22

			Analysis of Pooled Data
Slope	0.1648	0.1631	0.1640
$\pm$ SE Slope	1.291×10^{-3}	1.993×10^{-3}	1.568×10^{-3}
r	0.9998	0.9994	0.9996
Intercept	5.993×10^{-2}	5.600×10^{-2}	5.767×10^{-2}
$\pm$ SE Intercept	8.013×10^{-3}	1.237×10^{-2}	9.728×10^{-3}

Table 2.3.9.1 Verification of Beer-Lambert Relationship for Sulphadimidine in Aqueous Solution at 546 nm

(r is the Correlation Coefficient)

($t_{calc} = 0.716$; $t_{tab} = 2.12$; $n = 20$; $p = 0.05$)

Sulphamethizole Concentration ($\mu g\ ml^{-1}$)	Absorbance of Azo Complex of Sulphamethizole at 544 nm	
	A	B
10	1.73	1.72
9	1.59	1.58
8	1.43	1.41
7	1.26	1.25
6	1.10	1.10
5	0.92	0.91
4	0.76	0.73
3	0.56	0.55
2	0.37	0.36
1	0.23	0.22

			Analysis of Pooled Data
Slope	0.1701	0.1702	0.1702
$\pm$ SE Slope	2.132×10^{-3}	2.116×10^{-3}	2.073×10^{-3}
r	0.9994	0.9994	0.9994
Intercept	5.933×10^{-2}	4.667×10^{-2}	5.300×10^{-2}
$\pm$ SE Intercept	1.323×10^{-2}	1.313×10^{-2}	1.286×10^{-2}

Table 2.3.9.2. Verification of Beer-Lambert Relationship for Sulphamethizole in Aqueous Solution at 544 nm
(r is the Correlation Coefficient)

($t_{calc} = 0.033$; $t_{tab} = 2.12$; $n = 20$; $p = 0.05$)

Sulphathiazole Concentration ($\mu g\ ml^{-1}$)	Absorbance of Azo Complex of Sulphathiazole at 546 nm	
	A	B
1	0.205	0.205
0.9	0.184	0.184
0.8	0.161	0.166
0.7	0.144	0.145
0.6	0.129	0.128
0.5	0.106	0.106
0.4	0.082	0.083
0.3	0.060	0.061
0.2	0.040	0.038
0.1	0.021	0.020

			Analysis of Pooled Data
Slope	0.2047	0.2073	0.2060
$\pm$SE Slope	2.994×10^{-3}	2.545×10^{-3}	2.588×10^{-3}
r	0.9991	0.9994	0.9994
Intercept	6.000×10^{-4}	-4.000×10^{-4}	1.000×10^{-4}
$\pm$SE Intercept	1.858×10^{-3}	1.579×10^{-3}	1.606×10^{-3}

Table 2.3.9.3 Verification of Beer-Lambert Relationship for Sulphathiazole in Aqueous Solution at 546 nm.

(r is the Correlation Coefficient)

($t_{calc} = 0.662$; $t_{tab} = 2.12$; $n = 20$; $p = 0.05$)

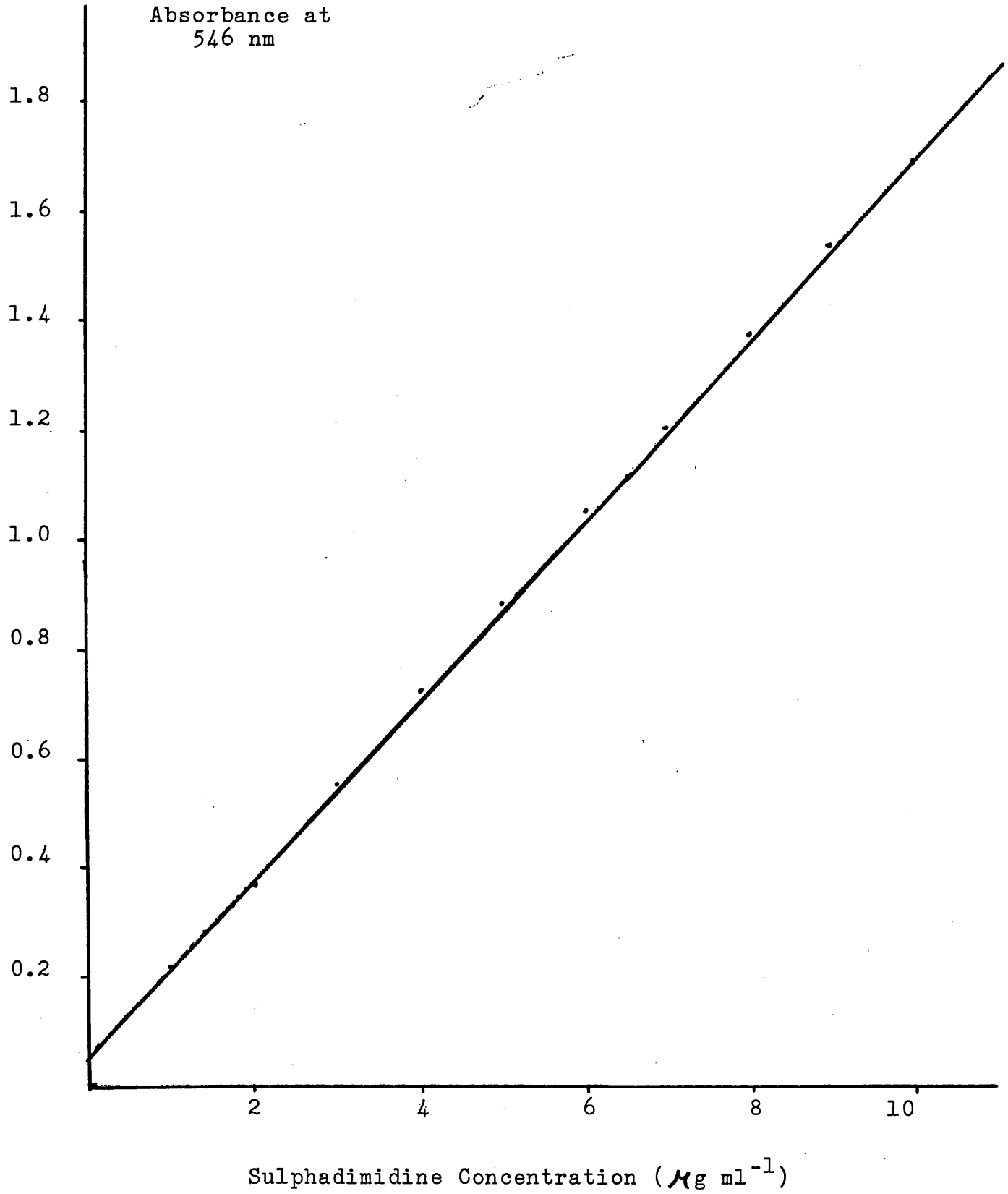

Fig.2.3.9.6 Beer-Lambert Calibration Curves for Sulphadimidine Azo Complex Absorbance at 546 nm (Aqueous)

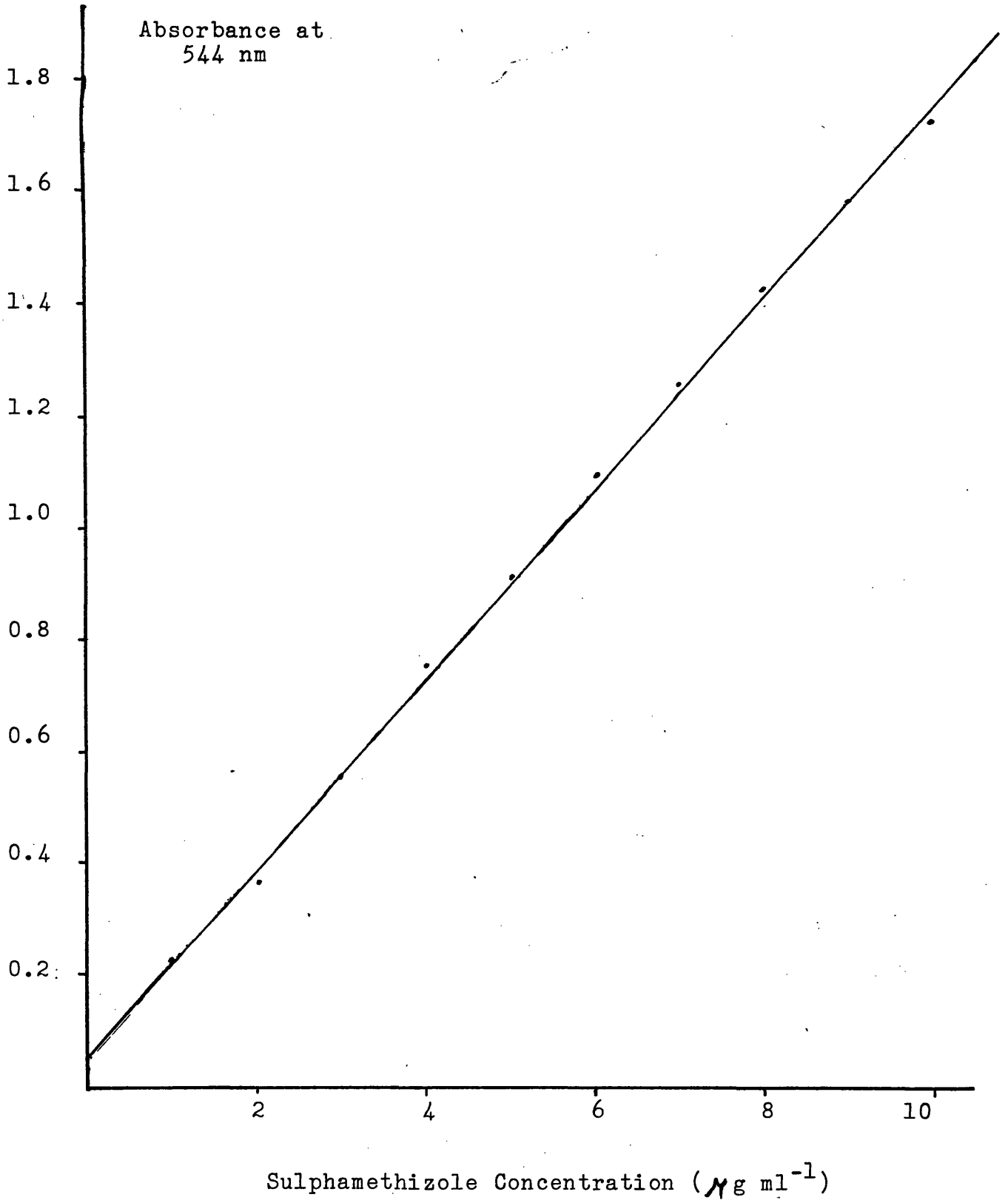

Figure 2.3.9.7 Beer-Lambert Calibration Curves for Sulphamethizole Azo Complex Absorbance at 544 nm (Aqueous)

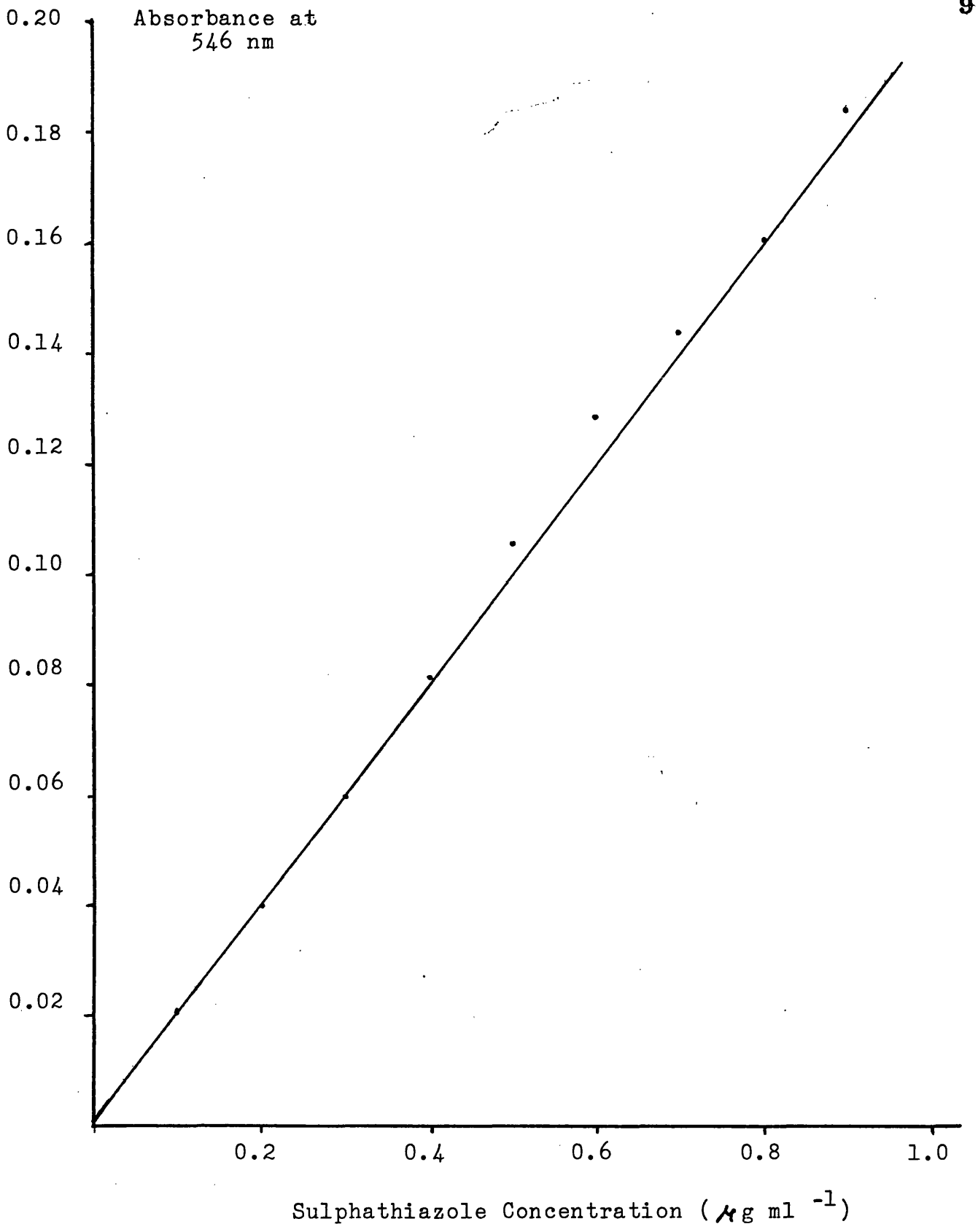

Fig.2.3.9.8 Beer-Lambert Calibration Curves for Sulphathiazole - Azo Complex Absorbance at 546 nm (Aqueous)

up to 10 ml. with distilled water, thereby effecting a 1 in 10 dilution of the original standard sulphonamide solution. The flasks were then shaken and left in the dark for fifteen minutes to allow full colour development. A blank was prepared in the same manner omitting the sulphonamide solution. The absorbance value obtained appeared to be constant over a two minute period. The results shown in Tables 2.3.9.1, 2.3.9.2 and 2.3.9.3 and Figs. 2.3.9.6, 2.3.9.7 and 2.3.9.8 for the determinationsverify that the Beer-Lambert Law is obeyed. Comparison of the duplicates by a Student 't' test (Appendix I) shows them not to be significantly different. The duplicate data was consequently pooled and submitted to linear least-squares regression analysis to provide the calibration line used in all subsequent aqueous sulphonamide determinations. The absorption coefficients $E^{1\%}_{1cm}$ and the molar absorption coefficients ε were calculated using the following equations:-

$$E^{1\%}_{1cm} = \frac{A}{C\ell} \quad \text{.....(18)}$$

where A = absorbance

C = percentage concentration

ℓ = 1cm path length of cell

and $\varepsilon = \frac{A}{C_m \ell}$ .....(19)

where A = absorbance

C_m = molar concentration

ℓ = path length of cell = 1cm

and found to be 1640.0 and 45641.2 respectively for the azo complex of sulphadimidine, 1702.0 and 46005.06 for the azo complex of sulphamethizole, and 2060 and 52591.8 for the azo complex of sulphathiazole.

2.3.10 ASSAY OF SULPHAMETHIZOLE IN 95% ETHANOL

Basically the same analytical procedure was employed for the analysis of sulphamethizole in 95% ethanol. Visible absorption spectra were obtained from a 100 μg ml^{-1} standard solution of sulphamethizole in 95% ethanol which had undergone the modified Bratton-Marshall reaction, and thus a 1 in 10 dilution. This was scanned over the range 450 - 610 nm to determine λmax. The spectra (Fig.2.3.10.1) showed an absorbance maximum at 544 nm and hence the calibration curve and quantitative determinations for sulphamethizole in 95% ethanol were carried out at this wavelength.

Adherence to the Beer-Lambert Law. A stock solution of sulphamethizole was prepared by dissolving 100 mg of sulphamethizole in about 75 mls of 95% ethanol and making up to 100 ml in a volumetric flask. From this stock solution a series of dilutions were performed to give standard solutions of 10 to 100 μg ml^{-1} of sulphamethizole in 95% ethanol. One ml of each of these solutions was pipetted into a 10 ml volumetric flask and treated as before. Each solution was made up to volume with distilled water and the flasks were left in the dark for fifteen minutes to allow full colour development. A blank was prepared in the same manner excluding sulphamethizole but including 1 ml of 95% ethanol. The absorbance values obtained appeared constant over a two minute period. The results shown

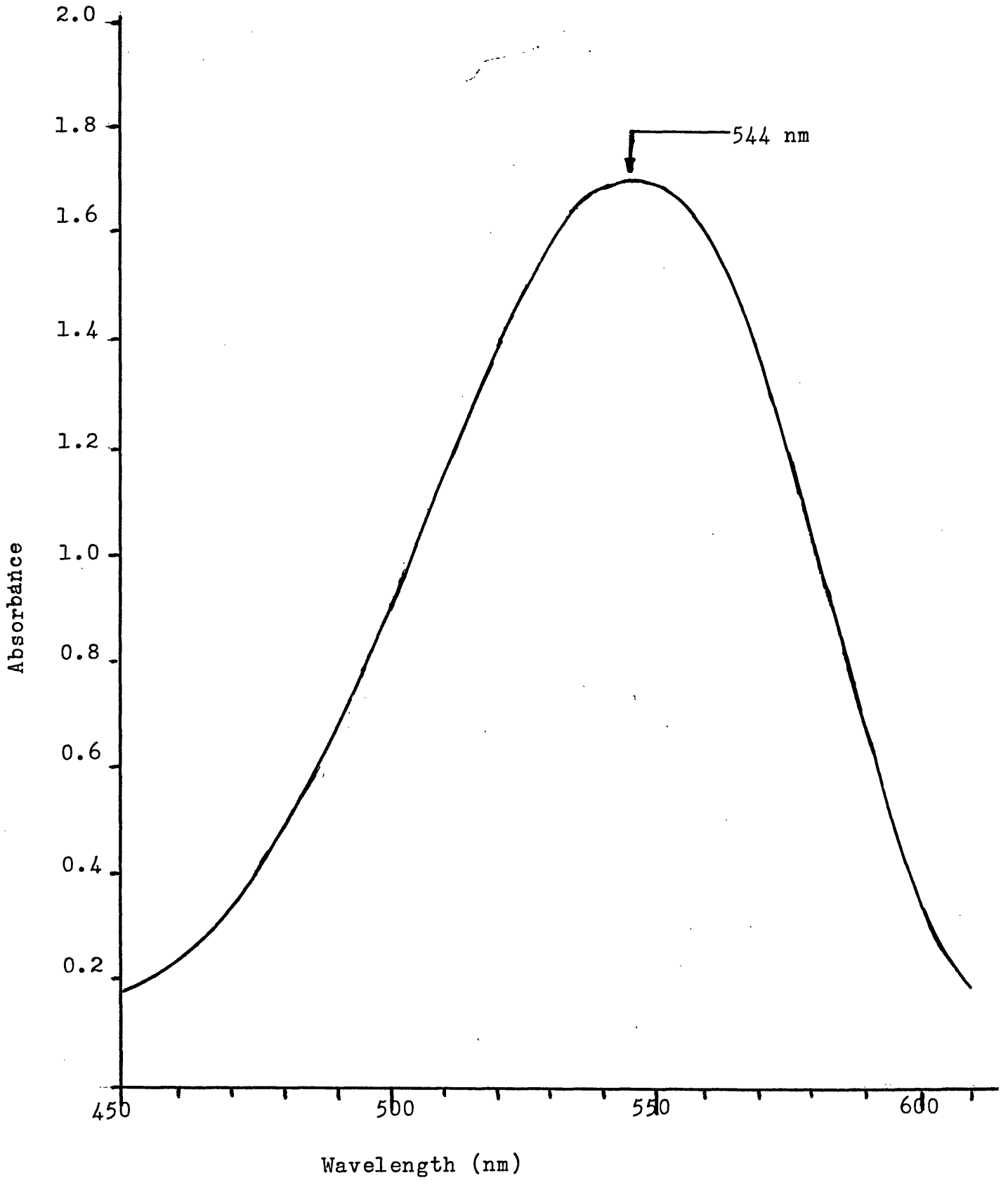

Fig. 2.3.10.1 Ultraviolet Absorption Spectrum for the Azo Complex of Sulphamethizole in 95% Ethanol

Sulphamethizole Concentration in 95% Ethanol ($\mu g\ ml^{-1}$)	Absorbance of Azo Complex of Sulphamethizole at 544 nm	
	A	B
10	1.80	1.79
9	1.62	1.61
8	1.45	1.44
7	1.27	1.27
6	1.10	1.09
5	0.91	0.91
4	0.73	0.73
3	0.55	0.55
2	0.37	0.37
1	0.20	0.20

Analysis of Pooled Data			
Slope	0.1785	0.1772	0.1779
$\pm$ SE Slope	5.845×10^{-4}	5.488×10^{-4}	5.348×10^{-4}
r	0.9999	0.9999	0.9999
Intercept	1.800×10^{-2}	2.133×10^{-2}	1.967×10^{-2}
$\pm$ SE Intercept	3.627×10^{-3}	3.405×10^{-3}	3.319×10^{-3}

Table 2.3.10.1 Verification of Beer-Lambert Relationship for Sulphamethizole in 95% Ethanol at 544 nm (r is the Correlation Coefficient)

($t_{calc} = 1.621$; $t_{tab} = 2.12$; $n = 20$; $p = 0.05$)

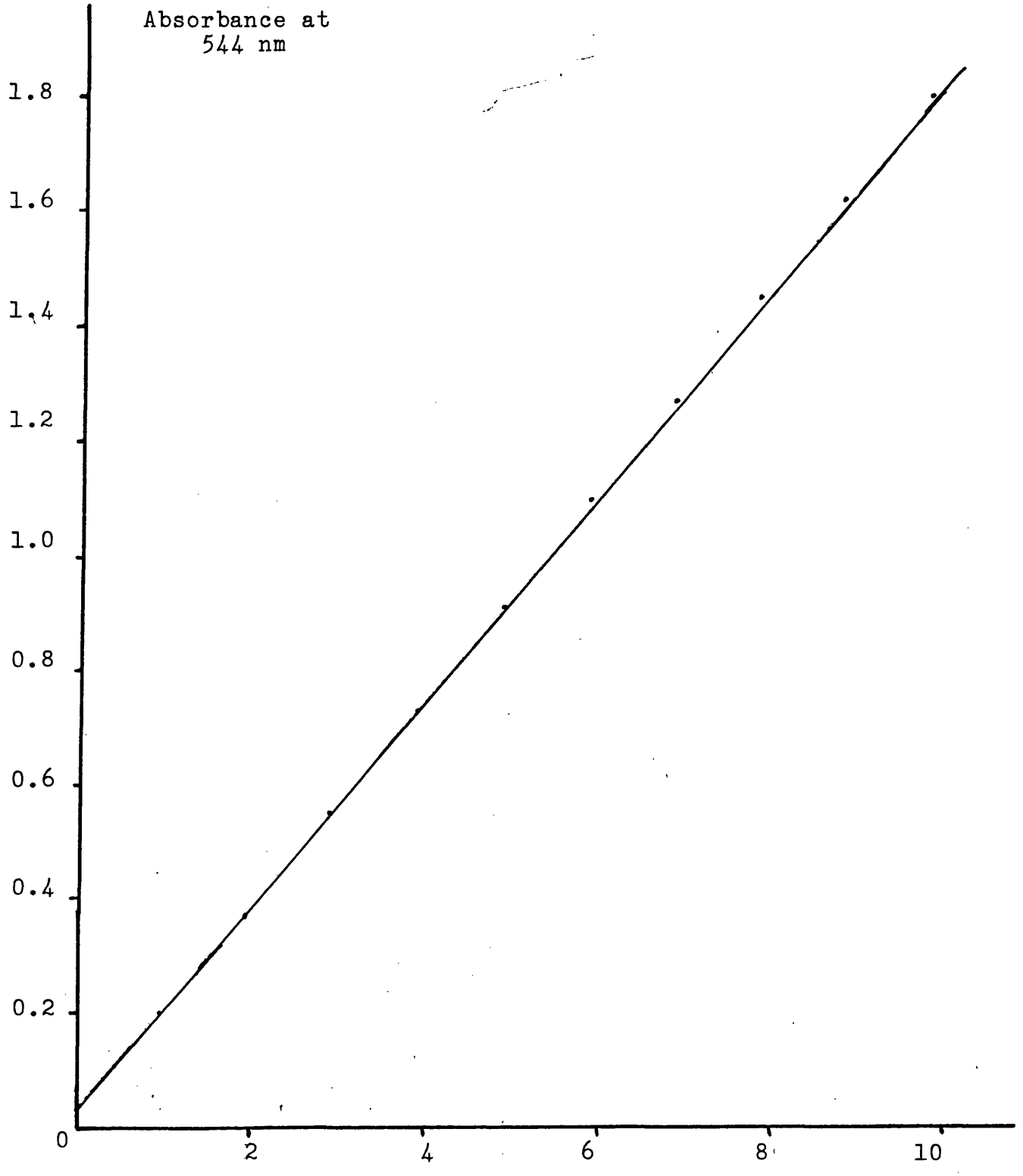

Fig.2.3.10.2 Beer-Lambert Calibration Curves for Sulphamethizole Azo Complex Absorbance at 544 nm in 95% Ethanol

in Table 2.3.10.1 and Fig.2.3.10.2 for the determinations verify that the Beer-Lambert Law was obeyed. Comparison of the duplicates by a Student 't' test (Appendix I) showed them not to be significantly different. The duplicate data was consequently pooled and submitted to linear least-squares regression analysis to provide the equation for the calibration line used in all subsequent sulphamethizole in 95% ethanol determinations. The absorption coefficient, $E^{1\%}_{1cm}$ and the molar absorption coefficient, ε were calculated as before and found to be 1779.0 and 48086.37 respectively.

2.3.11 SOLUBILITY OF THE SULPHONAMIDES

The saturation solubilities of sulphadimidine, sulphamethizole and sulphathiazole in distilled water and also of sulphamethizole in 95% ethanol were determined.

Method. Equilibrium was approached from the supersaturated state. Excess material was added to 30 mls of solvent previously equilibrated to 70°C, and rapidly stirred. The solute and solvent mixture was held at this temperature for four hours, with constant stirring. The temperature was then brought down slowly to the required temperature and held at this temperature for 48 hours. Samples were removed at 24 and 48 hours after reaching the required temperature. Before assay, the mixture was allowed to stand for one hour still at

constant temperature to enable any finely dispersed solids to settle. Removal of the sample was performed using a pre-warmed sintered glass tube and a pre-warmed pipette. A weighed quantity, after suitable dilution, was analysed as previously described. The temperature at the time of sampling was recorded. Agreement between the two samples was taken to show equilibrim had been reached. Tables 2.3.11.1, 2.3.11.2, 2.3.11.3 and 2.3.11.4 and Figs. 2.3.11.1 and 2.3.11.2 show the relationship between the saturation solubilities of the sulphonamides and temperature. Figs. 2.3.11.3 and 2.3.11.4 show this data expressed as van't Hoff plots showing curvilinear profiles. Both the solubility profile and the van't Hoff plots show that the solubility of all three sulphonamides in distilled water and that of sulphamethizole in 95% ethanol increased as the temperature was raised. However this increase is less marked in the case of sulphadimidine.

Temperature ^{o}C	$^{1}/_{T}$ ($\times 10^{-3} K^{-1}$)	Equilibrium Concentration of Sulphadimidine in Distilled Water ($\mu g\ ml^{-1}$)
23.0	3.378	339.8
28.5	3.317	391.7
33.0	3.268	446.5
38.5	3.210	522.8
48.0	3.115	649.6
54.0	3.058	733.1

Table 2.3.11.1 Influence of Temperature on the Equilibrium Solubility of Sulphadimidine in Distilled Water.

Temperature °C	$^1/_T$ (x $10^{-3}K^{-1}$)	Equilibrium Concentration of Sulphathiazole in Distilled Water ($\mu g\ ml^{-1}$)
23.0	3.378	507.3
28.0	3.322	628.6
33.0	3.268	774.3
38.0	3.215	968.4
42.5	3.170	1199.0
52.0	3.077	1818.0

Table 2.3.11.2 Influence of Temperature on the Equilibrium Solubility of Sulphathiazole in Distilled Water

Temperature °C	$^1/_T$ (x 10^{-3} K^{-1})	Equilibrium Concentration of Sulphamethizole in Distilled Water ($\mu g\ ml^{-1}$)
23.5	3.373	443.0
28.0	3.322	607.5
32.5	3.273	766.2
37.5	3.221	971.8
42.0	3.175	1171.6
50.0	3.096	1653.3

Table 2.3.11.3 Influence of Temperature on the Equilibrium Solubility of Sulphamethizole in Distilled Water

Temperature °C	$^1/_T$ (x $10^{-3}K^{-1}$)	Equilibrium Concentration of Sulphamethizole in 95% Ethanol ($\mu g\ ml^{-1}$)
23.5	3.373	13,318
28.0	3.322	16,885
33.0	3.268	19,739
38.0	3.215	24,733
44.5	3.150	31,868
56.0	3.040	44,710

Table 2.3.11.4 Influence of Temperature on the Equilibrium Solubility of Sulphamethizole in 95% Ethanol

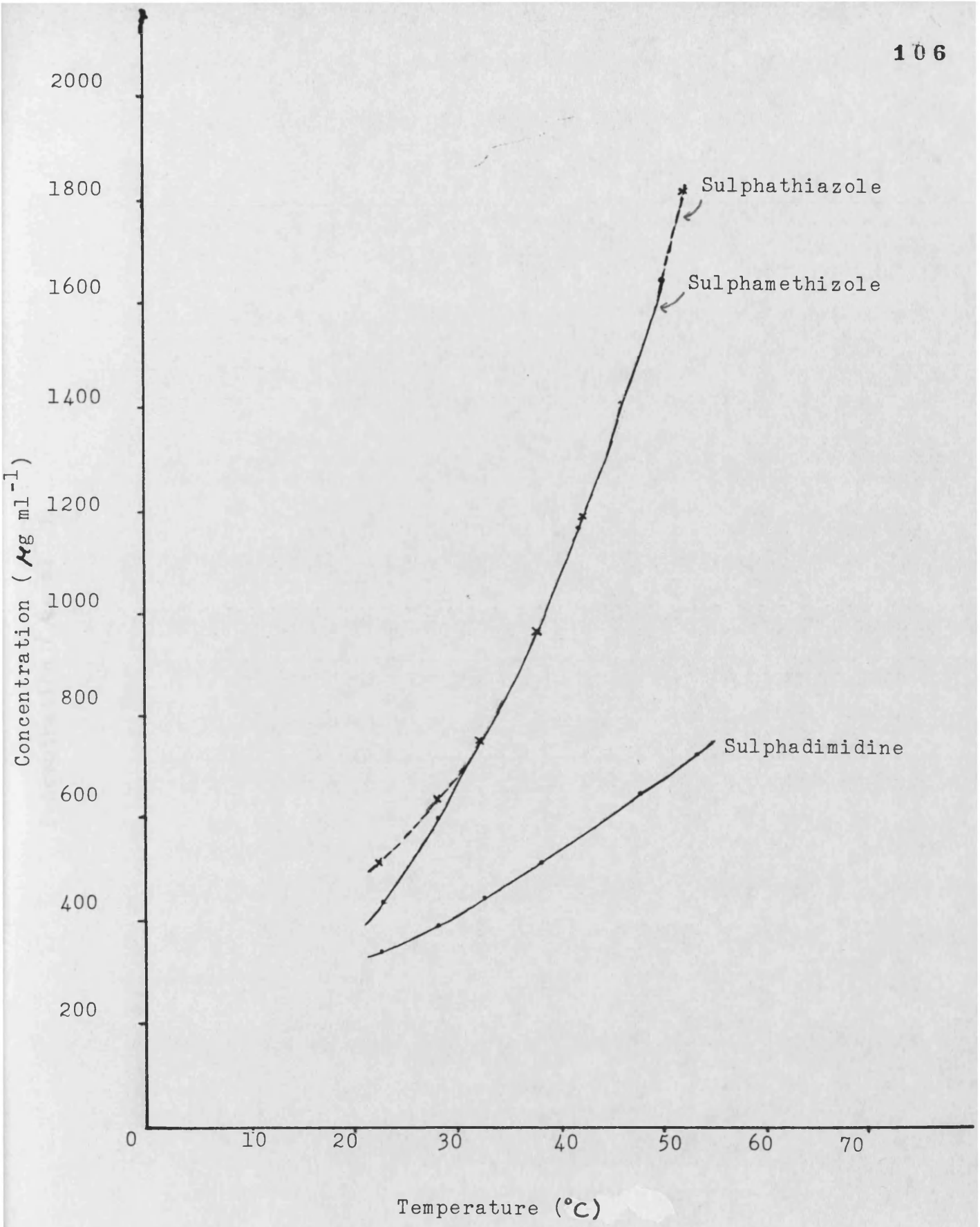

Fig.2.3.11.1 Solubility Profile of Sulphadimidine, Sulphamethizole and Sulphathiazole in Distilled Water.

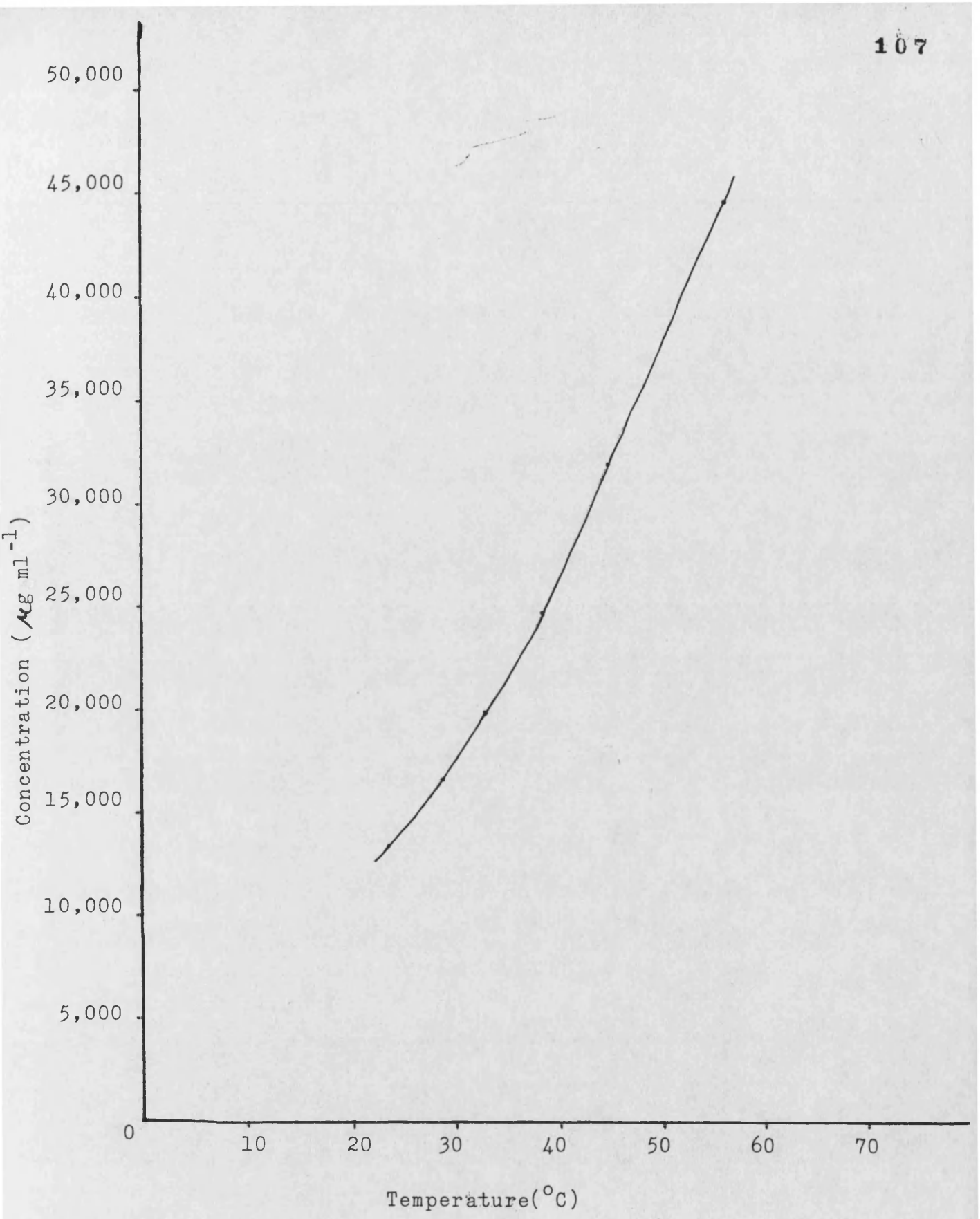

Fig.2.3.11.2 Solubility Profile of Sulphamethizole in 95% Ethanol

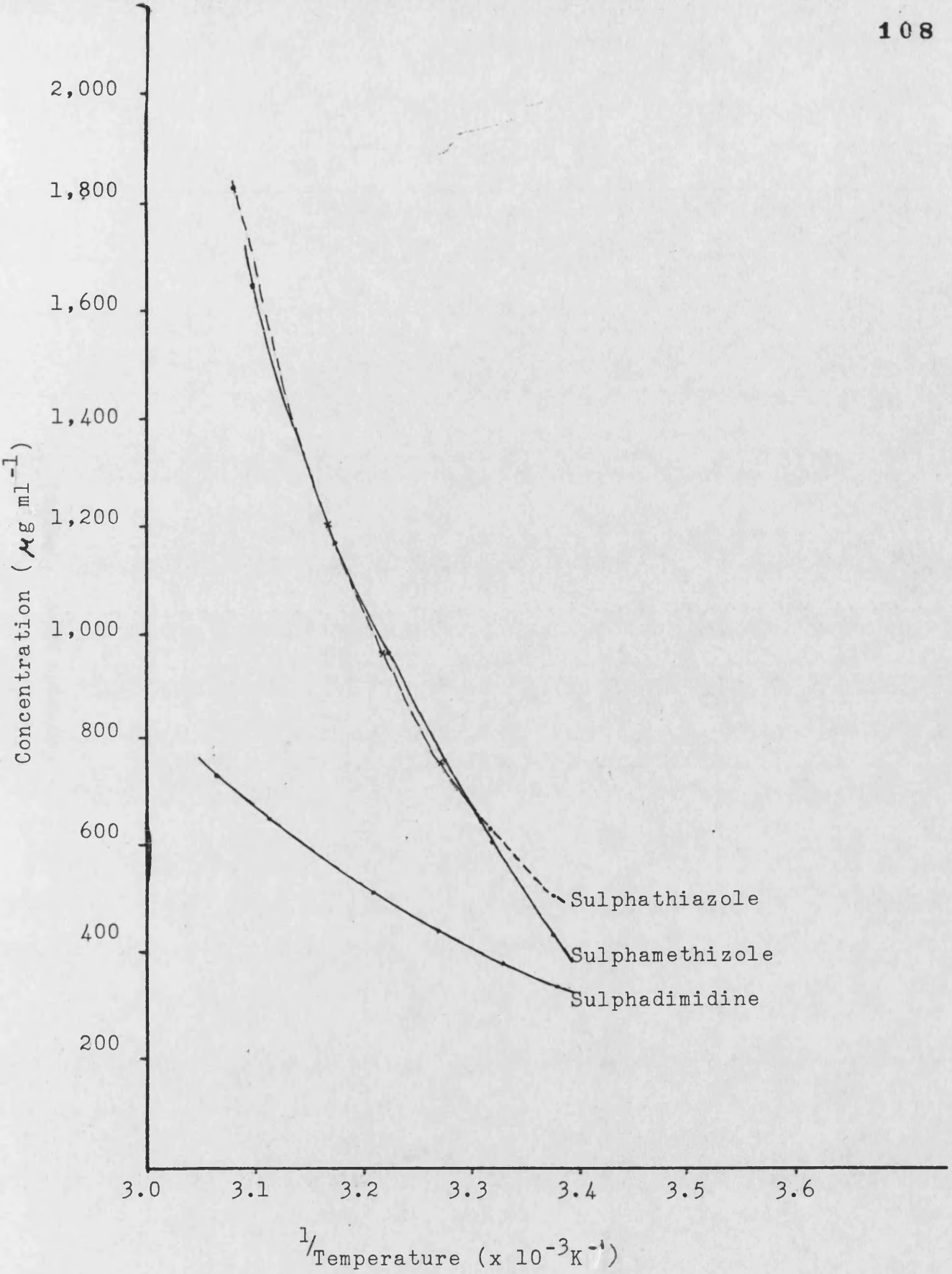

Fig.2.3.11.3. Van't Hoff Plot of Saturation Solubility of Sulphadimidine, Sulphamethizole and Sulphathiazole in Distilled Water

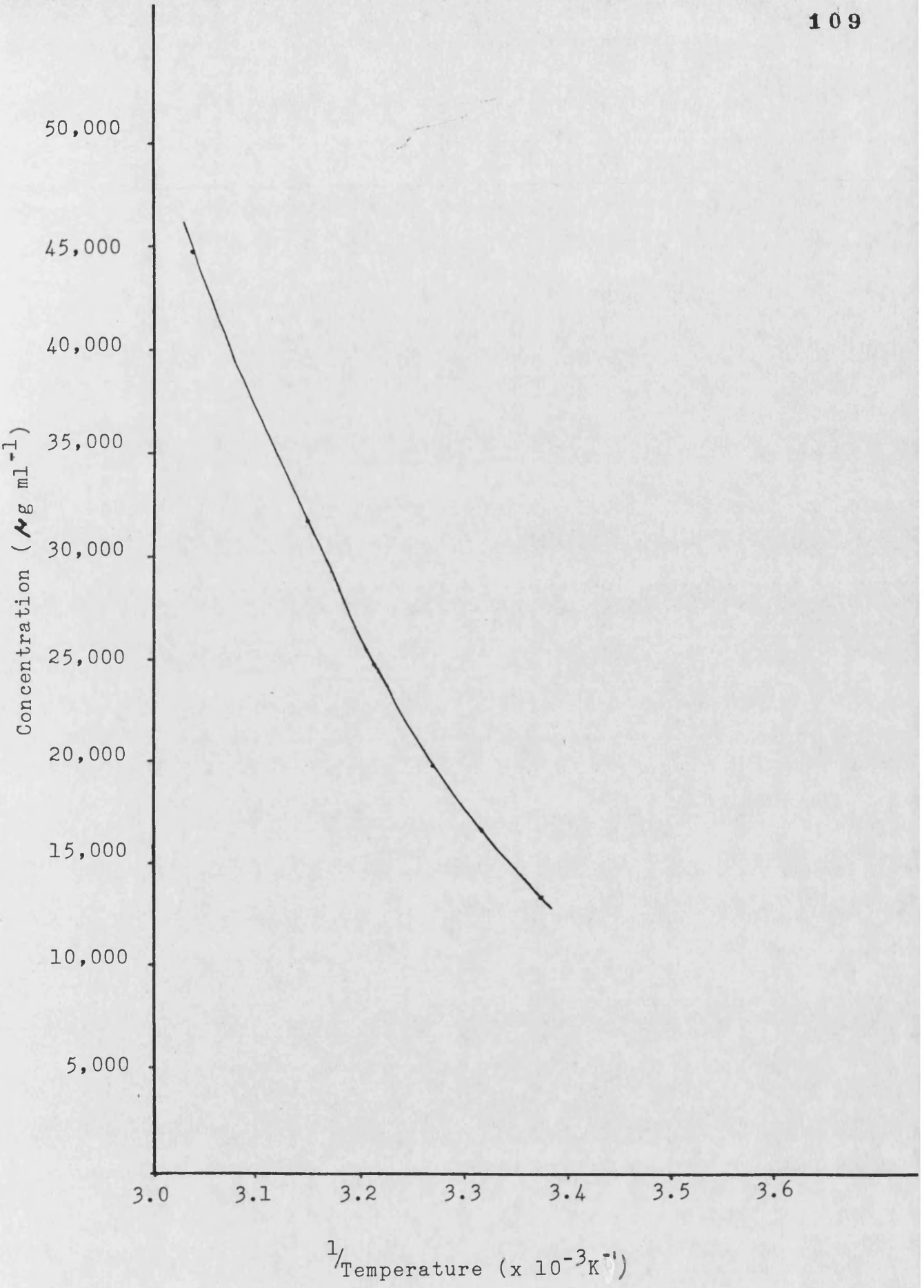

Fig.2.3.11.4 Van't Hoff Plot of Saturation Solubility of Sulphamethizole in 95% Ethanol

2.4 COMPUTER PROGRAMS

2.4.1 Magiscan Image Analysis System

Initially shape assessment was carried out using the Magiscan Image Analysis System. A Fortran program was written to facilitate this. By means of a light pen a point on the crystal surface could be positioned on the screen. On the positioning of another point a circle was generated between the two points so that they formed the diameter of the circle. The circle could then be accepted or rejected. This operation was then repeated so that the inscribed and circumscribed circle of the selected crystal appeared on the screen. If both circles were accepted the resulting ratio was generated and appeared on the screen. The ratios were stored in memory and printed out after 100 crystals had been analysed, together with the mean and standard deviation of the ratios.

This proved to be a relatively fast method, but the cost of the Magiscan prevented its use as a routine quality control method. Therefore an alternative image analysis system was sought that was based on a microcomputer and was therefore within financial reach of most research workers.

2.4.2 Microsight 1 Image Analysis System - "CRYSTAL"

A program "CRYSTAL" was written (J.Hart, Bath) for use in conjunction with the Digithurst Microeye System and its associated Microsight and Microscale software. The software was modified in order to allow the collection of data from ten screens on each image storage disc, as opposed to four screens. Thus by using ten image storage discs it was possible to collect and process 100 crystal images from each experimental treatment. The screen files saved in this way could be reloaded in the computer and processed subsequently to determine the ratio of the radii of the inscribed and circumscribed circles.

The program "CRYSTAL" provides a semi-automatic image analysis method. A cursor appears on the screen containing the crystal image; this may be moved to the required position on the image outline and saved by indicating with a cross. The cursor may then be repositioned to give a second point. There is a facility to accept or reject the position of the cursor. Acceptance of the second point will generate a circle with the two cursor positions as a diameter. This circle may be accepted or rejected. This operation is repeated to generate a second circle. The user positions the cursor appropriately in order to generate the inscribed and circumscribed circle for each crystal image. Acceptance of the second circle

will initiate the calculation of the ratio of the radii of the inscribed to circumscribed circles and this value appears on the screen. The area and perimeter of the crystal image may also be generated at this stage. The screen image of the crystal may be printed out, if desired. The program then proceeds to the next screen file.

When all the screen files have been processed the program calculates the mean and standard deviation of the ratio values. The radii of the inscribed and circumscribed circles, the resulting ratio and also the area and perimeter of each individual crystal image appear on the screen. These, together with the mean and standard deviation of the ratios, may be printed out if required or alternatively stored on disc for future statistical calculations.

2.4.3 Fractal Dimension

The fractal dimensions of the crystals were determined using the Digithurst Microsight 1 Image Analysis System and its associated software together with a specially written program "FRACTAL" (J.Hart, Bath). The same 100 screen files containing the digitised crystal images collected for the "CRYSTAL" program were analysed by "FRACTAL". After each image is loaded into the computer the digitised crystal

image is displayed on the video screen. A cross also appears on the screen which the operator is required to move by means of the cursor keys to place it within the crystal image. The crystal image is then processed by the computer which counts the total number of steps it takes to "walk" around the perimeter of the crystal for each different step length. The initial step length used was one picture point which was the minimum resolution of the system. The step lengths were then increased using the geometric progression of 1, 2, 4, 8, 16, 32..... etc. and each perimeter estimate recorded. The program ceases to estimate perimeter length of the crystal when the total number of step lengths around the crystal is less than seven. The computer did not provide enough memory space to cope with more than 15 perimeter estimates. It was found by using a geometric progression of step lengths and limiting the minimum number of step lengths to seven this maximum was not exceeded for the crystals studied. It may be necessary to alter these two conditions according to the samples being examined. From these data, estimates of the perimeter length of the crystal for each step length were calculated and a linear regression analysis performed to obtain the slope of the line of best fit for the log "step" length versus log "perimeter" estimate. This graph was then plotted on the video screen. The perimeter

estimates, slope, intercept, correlation coefficient and fractal dimension also appear on the screen and this information, together with the graph, was then dumped on the printer and printed out. This operation was repeated for each crystal image. Finally the user is asked if a printout of the mean and standard deviation of the results is required. If affirmative, this information is also printed out. In addition the individual fractal dimensions may be saved on a data file on disc and analysed statistically at a later date.

2.4.4 Validation of 'CRYSTAL' and 'FRACTAL' Programs

Both the 'CRYSTAL' and 'FRACTAL' programs were run using a circle generated by the computer, instead of a crystal image. Both programs gave a value of 1.00 for the I_i / I_c ratio and also for the fractal dimension, which agreed with the expected result in both cases.

2.5 KEY TO ABBREVIATIONS

The following lists the designations used in the Results and Discussion chapter of the thesis to identify each sulphonamide, the batch size and the associated temperature cycling conditions:

Sulphadimidine

The solvent used for each batch was distilled water

SDSM	-	starting material
SD 2L100	-	2 litre batch size, 100 cycles
SD 5L100	-	5 litre batch size, 100 cycles
SD 5L190	-	5 litre batch size, 190 cycles

Sulphathiazole

The solvent used for each batch was distilled water

STSM	-	starting material
ST 2L100	-	2 litre batch size, 100 cycles
ST 5L100	-	5 litre batch size, 100 cycles
ST 5L190	-	5 litre batch size, 190 cycles

Sulphamethizole

The solvent used for each batch was distilled water

SMSM	-	starting material
SM 2L100	-	2 litre batch size, 100 cycles
SM 2L190	-	2 litre batch size, 190 cycles
SM 5L50	-	5 litre batch size, 50 cycles
SM 5L100	-	5 litre batch size, 100 cycles
SM 5L150	-	5 litre batch size, 150 cycles
SM 5L190	-	5 litre batch size, 190 cycles

The above batches of all three sulphonamides (apart from the starting materials) underwent the stated number of 30 minute cycles, each cycle consisting of 15 minutes successive heating and cooling between 30°C and 40°C.

The following 5 litre batches of sulphamethizole in distilled water were prepared with different numbers of cycles of specified duration as indicated:-

SM 20H/10C 50 - 50 thirty minute cycles of twenty minutes heating and ten minutes cooling between 30°C and 40°C.

SM 20H/10C 100 - 100 cycles with the above conditions.

SM 20H/10C 150 - 150 cycles with the above conditions.

SM 20H/10C 200 - 200 cycles with the above conditions.

SM 40H/20C 50 - 50 hourly cycles of forty minutes heating and twenty minutes cooling between 30°C and 40°C.

SM 40H/20C 75 - 75 cycles with the above conditions.

SM 40H/20C 100 - 100 cycles with the above conditions.

SM 50H/10C 50 - 50 hourly cycles consisting of fifty minutes heating and ten minutes cooling between 30°C and 40°C.

SM 50H/10C 75 - 75 cycles with the above conditions.

SM 10H/20C 50 - 50 thirty minute cycles consisting of ten minutes heating and twenty minutes cooling between 30°C and 40°C.

SM 10H/20C 100 - 100 cycles with the above conditions

SM 10H/20C 150 - 150 cycles with the above conditions

SM 20H/40C 50 - 50 hourly cycles consisting of twenty minutes heating and forty minutes cooling between 30°C and 40°C.

SM 20H/40C 75 - 75 cycles with the above conditions.

SM 20H/40C 100 - 100 cycles with the above conditions.

SM 10H/50C 50 - 50 hourly cycles consisting of ten minutes heating and fifty minutes cooling between 30°C and 40°C.

SM 10H/50C 75 - 75 cycles with the above conditions

SM 10H/50C 100 - 100 cycles with the above conditions.

SM 10H/10C 50 - 50 twenty minute cycles consisting of ten minutes successive heating and cooling between 30°C and 40°C.

SM 10H/10C 100 - 100 cycles with the above conditions.

SM 10H/10C 200 - 200 cycles with the above conditions.

The following batches were prepared using 95% ethanol as the solvent. The batch size was 200mls in each case and the batches underwent thirty minute cycles consisting of fifteen minutes successive heating and cooling between 30°C and 40°C.

SMA 50 - 50 cycles with the above conditions.

SMA 100 - 100 cycles with the above conditions.

SMA 150 - 150 cycles with the above conditions.

SMA 200 - 200 cycles with the above conditions.

2.6 SLIDE PREPARATION AND EXAMINATION

A random sample of crystals from the batch being examined was taken and mounted in distilled water on a glass slide. The slide was examined under the microscope by a systematic scanning method to ensure that no field of view was examined more than once, in order to obtain a representative sample of unaggregated crystals.

2.7 INDEX OF PHOTOGRAPHS

The numbers listed in this index correspond to the numbers on the back of the photographs in the plastic wallet at the end of this thesis. Each photograph was taken at a magnification of 600. The photographs show the starting materials and the materials after temperature cycling.

1 - SMSM

2 - SM5L190

3 - SDSM

4 - SD5L190

5 - STSM

6 - ST2L100

RESULTS AND DISCUSSION

3.1 SOLUBILITY STUDIES

In the original work by Nyvlt (1973), very soluble crystalline materials were used, such as urea, sodium nitrate and sodium thiosulphate. These materials all exhibited a rounded crystal habit after undergoing periodic temperature cycling. Nyvlt's hypothesis was that this rounding effect was produced by successive dissolution of the corners of the crystals and deposition on the slower growing faces. It was thought that if this process could be applied to less soluble crystalline compounds, with the same result, it might be useful pharmaceutically for improving the handling and processing characteristics of crystalline solids.

In order to achieve significant dissolution and growth of these less soluble crystalline materials during the temperature cycling process, a crystalline drug material was chosen that had a high temperature coefficient of its solubility in a given solvent. The aqueous solubility data of the sulphonamides appeared to fit this requirement. Three of the sulphonamides were studied: sulphadimidine, sulphamethizole and sulphathiazole. Water was the preferred solvent for this study because of the advantages of it being innocuous, readily available and inexpensive.

The aqueous solubility profiles of sulphamethizole and sulphathiazole with respect to temperature are similar

(see Fig.2.3.11.1). Sulphamethizole has an initial aqueous solubility of 490 μg ml^{-1} at 25°C rising to 1650 μg ml^{-1} at 50°C. Sulphathiazole has an initial solubility of 555 μg ml^{-1} at 25°C rising to 1650 μg ml^{-1} at 50°C. The aqueous solubility profile of sulphadimidine (see Fig.2.3.11.1) shows a less pronounced increase with temperature, having an initial solubility of 355 μg ml^{-1} at 25°C rising to 675 μg ml^{-1} at 50°C. Sulphamethizole is much more soluble in 95% ethanol than in water. The effect of the periodic temperature cycling process on this same compound in a more efficient solvent could therefore be studied and the results compared with the less efficient solvent. The initial solubility of sulphamethizole in 95% ethanol is 1450 μg ml^{-1} at 25°C rising to 3775 μg ml^{-1} at 50°C (see Fig. 2.3.11.2).

The solubility of a substance depends on its physical and chemical properties and also on those of the solvent. Furthermore, solubility is dependent on temperature, pressure, p H of the solution and to a lesser degree the state of sub-division of the solute. The structural features of a substance, for example the ratio of polar to non-polar groups affects the solubility. Solubility can only be predicted qualitatively because of its dependence on these structural, chemical and electrical effects which determine the mutual interaction between solute and solvent. It was therefore necessary to determine the exact aqueous solubility profiles of all

three sulphonamides and also the solubility profile of sulphamethizole in 95% ethanol so that the saturation concentration at a given temperature could be determined. From these data the quantity of the drug could be calculated so that at the peak temperature of a chosen temperature cycle the concentration of the drug was slightly below saturation; this allowed limited dissolution to occur whilst, at the minimum temperature of the cycle, the drug concentration was above the point of saturation in order to allow deposition to occur.

Most drugs are weak acids or weak bases. In the case of the sulphonamides the aliphatic nitrogen is sufficiently positive for these compounds to act as slightly soluble weak acids, rather than bases. In water, which is a polar solvent, they act as weak electrolytes and therefore are not appreciably ionised. Their partial solubility in water is attributed to hydrogen bond formation with water. Sulphamethizole is more soluble in 95% ethanol than in water because alcohol is a semi-polar solvent. Increasing temperature increases the solubility of endothermic solids, according to Le Chatelier's principle - a system tends to adjust itself in a manner so as to minimise the influence of a stress.

The values chosen as the minimum and maximum temperatures of the cycle were on the lower part of the steeper gradient of the solubility profiles. This was in order to achieve maximum dissolution and deposition with

minimum risk of degradation. The latter requirement is important as pharmaceutical products must be of a high purity to comply with the official standards. It is possible that the presence of some degradation products in a medicinal product may produce undesirable side effects in the patient. It can be seen from Figs. 2.3.11.1 and 2.3.11.2 that the temperature range between 30°C and 40°C is on the lower part of the steepest gradient of the solubility profiles for all three sulphonamides in aqueous solution and also sulphamethizole in 95% ethanol. The concentration of sulphonamides used are given in Table 3.1.1. The concentrations of the compounds used by Nyvlt (1973) were not stated.

Sulphonamide	Aqueous Suspension Concentration (g/l)
Sulphamethizole	1.15
Sulphathiazole	1.50
Sulphadimidine	1.00

Sulphonamide	Ethanolic Suspension Concentration (g/l)
Sulphamethizole	27.50

Table 3.1.1 The Concentration of Sulphonamides Used in the Periodic Temperature Cycling Studies.

Initially 2 litre batches of each of the three sulphonamides were cycled in water as described in Materials and Methods (2.2). The batch was subjected to thirty minute cycles, each consisting of fifteen minutes heating to 40°C followed by

cooling to 30°C for 100 and 190 cycles. These time periods allowed equilibration of the system and also gave equal periods of dissolution and deposition (see Fig.2.2.2). Running the system continuously for five working days enabled 190 cycles to be completed. The batch size was then increased to 5 litres to investigate the effect of scaling up. The agitation rate of 2000 r.p.m. was kept constant throughout. This was found to be the minimum speed necessary to keep the crystals suspended in contact with the solvent and to prevent deposition on the walls of the vessel. Subsequently the effect of increasing the period of dissolution and also the effect of increasing the period of deposition were investigated. Finally the effect of periodic temperature cycling on sulphamethizole in the more efficient solvent was investigated.

3.2 SHAPE ASSESSMENT

The problem arose of how to assess changes in crystal habit that might occur as a result of the temperature cycling process. Shape is a complex parameter to define and even more difficult to quantify. A quantitative measure of the overall shape change was needed to establish whether or not the products were significantly different from the starting materials. However the choice of shape factor was limited by restrictions on the choice of size analysis method. The small amount of product in each batch was insufficient for sieving and sedimentation

Fig. 3.2.1 Shape Ratio

I_i / I_c = Inscribed Circle Radius / Circumscribed Circle Radius

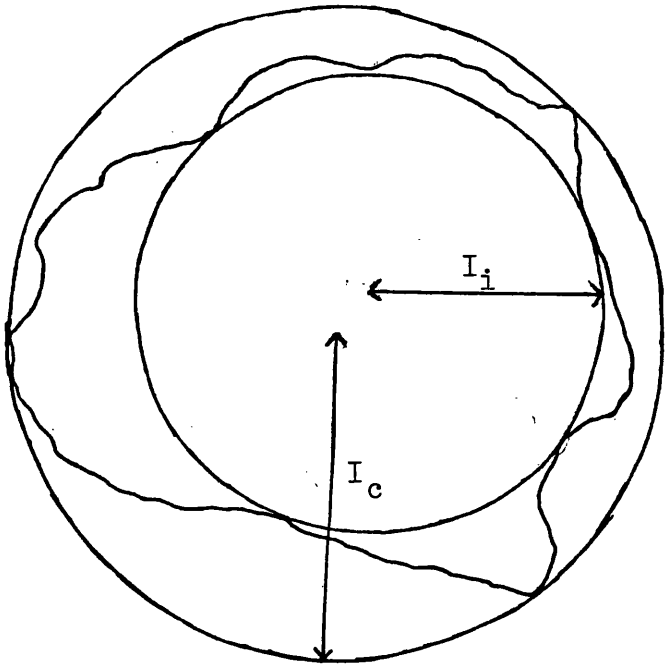

Table 3.2.1 I_i / I_c Ratios for some Standard Geometric Figures

Figure	Dimensions	I_i / I_c
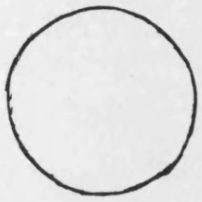	Circle	1.000
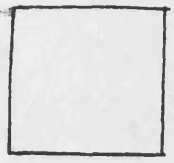	Square	0.714
	Rectangle 2:3	0.555
	Rectangle 1:2	0.435
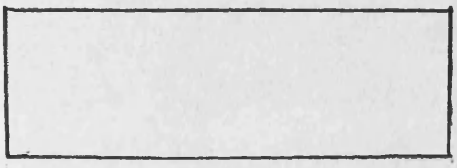	Rectangle 1:3	0.312

Table 3.2.1 (continued)

Figure	Dimensions	I_i / I_c
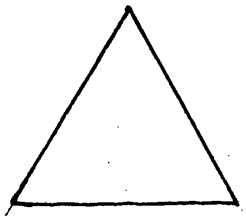	Equilateral Triangle	0.500
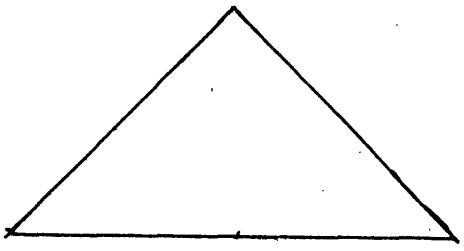	Isosceles Triangle (h = 1, a = 2)	0.364
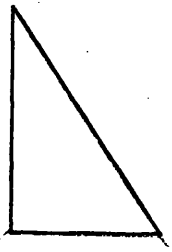	Right Angled Triangle (h = 3, a = 2)	0.368
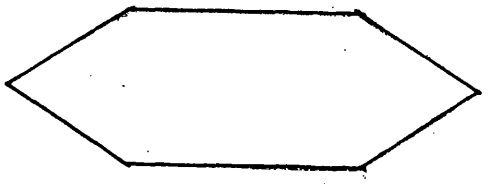	Elongated Hexagon	0.317
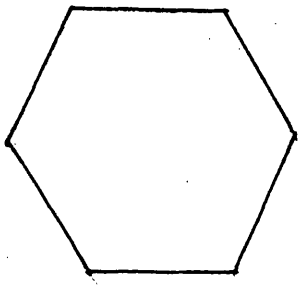	Equal Sided Hexagon	0.850

methods, and since the sulphonamides are slightly soluble in aqueous electrolytes, the electrical sensing zone method would not provide accurate information regarding the starting materials and products. Use of the Heywood shape factors is therefore difficult. A shape factor was required that could be determined from microscopy alone. The shape factor chosen was the ratio of the radius of the inscribed circle, (I_i), to that of the circumscribed circle, (I_c). The inscribed circle is the largest circle that can be drawn completely within the crystal image. The circumscribed circle is the smallest circle which encompasses the whole of the crystal image (see Fig.3.2.1). The closer the ratio I_i / I_c is to unity, the more isodiametric the crystal. Ratios for some standard geometrical figures are given in Table 3.2.1. This shape factor gives a fairly sensitive measure of circularity and can be readily obtained by image analysis.

3.3 STATISTICS

An analysis of variance was carried out on the shape factors and the fractal dimensions of the crystals (see Appendix II) to assess whether the variance between the results was due to within - treatment differences caused by random variation or to the effect of the treatment, in this case the temperature cycling conditions. The total variance of a set of results is due to the sum of these factors. The purpose of analysis

of variance is to separate the two contributing variances so that the effects of the treatment may be established. If the calculated variance ratio is greater than that of the corresponding tabulated value it may be stated that, given a certain probability level of being incorrect, the treatment has a significant effect on the crystal habit. The analysis shows whether or not the treatment has a significant effect on crystal habit. It does not show whether any given pair of treatments have significantly different effects. To compare any pair of treatments a Student t test must be performed (see Appendix I) to detect any significant differences.

The analysis of variance depends on a normal distribution of the variable. The results of the effect of temperature cycling on crystal habit are expressed as a change in the ratio I_i / I_c; this parameter is a proportion and therefore will not usually have a normal distribution. Nevertheless provided the results show distinct differences, reliable conclusions may still be drawn from an analysis of variance. However, in the present study, since the results lie fairly close together, the exact form of the distribution becomes of greater importance. When proportions are scattered around a mean value of 0.5 their distribution is often approximately normal. Difficulties arise when the mean value approaches 0 or 1. Proportions cannot be less than 0 or greater than 1. In the case of a normal distribution it is assumed that the tails of the curve extend to

infinity on either side of the mean. As a result the closer the sample mean is to 0 or 1, the smaller the standard deviation will be. As the mean value approaches 0 or 1, the data will deviate from a normal distribution. Thus, instead of there being a constant value for the standard deviation, there will be a maximum standard deviation for proportions around 0.5 and decreasing standard deviation values at either end of the range. To overcome this effect the arcsin transformation (see Appendix III) was applied to the ratios I_i / I_c before applying the analysis of variance.

3.4 I_i / I_c RATIOS OBTAINED USING THE MAGISCAN IMAGE ANALYSIS SYSTEM

The Student t test was applied to pairs of I_i / I_c ratios obtained by the Magiscan Image Analysis method for each sulphonamide (see Tables 3.4.1, 3.4.2, 3.4.3 and 3.4.4). There is a significant change in the crystal habits of the products after undergoing thirty minute temperature cycles consisting of fifteen minutes successive heating to 40°C and cooling to 30°C, compared with their respective starting materials. The one exception to this being ST2L100. The results also showed that there was a greater degree of rounding in the products of sulphadimidine and sulphamethizole when compared with their respective starting materials, than in the case of sulphathiazole.

It is interesting to note that the solubility

	NUMBER OF CYCLES	SULPHA-DIMIDINE	SULPHA-METHIZOLE	SULPHA-THIAZOLE
STARTING MATERIAL	0	0.56	0.60	0.52
2 LITRE BATCH	100	0.67	0.71	0.55
2 LITRE BATCH	190	0.68	0.70	0.59
5 LITRE BATCH	190	0.66	0.71	0.59

Table 3.4.1 Mean I_i / I_c Ratios of Three Sulphonamides and their Product Batches After Undergoing Differing Numbers of Thirty Minute Temperature Cycles Consisting of Fifteen Minutes Successive Heating to 40^0C and Cooling to 30^0C, Measured by the Magiscan Image Analysis System.

Table 3.4.2 Student t-Test Results for Pairs of I_i / I_c Ratios for Sulphathiazole Obtained by the Magiscan Image Analysis Method.

Pairs of Sulphathiazole Batches	t_{tab}	t_{calc}	n	p
STSM/ST2L100	1.65	1.30	200	>0.1
STSM/ST2L190	3.29	3.98	200	0.001
STSM/ST5L190	3.29	3.91	200	0.001
ST2L100/ST2L190	2.33	2.44	200	0.02
ST2L100/ST5L190	2.33	2.43	200	0.02
ST2L190/ST5L190	1.65	0.11	200	>0.1

t_{tab} = tabulated value of t

t_{calc} = calculated value of t

n = total number of results

p = probability

Table 3.4.3 Student t-Test Results for Pairs of I_i / I_c Ratios for Sulphadimidine Obtained by the Magiscan Image Analysis Method.

Pair of Sulphadimidine Batches	t_{tab}	t_{calc}	n	p
SDSM/SD2L100	3.29	7.66	200	0.001
SDSM/SD2L190	3.29	7.96	200	0.001
SDSM/SD5L190	3.29	7.81	200	0.001
SD2L100/SD2L190	1.65	0.39	200	>0.1
SD2L100/SD5L190	1.65	0.65	200	>0.1
SD2L190/SD5L190	1.65	1.14	200	>0.1

t_{tab} = tabulated value of t

t_{calc} = calculated value of t

n = total number of results

p = probability

Table 3.4.4 Student t-Test Results for Pairs of I_i / I_c Ratios for Sulphamethizole Obtained by The Magiscan Image Analysis Method

Pair of Sulphamethizole Batches	t_{tab}	t_{calc}	n	p
SMSM/SM2L100	3.29	6.54	200	0.001
SMSM/SM2L190	3.29	6.32	200	0.001
SMSM/SM5L190	3.29	6.38	200	0.001
SM2L100/SM2L190	1.65	0.33	200	>0.1
SM2L100/SM5L190	1.65	0.26	200	>0.1
SM2L190/SM5L190	1.65	0.07	200	>0.1

t_{tab} = tabulated value of t

t_{calc} = calculated value of t

n = total number of results

p = probability

profiles of sulphamethizole and sulphathiazole are very similar, both showing an approximate three-fold increase in solubility over the temperature range 25°C to 50°C, whereas the increase for sulphadimidine over the same temperature range was only two-fold. Therefore it might have been expected that sulphamethizole and sulphathiazole would show the most marked degree of rounding, since they would be undergoing greater growth and dissolution than sulphadimidine during the same temperature cycle. It is possible that the less marked shape change of sulphathiazole under these conditions is due to the different habit of the starting materials. Sulphadimidine and sulphamethizole both have irregular but approximately equidimensional crystals, whereas sulphathiazole has a characteristic elongated hexagonal shape. It may be that the crystal habit of the starting material is an important factor in determining the efficiency of the process for sparingly soluble crystalline materials. This does not appear to be a critical factor in very soluble systems such as those reported by Nyvlt (1973).

The Student t test (see Tables 3.4.2, 3.4.3 and 3.4.4) also showed that in the case of sulphamethizole and sulphadimidine there was no significant difference between the 2 litre batches that were cycled for 100 and 190 cycles and the 5 litre batch that was cycled for 190 cycles. It would appear that for these two materials there is no significant advantage in increasing the

number of cycles above 100 for the 2 litre batch size. Considering the 2 litre and 5 litre batches that have both undergone 190 cycles; it would appear that scaling up the batch size from 2 litres to 5 litres has not adversely affected the product.

In the case of sulphathiazole there was a significant difference in crystal habit at the 2% level between the 2 litre batches that had undergone 100 and 190 cycles, the latter being the most rounded. There was the same significant difference between the 2 litre batch that had undergone 100 cycles and the 5 litre batch that had undergone 190 cycles. There was no significant difference between the 2 litre and 5 litre batches that had both undergone 190 cycles. This indicates that in this case there may be some advantage in increasing the number of cycles but there is no reduction in rounding effect on increasing the batch size from 2 to 5 litres.

From the initial results obtained using the Magiscan Image Analysis System it was decided to single out one of the sulphonamides and investigate the effect of altering the temperature cycling conditions. Sulphamethizole was chosen as this had shown the most marked degree of rounding under the original conditions. The effects of prolonging and decreasing the periods of heating and cooling within each temperature cycle were studied. The batch size studied was 5 litres. The effect of using a more

efficient solvent system was also investigated; the batch size used in that case was 200 mls. A number of batches that had undergone different temperature cycling conditions for differing numbers of cycles were prepared.

3.5 I_i / I_c RATIOS OBTAINED USING THE MICROSIGHT 1 IMAGE ANALYSIS SYSTEM

The three sulphonamide starting materials and their products which had been previously examined on the Magiscan Image Analysis System were re-examined using the Microsight 1 Image Analysis System, in order to compare the two methods. In addition a 5 litre batch of each sulphonamide that had undergone 100 thirty-minute temperature cycles consisting of fifteen minutes successive heating to 40°C and cooling to 30°C were examined. The results obtained using the Microsight 1 Image Analysis System (see Tables 3.5.1, 3.5.2 and 3.5.3) were compared with the results obtained using the Magiscan Image Analysis System(see Table 3.4.1) using the Student t test (see Table 3.5.4). The comparison showed no significant differences between the results obtained using the two instrument systems for sulphamethizole and sulphathiazole. However for sulphadimidine starting material the two instruments gave significantly different results at the 0.1% level of significance. Likewise the SD2L100

	STSM	ST2L100	ST5L100	ST5L190
I_i / I_c	0.53	0.57	0.55	0.57
6_{n-1}	0.098	0.108	0.108	0.111
I_i (μm)	17.69	19.69	18.31	18.74
I_c (μm)	33.94	35.06	33.78	33.31
Fractal Dimension	1.07	1.06	1.08	1.06
6_{n-1}	0.020	0.016	0.021	0.015
Perimeter (μm)	192	203	198	193
Area (μm^2)	1842	2136	1888	1930

Table 3.5.1 Mean Dimensional Measurements of Sulphathiazole Crystals and of Batches After Temperature Cycling in Distilled Water, Measured by the Microsight 1 Image Analysis System.

6_{n-1} = standard deviation

n = total number of results = 100

	SDSM	SD2L100	SD5L100	SD5L190
I_i / I_c	0.66	0.72	0.69	0.69
6_{n-1}	0.083	0.072	0.071	0.073
I_i (μm)	17.07	17.49	16.97	17.58
I_c (μm)	25.91	24.47	24.76	25.67
Fractal Dimension	1.08	1.06	1.07	1.06
6_{n-1}	0.022	0.015	0.018	0.018
Perimeter (μm)	160	153	153	158
Area (μm^2)	1371	1329	1273	1383

Table 3.5.2 Mean Dimensional Measurements of Sulphadimidine Crystals and of Batches After Temperature Cycling in Distilled Water, Measured by the Microsight 1 Image Analysis System.

6_{n-1} = standard deviation

n = total number of results = 100

	SMSM	SM2L100	SM2L190	SM5L50	SM5L100	SM5L150	SM5L200
I_i / I_c	0.62	0.69	0.70	0.68	0.69	0.64	0.70
6_{n-1}	0.096	0.081	0.066	0.081	0.066	0.068	0.060
I_i (μm)	16.42	22.07	22.66	22.03	21.18	21.09	21.99
I_c (μm)	26.85	32.08	32.58	32.62	30.76	33.29	31.38
Fractal Dimension	1.08	1.03	1.02	1.03	1.03	1.03	1.03
6_{n-1}	0.024	0.016	0.009	0.010	0.010	0.015	0.012
Perimeter (μm)	162	201	206	203	193	204	197
Area (μm^2)	1369	2319	2457	2290	2125	2288	2316

Table 3.5.3 Mean Dimensional Measurements of Sulphamethizole Crystals and of Batches After Temperature Cycling in Distilled Water, Measured by the Microsight 1 Image Analysis System.

6_{n-1} = standard deviation

n = total number of results = 100

Table 3.5.4 Student t-Test Results for the Comparison of the Magiscan and Microsight 1 Image Analysis Systems

Batch	t_{tab}	t_{calc}	n	p
SMSM	1.65	1.11	200	>0.1
SM2L100	1.65	1.18	200	>0.1
SM5L190	1.65	0.41	200	>0.1
SDSM	3.29	7.85	200	0.001
SD2L100	2.58	3.23	200	0.01
SD5L190	1.96	2.28	200	0.05
STSM	1.65	0.50	200	>0.1
ST2L100	1.65	1.55	200	>0.1
ST5L190	1.65	1.19	200	>0.1

t_{tab} = tabulated value of t

t_{calc} = calculated value of t

n = total number of results

p = probability

batch results were significantly different at the 1% level and the SD5L190 batch results were significantly different at the 5% level. It is probable that the difference in resolution between the two image analysis systems accounts for these results. It was therefore obvious that one image analysis system would need to be selected, in order to be able to compare results and draw conclusions about their significance. The Digithurst Microsight 1 Image Analysis System was chosen because of its advantages of being readily available, easily programmable and relatively inexpensive.

One disadvantage however was the time factor involved in processing the data. To analyse 100 crystals, 100 digitised crystal pictures must be collected on disc and these then further processed using the "CRYSTAL" program. The Magiscan does not require collection of digitised pictures - the crystal data can be processed directly from the video screen in a shorter time. It must be remembered that the former system is very much less expensive than the Magiscan and therefore the time and resolution disadvantages might be expected. The essential consideration is whether or not the lower cost system can produce meaningful results in an acceptable period of time for the purposes of the operator.

3.6 I_i / I_c RATIOS OBTAINED FOR SULPHATHIAZOLE USING THE MICROSIGHT 1 IMAGE ANALYSIS SYSTEM

The analysis of variance indicated a 2.5% probability of error in concluding that there was a significant difference between the sulphathiazole starting material and batches ST2L100, ST5L100 and ST5L190 following the temperature cycling. The Student t test was applied to pairs of results (see Table 3.6.1) and this indicated that there was a significant difference at the 1% level between sulphathiazole starting material and each batch ST2L100 and ST5L190. There was no significant difference between the starting material and the batch ST5L100. This would appear to indicate that in this case when the batch size is increased from 2 litres to 5 litres, a larger number of temperature cycles is necessary to produce a significant rounding effect. It should be noted that the significance is at the 1% level and therefore the observed rounding effect would appear to be less than that observed with sulphamethizole and sulphadimidine. This may be attributed to the differing crystal habits of the starting materials as mentioned previously. There was no significant difference between the three products indicating that none of the batches appears to be superior overall in terms of rounding effect. It can be concluded that under

Table 3.6.1 Student t-Test Results for Pairs of I_i / I_c Ratios for Sulphathiazole Obtained by the Microsight 1 Image Analysis Method.

Pairs of Sulphathiazole Batches	t_{tab}	t_{calc}	n	p
STSM/ST2L100	2.58	2.80	200	0.01
STSM/ST5L100	1.65	1.60	200	>0.1
STSM/ST5L190	2.58	2.67	200	0.01
ST2L100/ST5L100	1.65	1.15	200	>0.1
ST2L100/ST5L190	1.65	0.08	200	>0.1
ST5L100/ST5L190	1.65	1.05	200	>0.1

t_{tab} = tabulated value of t
t_{calc} = calculated value of t
n = total number of results
p = probability

these conditions it is arguable whether or not the rounding effect produced is significant. The process for sulphathiazole certainly would not appear to be economically viable, although it is possible that further investigation into the effects of other temperature cycling conditions might produce more significant results.

3.7 I_i / I_c RATIOS OBTAINED FOR SULPHADIMIDINE USING THE MICROSIGHT 1 IMAGE ANALYSIS SYSTEM

Analysis of variance gave a nil probability of being incorrect, thus indicating the certainty of a significant difference between the starting material and the batches SD2L100, SD5L100 and SD5L190 produced by temperature cycling. The t-test (see Table 3.7.1) indicated that batch SD2L100 was significantly different from SDSM ($p = 0.1\%$) and the two batches SD5L100 and SD5L190 were also significantly different from SDSM ($p = 2\%$). The SD2L100 batch was significantly different from batch SD5L100 ($p = 2\%$) and from batch SD5L190 ($p = 1\%$). This shows that in this case an increase in batch size adversely affected the product. Batches SD5L100 and SD5L190 were not significantly different from one another so for the larger batch size there is no apparent advantage in increasing the number of temperature cycles above 100.

Table 3.7.1 Student t-Test Results for Pairs of I_i/I_c Ratios for Sulphadimidine Obtained by the Microsight 1 Image Analysis Method.

Pairs of Sulphadimidine Batches	t_{tab}	t_{calc}	n	p
SDSM/SD2L100	3.29	4.88	200	0.001
SDSM/SD5L100	2.33	2.56	200	0.02
SDSM/SD5L190	2.33	2.42	200	0.02
SD2L100/SD5L100	2.33	2.52	200	0.02
SD2L100/SD5L190	2.58	2.61	200	0.01
SD5L100/SD5L190	1.65	0.13	200	>0.1

t_{tab} = tabulated value of t

t_{calc} = calculated value of t

n = total number of results

p = probability

3.8 I_i / I_c RATIOS OBTAINED FOR SULPHAMETHIZOLE USING THE MICROSIGHT 1 IMAGE ANALYSIS SYSTEM

Sulphamethizole was considered suitable for investigation of a further increase in batch size and of the minimum number of cycles required to produce a significant rounding effect (see Table 3.5.3). All the following batches SM2L100, SM2L190, SM5L50, SM5L100 and SM5L190 were found to be significantly different from the starting material ($p = 0.1\%$) when the t-test was applied (see Table 3.8.1). Batch SM5L150 was not found to be significantly different from the starting material. None of these batches differed significantly from one another, with the exception of SM5L150 which was significantly different from each of the other batches ($p = 0.1\%$). It may be inferred that for the 2 litre batch size there is no apparent advantage in increasing the number of temperature cycles beyond 100. There was no adverse effect on the product when the batch size was scaled up to 5 litres, but for this set of temperature cycling conditions at this batch size there was no significant advantage in increasing the number of cycles above 50. Batch SM5L150 was not significantly different from the starting material but it was significantly less rounded than all the other products. Since the results for the other batches were so consistent it is possible that this was due to the sticking of crystals on the side of the glass vessel or to poor sampling.

Table 3.8.1 Student t-Test Results for Pairs of I_i / I_c Ratios of Sulphamethizole After Undergoing 30 Minute Cycles of 15 Minutes Successive Heating to 40°C and Cooling to 30°C Obtained by the Microsight 1 Image Analysis Method.

Pairs of Sulphamethizole Batches	t_{tab}	t_{calc}	n	p
SMSM/SM2L100	3.29	6.03	200	0.001
SMSM/SM2L190	3.29	6.71	200	0.001
SMSM/SM5L50	3.29	4.93	200	0.001
SMSM/SM5L100	3.29	6.26	200	0.001
SMSM/SM5L150	1.65	1.81	200	0.1
SMSM/SM5L190	3.29	7.29	200	0.001
SM2L100/SM2L190	1.65	0.22	200	>0.1
SM2L100/SM5L50	1.65	1.23	200	>0.1
SM2L100/SM5L100	1.65	0.30	200	>0.1
SM2L100/SM5L150	3.29	5.16	200	0.001
SM2L100/SM5L190	1.65	0.65	200	>0.1
SM2L190/SM5L50	1.65	1.57	200	>0.1
SM2L190/SM5L100	1.65	0.58	200	>0.1
SM2L190/SM5L150	3.29	6.01	200	0.001
SM2L190/SM5L190	1.65	0.48	200	>0.1
SM5L50/SM5L100	1.65	1.06	200	>0.1
SM5L50/SM5L150	3.29	3.84	200	0.001
SM5L50/SM5L190	1.96	2.06	200	0.05

Table 3.8.1 (continued)

Pairs of Sulphamethizole Batches	t_{tab}	t_{calc}	n	p
SM5L100/SM5L150	3.29	5.45	200	0.001
SM5L100/SM5L190	1.65	1.09	200	0.1
SM5L150/SM5L190	3.29	6.76	200	0.001

t_{tab} = tabulated value of t

t_{calc} = calculated value of t

n = total number of results

p = probability

3.9 THE EFFECT OF PROLONGING THE HEATING PHASE OF THE TEMPERATURE CYCLE ON SULPHAMETHIZOLE I_i/I_c RATIOS

The effect of prolonging the period of heating, and therefore the period of dissolution, was investigated. The period of heating was extended from 15 minutes to 20 minutes with 10 minutes cooling, 40 minutes with 20 minutes cooling and 50 minutes with 10 minutes cooling, cycling between 30°C and 40°C. (see Table 3.9.1). Considering batches SM20H/10C50, SM20H/10C100, SM20H/10C150 and SM20H/10C200, the analysis of variance indicated a significant difference between these products and the starting material due to the treatment. However when the t-test was applied (see Table 3.9.2) the only batch that was significantly different from the starting material where p = 0.1% was SM20H/10C150. Batches SM20H/10C50 and SM20H/10C200 were significantly different from SMSM (p = 1%) and also SM20H/10C100 (p = 2%). None of these batches differed significantly from each other at less than the 5% level of significance. It is concluded that temperature cycles of 20 minutes heating to 40°C and 10 minutes cooling to 30°C did not appear to have any significant advantage over 15 minutes successive heating and cooling between these temperature limits.

An hourly temperature cycle of 40 minutes heating and 20 minutes cooling between 30°C and 40°C was

	SMSM	SM20H/10C				SM40H/20C			SM50H/10C	
		50	100	150	200	50	75	100	50	75
I_i / I_c	0.62	0.66	0.65	0.67	0.65	0.68	0.66	0.69	0.66	0.68
6_{n-1}	0.096	0.084	0.083	0.085	0.083	0.089	0.110	0.089	0.103	0.078
I_i (μm)	16.42	21.82	20.30	23.26	24.10	21.41	22.53	22.13	21.91	20.73
I_c (μm)	26.85	33.52	31.54	34.65	37.03	31.70	34.28	32.20	33.62	30.79
Fractal Dimension	1.08	1.03	1.03	1.02	1.02	1.02	1.05	1.06	1.06	1.05
6_{n-1}	0.024	0.010	0.010	0.008	0.007	0.011	0.014	0.013	0.014	0.014
Perimeter(μm)	162	207	194	213	230	195	211	200	206	189
Area (μm^2)	1369	2371	2057	2521	2888	2159	2419	2240	2336	1983

Table 3.9.1 Mean Dimensional Measurements of Sulphamethizole Crystals and of Batches After Temperature Cycling in Distilled Water, Measured by the Microsight 1 Image Analysis System.

6_{n-1} = standard deviation

n = number of results = 100

Table 3.9.2. Student t Test Results for Pairs of I_i / I_c Ratios for Sulphamethizole After Undergoing Temperature Cycling With a Prolonged Heating Period Obtained by the Microsight 1 Image Analysis Method.

Pairs of Sulphamethizole Batches	t_{tab}	t_{calc}	n	p
SMSM/SM20H/10C50	2.58	3.00	200	0.01
SMSM/SM20H/10C100	2.33	2.38	200	0.02
SMSM/SM20H/10C150	3.29	4.47	200	0.001
SMSM/SM20H/10C200	2.58	2.92	200	0.01
SM20H/10C50/SM20H/10C100	1.65	0.69	200	>0.1
SM20H/10C50/SM20H/10C150	1.65	1.60	200	>0.1
SM20H/10C50/SM20H/10C200	1.65	0.10	200	>0.1
SM20H/10C100/SM20H/10C150	1.96	2.29	200	0.05
SM20H/10C100/SM20H/10C200	1.65	0.59	200	>0.1
SM20H/10C150/SM20H/10C200	1.65	1.70	200	0.1
SMSM/SM40H/20C50	3.29	4.61	200	0.001
SMSM/SM40H/20C75	2.58	3.14	200	0.01
SMSM/SM40H/20C100	3.29	5.57	200	0.001
SM40H/20C50/SM40H/20C75	1.65	1.02	200	>0.1
SM40H/20C50/SM40H/20C100	1.65	0.99	200	>0.1
SM40H/20C75/SM40H/20C100	1.65	1.90	200	0.1
SMSM/SM50H/10C50	2.58	2.83	200	0.01
SMSM/SM50H/10C100	3.29	5.07	200	0.001
SM50H/10C50/SM50H/10C100	1.65	1.76	200	0.1

t_{tab} = tabulated value of t n = total number of results

t_{calc} = calculated value of t p = probability

used to investigate the effect of prolonging the heating period of the cycle further. Analysis of variance (P =0) indicated that there was a significant difference between the starting material and each product batch SM40H/20C50, SM40H/20C75, and SM40H/20C100, due to the treatment. The t-test (see Table 3.9.2) showed that the batches SM40H/20C50 and SM40H/20C100 were significantly different at the 0.1% level from the starting material. Batch SM40H/20C75 was significantly different from the starting material at the 1% level. None of the product batches were significantly different from each other. It can be concluded that, under these conditions there is no advantage in increasing the number of cycles beyond 50.

The longest period of heating studied was 50 minutes with 10 minutes cooling. Analysis of variance (P = 0) again indicated that there was a significant difference between the starting material and the product batches SM50H/10C50 and SM50H/10C100. The t-test (see Table 3.9.2) showed that batch SM50H/10C50 was significantly different from the starting material at the 1% level. Batch SM50H/10C100 was significantly different from the starting material at the 0.1% level. The two product batches were not significantly different from each other. In this case there may be some slight advantage in increasing the number of temperature cycles but it is arguable as to whether or not the small increase in rounding justifies the costs associated with a longer process.

Table 3.9.3 Student t-Test Results for Pairs of I_i / I_c Ratios for Sulphamethizole Batches that Were Significantly Different from the Starting Material at the 0.1% Level.

Pairs of Sulphamethizole Batches	t_{tab}	t_{calc}	n	p
SM20H/10C150/SM40H/20C50	1.65	0.24	200	>0.1
SM20H/10C150/SM40H/20C100	1.65	1.25	200	>0.1
SM20H/10C150/SM50H/10C75	1.65	0.46	200	>0.1
SM40H/20C50/SM40H/20C100	1.65	0.99	200	>0.1
SM40H/20C50/SM50H/10C75	1.65	0.19	200	>0.1
SM40H/20C100/SM50H/10C75	1.65	0.86	200	>0.1
SM2L100/SM20H/10C150	1.65	1.57	200	>0.1
SM2L100/SM40H/20C50	1.65	1.28	200	>0.1
SM2L100/SM40H/20C100	1.65	0.26	200	>0.1
SM2L100/SM50H/10C75	1.65	1.17	200	>0.1
SM2L190/SM20H/10C150	1.65	1.93	200	>0.1
SM2L190/SM40H/20C50	1.65	1.60	200	>0.1
SM2L190/SM40H/20C100	1.65	0.49	200	>0.1
SM2L190/SM50H/10C75	1.65	1.52	200	>0.1
SM5L50/SM20H/10C150	1.65	0.38	200	>0.1
SM5L50/SM40H/20C50	1.65	0.12	200	>0.1
SM5L50/SM40H/20C100	1.65	0.92	200	>0.1
SM5L50/SM50H/10C75	1.65	0.08	200	>0.1

Table 3.9.3 (continued)

Pairs of Sulphamethizole Batches	t_{tab}	t_{calc}	n	p
SM5L100/SM20H/10C150	1.65	1.43	200	> 0.1
SM5L100/SM40H/20C50	1.65	1.12	200	> 0.1
SM5L100/SM40H/20C100	1.65	0.00	200	> 0.1
SM5L100/SM50H/10C75	1.65	0.99	200	> 0.1
SM5L190/SM20H/10C150	2.33	2.41	200	0.02
SM5L190/SM40H/20C50	1.96	2.06	200	0.05
SM5L190/SM40H/20C100	1.65	0.91	200	> 0.1
SM5L190/SM50H/10C75	1.96	2.02	200	0.05
SM20C/10H100/SM40C/20H50	3.29	4.14	200	0.001
SM20C/10H100/SM40C/20H75	3.29	5.59	200	0.001
SM20C/10H100/SM50C/10H75	1.65	0.42	200	> 0.1
SM40C/20H50/SM40C/20H75	1.65	1.47	200	> 0.1
SM40C/20H50/SM50C/10H75	3.29	4.71	200	0.001
SM40C/20H75/SM50C/10H75	3.29	6.22	200	0.001
SM2L100/SM40C/20H50	1.65	1.37	200	> 0.1
SM2L100/SM40C/20H75	2.58	2.77	200	0.01
SM2L200/SM40C/20H50	1.65	1.29	200	> 0.1
SM2L200/SM40C/20H75	2.58	2.85	200	0.01
SM5L50/SM40C/20H50	2.58	2.68	200	0.01
SM5L50/SM40C/20H75	3.29	4.11	200	0.001
SM5L100/SM40C/20H50	1.65	1.85	200	0.1
SM5L100/SM40C/20H75	3.29	3.42	200	0.001
SM5L190/SM40C/20H50	1.65	0.89	200	> 0.1
SM5L190/SM40C/20H75	2.33	2.51	200	0.02

Table 3.9.3 (continued)

Pairs of Sulphamethizole Batches	t_{tab}	t_{calc}	n	p
SM2L100/SMA50	1.65	1.63	200	>0.1
SM2L100/SMA100	1.96	2.17	200	0.05
SM2L100/SMA150	3.29	3.77	200	0.001
SM2L100/SMA200	3.29	3.35	200	0.001
SM2L190/SMA50	1.65	1.57	200	>0.1
SM2L190/SMA100	1.96	2.17	200	0.05
SM2L190/SMA150	3.29	4.00	200	0.001
SM2L190/SMA200	3.29	3.46	200	0.001
SM5L50/SMA50	2.58	2.85	200	0.01
SM5L50/SMA100	3.29	3.43	200	0.001
SM5L50/SMA150	3.29	5.17	200	0.001
SM5L50/SMA200	3.29	4.60	200	0.001
SM5L100/SMA50	1.96	2.08	200	0.05
SM5L100/SMA100	2.58	2.70	200	0.01
SM5L100/SMA150	3.29	4.61	200	0.001
SM5L100/SMA200	3.29	3.99	200	0.001
SM5L190/SMA50	1.65	1.21	200	>0.1
SM5L190/SMA100	1.65	1.81	200	0.1
SM5L190/SMA150	3.29	3.70	200	0.001
SM5L190/SMA200	2.58	3.16	200	0.01

Table 3.9.3 (continued)

Pairs of Sulphamethizole Batches	t_{tab}	t_{calc}	n	p
SM40C/20H50/SMA50	1.65	0.38	200	> 0.1
SM40C/20H50/SMA100	1.65	0.90	200	> 0.1
SM40C/20H50/SMA150	2.33	2.49	200	0.02
SM40C/20H50/SMA200	1.96	2.16	200	0.05
SM40C/20H75/SMA50	1.65	0.96	200	> 0.1
SM40C/20H75/SMA100	1.65	0.49	200	> 0.1
SM40C/20H75/SMA150	1.65	0.98	200	> 0.1
SM40C/20H75/SMA200	1.65	0.82	200	> 0.1

t_{tab} = tabulated value of t

t_{calc} = calculated value of t

n = total number of results

p = probability

All the batches that underwent a prolonged heating period and were found to be significantly more rounded than the starting material at the 0.1% level, were compared with each other using the t-test (see Table 3.9.3). Batches SM20H/10C150, SM40H/20C50, SM40H/20C100 and SM50H/10C75 were not found to be significantly better than each other. The t-test was also applied to the data for the above batches and those products that had undergone 30 minute temperature cycles of 15 minutes successive heating to 40°C and cooling to 30°C and were significantly different from the starting material at the 0.1% level. None of the products which underwent a prolonged period of heating was significantly better than those which underwent a 15 minute period of heating. Therefore it can be concluded that there is no significant advantage in prolonging the period of dissolution during the heating phase of the cycle in order to improve the rounding effect. It is inferred that the period of dissolution during temperature cycling is not the critical factor for rounding to occur.

3.10 THE EFFECT OF PROLONGING THE COOLING PHASE OF THE TEMPERATURE CYCLE ON SULPHAMETHIZOLE I_i / I_c RATIOS.

The effect of prolonging the period of cooling, and hence the deposition phase of the temperature cycle was also investigated (see Table 3.10.1). The period

	SMSM	SM10H/20C			SM20H/40C			SM10H/50C		
		50	100	150	50	75	100	50	75	100
I_i / I_c	0.62	0.64	0.66	0.66	0.71	0.72	0.61	0.56	0.66	0.56
6_{n-1}	0.096	0.088	0.081	0.077	0.072	0.070	0.117	0.099	0.076	0.090
I_i (μm)	16.42	20.28	19.71	21.54	21.84	22.93	23.80	23.13	19.82	23.13
I_c (μm)	26.85	31.98	29.81	32.67	31.10	31.77	39.90	42.49	30.40	41.70
Fractal Dimension	1.08	1.03	1.03	1.03	1.02	1.02	1.02	1.03	1.03	1.07
6_{n-1}	0.024	0.012	0.011	0.012	0.008	0.009	0.010	0.011	0.013	0.019
Perimeter (μm)	162	195	183	200	194	201	237	256	186	239
Area (μm^2)	1369	2073	1828	2245	2185	2318	3013	2984	1904	2916

Table 3.10.1 Mean Dimensional Measurements of Sulphamethizole Crystals and Product Batches After Temperature Cycling in Distilled Water, Measured by the Microsight 1 Image Analysis System.

6_{n-1} = standard deviation

n = total number of results = 100

Table 3.10.2 Student t-Test Results for Pairs of I_i / I_c Ratios for Sulphamethizole After Undergoing Temperature Cycling With a Prolonged Cooling Period Obtained by the Microsight 1 Image Analysis Method.

Pairs of Sulphamethizole Batches	t_{tab}	t_{calc}	n	p
SMSM/SM10H/20C50	1.65	1.55	200	> 0.1
SMSM/SM10H/20C100	3.29	3.67	200	0.001
SMSM/SM10H/20C150	2.58	3.27	200	0.01
SM10H/20C50/SM10H/20C100	1.96	2.16	200	0.05
SM10H/20C50/SM10H/20C150	1.65	1.71	200	0.10
SM10H/20C100/SM10H/20C150	1.65	0.51	200	> 0.1
SMSM/SM20H/40C50	3.29	7.56	200	0.001
SMSM/SM20H/40C75	3.29	8.90	200	0.001
SMSM/SM20H/40C100	1.65	0.32	200	> 0.1
SM20H/40C50/SM20H/40C75	1.65	1.47	200	> 0.1
SM20H/40C50/SM20H/40C100	3.29	6.94	200	0.001
SM20H/40C75/SM20H/40C100	3.29	8.08	200	0.001
SMSM/SM10H/50C50	3.29	4.32	200	0.001
SMSM/SM10H/50C75	3.29	3.38	200	0.001
SMSM/SM10H/50C100	3.29	4.06	200	0.001
SM10H/50C50/SM10H/50C75	3.29	8.10	200	0.001
SM10H/50C50/SM10H/50C100	1.65	0.44	200	> 0.1
SM10H/50C75/SM10H/50C100	3.29	8.04	200	0.001

t_{tab} = tabulated value of t n = total number of results

t_{calc} = calculated value of t p = probability

of cooling was extended to 20 minutes with 10 minutes heating, 40 minutes with 20 minutes heating and 50 minutes with 10 minutes heating between 30°C and 40°C. Considering the temperature cycle of 20 minutes cooling and 10 minutes heating, analysis of variance (P = 0.002) indicated a probable significant difference between the products and the starting material due to the treatment. The t-test (see Table 3.10.2) showed that SM10H/20C100 was significantly different at the 0.1% level and SM10H/20C150 at the 1% level from the starting material. Batch SM10H/20C50 was not significantly different from the starting material and there was no significant difference between the batches. It would appear that the optimum number of temperature cycles in this case would be 100.

When the period of cooling was increased to 40 minutes with 20 minutes heating between 30°C and 40°C, analysis of variance (P = 0) indicated there was a significant difference between the starting material and products due to the treatment. The t-test (see Table 3.10.2) showed that batches SM20H/40C50 and SM20H/40C75 were significantly different at the 0.1% level from the starting material but batch SM20H/40C/100 was not significantly different from SMSM. Batch SM20H/40C100 was also significantly different from batches SM20H/40C50 and SM20H/40C75 at the 0.1% level. In this case there appears to be

an adverse effect on the product shape if the number of temperature cycles is increased above 75.

On increasing the period of cooling still further to 50 minutes with 10 minutes heating, analysis of variance (P = 0) showed there was a significant difference between the products and starting material due to the treatment, but in this instance it appears to be an adverse effect. The t-test (see Table 3.10.2) showed that all the product batches (SM10H/50C50, SM10H/50C75 and SM10H/50C100) were significantly different from the starting material at the 0.1% level. Batches SM10H/50C50 and SM10H/50C100 were less rounded than the starting material (see Table 3.10.1). Batch SM10H/50C75 was more rounded than the starting material (see Table 3.10.1) and was significantly different from batches SM10H/50C50 and SM10H/50C100 at the 0.1% level. Batches SM10H/50C50 and SM10H/50C100 were not significantly different from each other.

All the product batches that had undergone a prolonged period of cooling and were significantly more rounded than the starting material at the 0.1% level, were compared with each other using the t-test (see Table 3.9.3). Batches SM20H/40C50 and SM20H/40C75 were significantly different from SM10H/20C100 and SM10H/50C75 at the 0.1% level. However they were not significantly different

from each other. It would appear that the 40 minute cooling period was the optimum deposition phase of the conditions studied. Increasing the number of cycles beyond 50 provided no significant advantage. There is some advantage in prolonging the period of deposition from 15 to 40 minutes. Batches SM20H/40C50 and SM20H/40C75 were compared to those that had undergone 30 minute cycles consisting of 15 minutes successive heating and cooling between 30°C and 40°C. Batch SM20H/40C50 was significantly more rounded than batch SM5L50 at the 1% level. Batch SM20H/40C75 was significantly more rounded than batches SM5L50 and SM5L100 at the 0.1% level; SM2L100 and SM2L190 at the 1% level and SM5L190 at the 2% level. It may be concluded that there is some advantage in prolonging the cooling period of the temperature cycle and hence the deposition phase, but there appears to be an optimum time after which this effect decreases. The period of deposition may have more effect on the rounding process than the period of dissolution.

3.11 THE EFFECT OF REDUCING BOTH PERIODS OF HEATING AND COOLING OF THE TEMPERATURE CYCLE ON SULPHAMETHIZOLE I_i / I_c RATIOS.

When periods of both heating and cooling were decreased to 10 minutes from 15 minutes, analysis of variance ($P = 0.001$) showed a significant difference between the products and the starting

	SMSM	SM10H/10C 50	100	200
I_i / I_c	0.62	0.66	0.65	0.65
6_{n-1}	0.096	0.087	0.090	0.091
I_i (μm)	16.42	20.88	21.00	21.07
I_c (μm)	26.85	31.96	32.51	32.68
Fractal Dimension	1.08	1.06	1.06	1.06
6_{n-1}	0.024	0.014	0.017	0.013
Perimeter (μm)	162	197	199	200
Area (μm^2)	1369	2083	2142	2129

Table 3.11.1 Mean Dimensional Measurements of Sulphamethizole Crystals and of Batches After Temperature Cycling in Distilled Water, Measured by the Microsight 1 Image Analysis System.

6_{n-1} = standard deviation

n = total number of results = 100

Table 3.11.2 Student t Test Results for Pairs of I_i / I_c Ratios for Sulphamethizole After Undergoing Temperature Cycling With Decreased Heating and Cooling Periods and for a Changed Solvent System Obtained by the Microsight 1 Image Analysis Method.

Pairs of Sulphamethizole Batches	t_{tab}	t_{calc}	n	p
SMSM/SM10H/10C50	2.58	3.06	200	0.01
SMSM/SM10H/10C100	2.58	2.76	200	0.01
SMSM/SM10H/10C200	2.33	2.57	200	0.02
SM10H/10C50/SM10H/10C/100	1.65	0.26	200	>0.1
SM10H/10C50/SM10H/10C200	1.65	0.45	200	>0.1
SM10H/10C100/SM10H/10C200	1.65	0.19	200	>0.1
SMSM/SMA50	3.29	7.43	200	0.001
SMSM/SMA100	3.29	8.09	200	0.001
SMSM/SMA150	3.29	9.98	200	0.001
SMSM/SMA200	3.29	9.11	200	0.001
SMA50/SMA100	1.65	0.47	200	> 0.1
SMA50/SMA150	1.65	1.87	200	0.1
SMA50/SMA200	1.65	1.65	200	>0.1
SMA100/SMA150	1.65	1.42	200	>0.1
SMA100/SMA200	1.65	1.23	200	>0.1
SMA150/SMA200	1.65	0.05	200	>0.1

t_{tab} = tabulated value of t

t_{calc} = calculated value of t

n = total number of results

p = probability

material due to the treatment. When the t-test (see Table 3.11.2) was applied, batches SM10H/10C50 and SM10H/10C100 were found to be significantly more rounded than the starting material (see Table 3.11.1) at the 1% level and batch SM10H/10C200 at the 2% level. None of the products were significantly different from each other. This indicates that there is no advantage in increasing the number of cycles beyond 50. However the rounding effect obtained under these temperature cycling conditions was not so great as that obtained with the 30 minute cycle of 15 minutes successive heating and cooling between the same temperatures. This is probably due to equilibration of the system only just being attained over the ten minute periods of heating and cooling. It is inferred that the efficiency of the process is not improved by decreasing the temperature cycling period.

3.12 THE EFFECT OF USING A MORE EFFICIENT SOLVENT ON SULPHAMETHIZOLE I_i / I_c RATIOS.

Analysis of variance ($P = 0.001$) indicated that there was a significant difference between the products and the starting material as a result of temperature cycling for 30 minute periods consisting of 15 minutes successive heating to 40°C and cooling to 30°C in 95% ethanol.(see Table 3.12.1). The t-test (see Table 3.11.2) showed that all the product batches were significantly different from the

	SMSM	SMA50	SMA100	SMA150	SMA200
I_i / I_c	0.62	0.71	0.72	0.73	0.73
6_{n-1}	0.096	0.084	0.078	0.063	0.081
I_i (μm)	16.42	22.63	24.12	24.83	24.74
I_c (μm)	26.85	31.78	33.38	33.94	34.13
Fractal Dimension	1.08	1.05	1.05	1.05	1.05
6_{n-1}	0.024	0.015	0.012	0.010	0.011
Perimeter (μm)	162	199	210	213	214
Area (μm^2)	1369	2288	2624	2660	2630

Table 3.12.1 Mean Dimensional Measurements of Sulphamethizole Crystals and Product Batches After Temperature Cycling in 95% Ethanol, Measured by the Microsight Image Analysis System.

6_{n-1} = standard deviation

n = total number of results = 100

starting material at the 0.1% level. However none of the products was found to be significantly different from another. Therefore it does not appear that increasing the number of cycles above 50 has any significant advantage. The products were also compared to batches of sulphamethizole that underwent the same temperature cycling conditions in an aqueous solvent system (see Table 3.9.3). Batches SMA150 and SMA200 were significantly more rounded than batches SM2L100, SM2L190 and SM5L100 at the 0.1% level. Together with batch SMA100 they were also significantly more rounded than batch SM5L50 at the 0.1% level. Batch SMA150 was significantly more rounded than SM5L190 at the 0.1% level. Batch SMA200 was also significantly more rounded than batch SM5L190 at the 1% level. These results indicate that an increased number of cycles using a solvent system in which the compound is more soluble does improve the rounding effect. This would be expected due to the greater degree of dissolution and deposition. However the beneficial effect of higher solubility was not seen until the number of cycles exceeded 100.

3.13 THE EFFECT OF TEMPERATURE CYCLING ON THE FRACTAL DIMENSIONS OF SULPHATHIAZOLE.

Fractal dimension (as defined in Section 1.8) can be used to assess the surface texture of fineparticles. It would be expected that a perfectly smooth round

Table 3.13.1 Student t-Test Results Comparing Fractal Dimensions of Sulphathiazole Starting Material and Products Obtained After Temperature Cycling.

Pairs of Sulphathiazole Batches	t_{tab}	t_{calc}	n	p
STSM/ST2L100	3.29	3.49	200	0.001
STSM/ST5L100	1.65	1.44	200	>0.1
STSM/SM5L190	2.58	3.04	200	0.01
ST2L100/ST5L100	3.29	5.02	200	0.001
ST2L100/ST5L190	1.65	0.59	200	>0.1
ST5L100/ST5L190	3.29	4.61	200	0.001

t_{tab} = tabulated value of t
t_{calc} = calculated value of t
n = total number of results
p = probability

particle would have a fractal dimension of 1. Therefore the closer the fractal dimension is to 1, the closer the particle will be to being perfectly smooth and round. The fractal dimension of sulphathiazole and its product batches are given in Table 3.5.1. Analysis of variance (P= 0) indicated that there was a significant difference in the fractal dimension between the products and the starting material due to the effect of the temperature cycling conditions. The t-test (see Table 3.13.1) showed there was a significant difference at the 0.1% level between ST2L100 and STSM and at the 1% level between ST5L190 and STSM. There was no significant difference between ST5L100 and STSM. There was also a significant difference at the 0.1% level between ST5L100 and each of the two batches ST2L100 and ST5L190. It would appear that in the case of sulphathiazole temperature cycling under the conditions described decreased the fractal dimension indicating that the products were smoother and rounder than the starting material. On scaling up the batch size from 2 to 5 litres, an increased number of cycles is necessary to produce the same effect.

3.14 THE EFFECT OF TEMPERATURE CYCLING ON THE FRACTAL DIMENSIONS OF SULPHADIMIDINE

The fractal dimensions for sulphadimidine starting

Table 3.14.1 Student t-Test Results Comparing Fractal Dimensions of Sulphadimidine Starting Material and Products Obtained After Temperature Cycling.

Pairs of Sulphadimidine Batches	t_{tab}	t_{calc}	n	p
SDSM/SD2L100	3.29	5.59	200	0.001
SDSM/SD5L100	3.29	3.54	200	0.001
SDSM/SD5L190	3.29	4.96	200	0.001
SD2L100/SD5L100	1.96	2.07	200	0.05
SD2L100/SD5L190	1.65	0.35	200	> 0.1
SD5L100/SD5L190	1.65	1.59	200	> 0.1

t_{tab} = tabulated value of t

t_{calc} = calculated value of t

n = total number of results

p = probability

material and its product batches (see Table 3.5.2) were shown by analysis of variance (P = 0) to be significantly different due to the effect of temperature cycling. The t-test (see Table 3.14.1) confirmed that all three product batches SD2L100, SD5L100 and SD5L190 were significantly different from the starting material at the 0.1% level. All three products had a lower fractal dimension than the starting material indicating a smoother, rounder product in each case. The products were not significantly different from each other, so that scaling up the batch size from 2 to 5 litres does not adversely affect the product. Increasing the number of temperature cycles above 100 does not appear to offer any significant advantage.

3.15 THE EFFECT OF TEMPERATURE CYCLING ON THE FRACTAL DIMENSIONS OF SULPHAMETHIZOLE.

The fractal dimensions of sulphamethizole starting material and its product batches that underwent 30 minutes temperature cycles consisting of 15 minutes successive heating to 40°C and cooling to 30°C (see Table 3.5.3) were shown by analysis of variance (P = 0) to be significantly different. The t-test (see Table 3.15.1) confirmed that all the product batches were significantly different from the starting material at the 0.1% level. None of the products was significantly

Table 3.15.1 Student t-Test Results Comparing Fractal Dimensions of Sulphamethizole Starting Material and Products Obtained After Thirty Minute Temperature Cycles Consisting of Fifteen Minutes Successive Heating to 40°C and Cooling to 30°C.

Pairs of Sulphamethizole Batches	t_{tab}	t_{calc}	n	p
SMSM/SM2L100	3.29	18.24	200	0.001
SMSM/SM2L190	3.29	21.79	200	0.001
SMSM/SM5L50	3.29	20.64	200	0.001
SMSM/SM5L100	3.29	19.60	200	0.001
SMSM/SM5L150	3.29	17.75	200	0.001
SMSM/SM5L190	3.29	20.11	200	0.001
SM2L100/SM2L190	1.96	2.09	200	0.05
SM2L100/SM5L50	1.65	0.70	200	>0.1
SM2L100/SM5L100	1.65	0.59	200	>0.1
SM2L100/SM5L150	1.65	1.03	200	>0.1
SM2L100/SM5L190	1.65	0.62	200	>0.1
SM2L190/SM5L50	1.65	1.82	200	>0.1
SM2L190/SM5L100	1.65	3.51	200	>0.1
SM2L190/SM5L150	1.65	3.44	200	>0.1
SM2L190/SM5L190	1.65	1.75	200	>0.1
SM5L50/SM5L100	1.65	1.68	200	0.1
SM5L50/SM5L150	1.96	1.97	200	0.05
SM5L50/SM5L190	1.65	0.07	200	>0.1

Table 3.15.1 (continued)

Pairs of Sulphamethizole Batches	t_{tab}	t_{calc}	n	p
SM5L100/SM5L150	1.65	0.61	200	>0.1
SM5L100/SM5L190	1.65	1.49	200	>0.1
SM5L150/SM5L190	1.65	1.83	200	0.1

t_{tab} = tabulated value of t

t_{calc} = calculated value of t

n = total number of results

p = probability

different from another. The fractal dimension was reduced from 1.08 for the starting material to 1.03 for all the product batches SM2L100, SM5L50, SM5L100, SM5L150 and SM5L200, and to 1.02 for batch SM2L190. This showed the temperature cycling to have a smoothing and rounding effect. The fractal dimensions of all the product batches was very consistent. There appears to be no adverse effect in scaling up the batch size from 2 to 5 litres, but for the 5 litre batch size there was no significant advantage in increasing the number of temperature cycles beyond 50.

3.16 THE EFFECT OF PROLONGING THE HEATING PERIOD OF THE TEMPERATURE CYCLE ON THE FRACTAL DIMENSION OF SULPHAMETHIZOLE.

The effect of prolonging the period of heating and thus the dissolution phase of the temperature cycle was studied (see Table 3.9.1). The 15 minute period of heating was extended to 20 minutes with 10 minutes cooling, 40 minutes with 20 minutes cooling and 50 minutes with 10 minutes cooling. Analysis of variance ($P = 0$) showed that for all three different temperature cycling conditions there was a significant difference between the products and the starting material due to the treatments. All the products that underwent

Table 3.16.1 Student t-Test Results Comparing Fractal Dimensions of Sulphamethizole Starting Material and Products Obtained After Temperature Cycling With a Prolonged Heating Period.

Pairs of Sulphamethizole Batches	t_{tab}	t_{calc}	n	p
SMSM/SM20H/10C50	3.29	21.01	200	0.001
SMSM/SM20H/10C100	3.29	20.18	200	0.001
SMSM/SM20H/10C150	3.29	22.57	200	0.001
SMSM/SM20H/10C200	3.29	22.97	200	0.001
SM20H/10C50/SM20H/10C100	1.65	1.62	200	> 0.1
SM20H/10C50/SM20H/10C150	1.96	2.27	200	0.05
SM20H/10C50/SM20H/10C200	2.33	2.50	200	0.02
SM20H/10C100/SM20H/10C150	3.29	4.02	200	0.001
SM20H/10C100/SM20H/10C200	3.29	4.37	200	0.001
SM20H/10C150/SM20H/10C200	1.65	0.09	200	> 0.1
SMSM/SM40H/20C50	3.29	20.95	200	0.001
SMSM/SM40H/20C75	3.29	8.99	200	0.001
SMSM/SM40H/20C100	3.29	8.54	200	0.001
SM40H/20C50/SM40H/20C75	3.29	16.55	200	0.001
SM40H/20C50/SM40H/20C100	3.29	18.11	200	0.001
SM40H/20C75/SM40H/20C100	1.65	0.82	200	> 0.1
SMSM/SM50H/10C50	3.29	8.41	200	0.001
SMSM/SM50H/10C75	3.29	9.43	200	0.001
SM50H/10C50/SM50H/10C75	1.65	1.34	200	> 0.1

t_{tab} = tabulated value of t n = total number of results

t_{calc} = calculated value of t p = probability

differing numbers of cycles consisting of 20 minutes heating and 10 minutes cooling between 30°C and 40°C were shown by the t-test (see Table 3.16.1) to be significantly different from the starting material at the 0.1% level. Batch SM20H/10C100 was significantly smoother and rounder than batches SM20H/10C150 and SM20H/10C200 at the 0.1% level. The fractal dimensions for all four product batches SM20H/10C50, SM20H/10C100, SM20H/10C150 and SM20H/10C200, were again very consistent and reduced compared to the starting material, indicating that the products were smoother and rounder. There appears to be no significant advantage in this case in extending the number of cycles beyond 50.

An hourly temperature cycle of 40 minutes heating and 20 minutes cooling between 30°C and 40°C was studied (see Table 3.9.1). The t-test (see Table 3.16.1) showed that the product batches SM40H/20C50, SM40H/20C75 and SM40H/20C100 were significantly smoother and rounder than the starting material at the 0.1% level. Batch SM40H/20C50 was significantly smoother and rounder than batches SM40H/20C75 and SM40H/20C100 at the 0.1% level. Batches SM40H/20C75 and SM40H/20C100 were not significantly different from each other. In this case increasing the number of temperature cycles above 50 appears to have an adverse effect on the smoothness and roundness of

the crystal product. The fractal dimension of batch SM40H/20C50 was reduced to 1.02 but rose to 1.05 and 1.06 for batches SM40H/20C75 and SM40H/20C100 respectively.

Further prolonging the period of heating to 50 minutes with 10 minutes cooling between the same temperatures also gave products with a reduced fractal dimension (see Table 3.9.1), The t-test (see Table 3.16.1) showed the product batches SM50H/10C50 and SM50H/10C75 were significantly different from the starting material at the 0.1% level. The products were not significantly different from each other. There would appear to be no significant advantage in increasing the number of cycles above 50 with the object of increasing smoothness and roundness.

From these results it would appear that prolonging the period of heating and hence dissolution above 20 minutes reduced the smoothing and rounding effects obtained. Increased heating periods of 40 and 50 minutes gave characteristic fractal dimensions of 1.05 and 1.06 as opposed to 1.02 and 1.03 for 15 and 20 minute periods. This compares with the fractal dimension of the starting material of 1.08. In all cases there appears to be no advantage in increasing the number of cycles beyond 50 and no significant advantage in prolonging the 15 minute heating period.

3.17 THE EFFECT OF PROLONGING THE PERIOD OF COOLING OF THE TEMPERATURE CYCLE ON THE FRACTAL DIMENSION OF SULPHAMETHIZOLE

The effect of prolonging the cooling period of the cycle and hence the deposition phase was investigated (see Table 3.10.1). Analysis of variance for all three temperature cycling conditions with a prolonged cooling phase (P =0) showed that there was a significant difference between the starting material and products due to the treatment. For the 30 minute cycle consisting of 20 minutes cooling with 10 minutes heating between 30°C and 40°C, the t-test (see Table 3.17.1) showed that all the product batches were significantly different from the starting material at the 0.1% level. None of the products was significantly different from any other. All the products had a lower fractal dimension indicating a smoothing and rounding effect.

Similar results were obtained when the period of cooling was extended to 40 minutes with 20 minutes heating between the same temperatures. When the period of cooling was extended still further to 50 minutes with 10 minutes heating between the same temperatures the products were still found to be significantly different from the starting material at the 0.1% level when the t-test was

Table 3.17.1 Student t-Test Results Comparing Fractal Dimensions of Sulphamethizole Starting Material and Products Obtained After Temperature Cycling With a Prolonged Cooling Period.

Pairs of Sulphamethizole Batches	t_{tab}	t_{calc}	n	p
SMSM/SM10H/20C50	3.29	18.86	200	0.001
SMSM/SM10H/20C100	3.29	19.76	200	0.001
SMSM/SM10H/20C150	3.29	19.44	200	0.001
SM10H/20C50/SM10H/20C100	1.65	0.75	200	>0.1
SM10H/20C50/SM10H/20C150	1.65	1.16	200	>0.1
SM10H/20C100/SM10H/20C150	1.65	0.49	200	>0.1
SMSM/SM20H/40C50	3.29	22.22	200	0.001
SMSM/SM20H/40C75	3.29	21.99	200	0.001
SMSM/SM20H/40C100	3.29	21.26	200	0.001
SM20H/40C50/SM20H/40C75	1.65	0.08	200	>0.1
SM20H/40C50/SM20H/40C100	1.65	0.53	200	>0.1
SM20H/40C75/SM20H/40C100	1.65	0.44	200	>0.1
SMSM/SM10H/50C50	3.29	19.62	200	0.001
SMSM/SM10H/50C75	3.29	17.32	200	0.001
SMSM/SM10H/50C/100	3.29	3.94	200	0.001
SM10H/50C50/SM10H/50C75	2.33	2.42	200	0.02
SM10H/50C50/SM10H/50C100	3.29	18.18	200	0.001
SM10H/50C75/SM10H/50C100	3.29	15.35	200	0.001

t_{tab} = tabulated value of t n = total number of results

t_{calc} = calculated value of t p = probability

applied (see Table 3.17.1) but in this case when the number of temperature cycles increased to 100, the fractal dimension also increased.

From these results it would appear that for the temperature cycles with a prolonged cooling phase studied, 40 minute cooling with 20 minutes heating produced the most marked smoothing and rounding effect and hence the lowest fractal dimension. Prolonging the cooling period further had an adverse effect on the product shape and texture causing the fractal dimension to increase again. This indicates that the deposition phase length plays an important part in the smoothing and rounding effect. However when the fractal dimension of 1.02 achieved for these products is compared with the fractal dimension of 1.03 for batches SM5L50, SM5L100, SM5L150 and SM5L200 it is debatable as to whether or not there is any significant advantage to be gained by prolonging the cooling period beyond 15 minutes.

3.18 THE EFFECT OF REDUCING THE HEATING AND COOLING PHASES OF THE TEMPERATURE CYCLE ON THE FRACTAL DIMENSION OF SULPHAMETHIZOLE

When the overall temperature cycling period was reduced to 20 minutes consisting of 10 minutes successive heating and cooling between 30°C and 40°C, the fractal dimensions were lower than the starting

Table 3.18.1 Student t-Test Results Comparing Fractal Dimensions of Sulphamethizole Starting Material and Products Obtained After Temperature Cycling With Reduced Periods of Heating and Cooling and With a Changed Solvent System.

Pairs of Sulphamethizole Batches	t_{tab}	t_{calc}	n	p
SMSM/SM10H/10C50	3.29	6.01	200	0.001
SMSM/SM10H/10C150	3.29	6.33	200	0.001
SMSM/SM10H/10C200	3.29	6.05	200	0.001
SM10H/10C50/SM10H/10C150	1.65	0.78	200	>0.1
SM10H/10C50/SM10H/10C200	1.65	0.10	200	>0.1
SM10H/10C150/SM10H/10C200	1.65	0.90	200	>0.1
SMSM/SMA50	3.29	9.60	200	0.001
SMSM/SMA100	3.29	11.87	200	0.001
SMSM/SMA150	3.29	12.64	200	0.001
SMSM/SMA200	3.29	11.97	200	0.001
SMA50/SMA100	2.33	2.38	200	0.02
SMA50/SMA150	2.58	3.08	200	0.01
SMA50/SMA200	1.96	2.26	200	0.05
SMA100/SMA150	1.65	0.63	200	>0.1
SMA100/SMA200	1.65	0.25	200	>0.1
SMA150/SMA200	1.65	0.94	200	>0.1

t_{tab} = tabulated value of t

t_{calc} = calculated value of t

n = total number of results

p = probability

material (see Table 3.11.1). Analysis of variance (P = 0) showed a significant difference between the starting material and products due to the treatment. The t-test (see Table 3.18.1) showed that all the products were significantly smoother and rounder than the starting material at the 0.1% level. The products were not significantly different from on another. However although the fractal dimensions of the products were lower than the starting material, this effect was less marked than that achieved with some of the other temperature cycling conditions. It is inferred that reducing both phases of the temperature cycle only marginally improve the product and therefore these would not be the temperature cycling conditions of choice.

3.19 THE EFFECT OF USING A MORE EFFICIENT SOLVENT AND TEMPERATURE CYCLING ON THE FRACTAL DIMENSION OF SULPHAMETHIZOLE

The fractal dimensions of all the products were 1.05 compared with the fractal dimension of the starting material of 1.08 (see Table 3.12.1). Analysis of variance (P = 0) indicated that there was a significant difference between the products cycled in 95% aqueous ethanol and the starting material. The t-test (see Table (3.18.1) showed that all the products were significantly different

from the starting material at the 0.1% level. They were not significantly different from one another at this probability level. Therefore it may be assumed that increasing the number of temperature cycles beyond 50 does not have any significant advantage. The fractal dimensions achieved with the more efficient solvent were not as low as those achieved with the less efficient aqueous solvent.

It is inferred that there is no advantage in using the more efficient solvent, especially when the increased cost and fire hazard of the 95% ethanol are considered.

3.19 DISCUSSION

The rounding of sulphamethizole crystals by periodic temperature cycles of 30 minutes consisting of 15 minutes successive heating to 40°C and cooling to 30°C was not significantly improved by changing the duration of the cycling phases. However there was some evidence to suggest that the period of deposition may have more effect on the rounding process than the period of dissolution. The dissolution rate is less dependent on the presence of corners and edges whereas the deposition rate on plane surfaces is significantly higher than at corners and edges. Batches SM20H/40C50 and SM20H/40C75 were significantly more rounded than the starting material, but this rounding effect decreased beyond 75 cycles. Batches

SM10H/50C50 and SM10H/50C100 were less rounded than the starting material but batch SM10H/50C75 was more rounded. Extending the number of cycles appears to cause a reversion of shape in these cases. It would appear that crystal habit modification occurs initially, but when the amount of deposition exceeds the amount of dissolution, crystal growth will occur and cause the observed shape reversion. It is interesting to note that, as a general trend the mean crystal area and perimeter increase during temperature cycling, indicating crystal growth as reported by Carless and Foster (1966).

Comparison of results using the circle ratio, I_i / I_c and fractal dimension showed that sulphamethizole underwent the most marked degree of rounding after 30 minute temperature cycles consisting of 15 minutes successive heating to 40°C and cooling to 30°C. In the case of sulphathiazole both factors showed it was necessary to increase the number of cycles when scaling up the batch size from 2 to 5 litres in order to achieve a more significant rounding effect. For sulphadimidine, both factors indicated no significant advantage in increasing the number of cycles beyond 100. In this case the fractal dimension indicated that scaling up the batch size from 2 to 5 litres had not adversely affected the product, whereas the I_i / I_c ratio indicated that it had. This apparent anomaly arises

because fractal dimension is concerned primarily with surface texture rather than roundness, with a perfectly smooth circular crystal image having a fractal dimension of unity. If the overall shape of a crystal is round but its surface texture is very rugged its fractal dimension will be higher than unity, but its I_i / I_c ratio may be close to unity as this ratio is not sensitive to surface structure. Conversely if the crystal image is smooth but not circular the fractal dimension may be closer to unity, but the I_i / I_c ratio will tend away from unity resulting in the anomaly that has occurred in this case. Both factors showed fairly good agreement for the sulphamethizole products that underwent either prolonged periods of heating or cooling, or reduced heating and cooling periods or treatment in a more efficient solvent.

Either of these factors - I_i / I_c ratio or fractal dimension-may be used on their own, or in conjunction with one another, depending on the information required. This could prove useful when investigating the flow properties of a bulk powder. Shape and surface texture are two important parameters that affect the flow of a particulate material, but neither parameter individually gives an accurate prediction of flow properties. It is possible that the two factors used in conjunction might improve the prediction and this

is an area which might benefit from further investigation.

Both the Magiscan and the Microsight 1 Image Analysis methods are semi-automatic and therefore may be user subjective. The associated errors may be reduced by using the same operator and by displaying the results on the video screen at the end of the program. The Microsight 1 system is somewhat time consuming compared to the Magiscan, but familiarity with the program allows the operator to become faster and more accurate. As a routine quality control image analysis method, this would probably not be very cost effective, but as a relatively low cost, research tool it could prove very useful and within the budgetary capacity of most institutions. Increased resolution of the digitised crystal image would lead to improved discrimination and therefore permit greater differentiation between crystal shapes.

The temperature cycling conditions studied produced only marginal improvement in the overall shape of the compounds investigated and due to the length of time involved in the process and the small yields obtained it is unlikely that this process will prove commercially viable. Spherical aggregation of crystals has been reported by Kawashima, Naito, Lin and Takenaka (1983). This

might prove to be an interesting field for further investigation. It is possible that crystallites could be prepared by their phase separation technique and used either as a seed core around which to apply a second drug, or alternatively a drug could be deposited on crystallites of excipient such as lactose.

CONCLUSIONS

(i) The rounding effect produced in sulphamethizole by periodic temperature cycles of 30 minutes consisting of 15 minutes successive heating to 40°C and cooling to 30°C was not significantly improved by prolonging the heating or cooling phases of the cycle.

(ii) For a 5 litre batch that underwent the above temperature cycling conditions there was no significant advantage in increasing the number of cycles above 50. However this still involved 25 hours of temperature cycling in order to achieve a rounding effect and produced only small yields. Therefore it is doubtful if this process would be commercially viable although it could be of use in small scale flow property studies.

(iii) Use of a solvent that provided higher solubility did significantly improve the rounding effect due to increased dissolution and deposition but this effect required over 100 cycles. The process appears to be useful only for extremely soluble compounds and therefore is unlikely to be of great value in the pharmaceutical industry.

(iv) The Microsight 1 Image Analysis System proved to be a very useful instrument for research purposes, although somewhat time consuming in comparison with the Magiscan system.

(v) . Fractal dimension in conjunction with the circle ratio, I_i / I_c, gives valuable information about crystal shape and surface texture.

APPENDICES

APPENDIX I

To Determine the Equality of Two Means of a Parameter (Students t-Test)

The equality of two means $\bar{x}_1$ and $\bar{x}_2$ with respective variances S_1^2 and S_2^2 of a parameter may be assessed by the following statistic:-

$$t = \frac{\bar{x}_1 - \bar{x}_2}{\sqrt{\frac{(n_1-1)\,S_1^2 + (n_2-1)\,S_2^2}{n_1 + n_2 - 2}}}$$

The value of t is compared with tabulated values, (t_{tab}) with $n_1 + n_2 - 2$ degrees of freedom where n_1 and n_2 are the number of observations used in the estimation of $\bar{x}_1$ and $\bar{x}_2$ respectively. If the value of t, (t_{calc}) does not exceed the tabulated value at the probability level indicated, the values are assumed to be indistinguishable at that level.

APPENDIX II

Analysis of Variance

The total variance of a whole set of results consists of variance due to random differences, d, and those differences due to the effect of the treatment, T. Each result may be written as;

$$x = \bar{x} + T + d$$

where $\bar{x}$ is the mean value of the set of results. The sums of squares of T are calculated as follows:-

$$\Sigma T^2 = \frac{\Sigma(\text{treatment totals})^2}{v} - \frac{(\Sigma x)^2}{n}$$

where the treatment totals are the totals of the set of observations, v is the number of observations in the set and n is the total number of observations. From these the total sum of squares of deviations are calculated:-

$$\Sigma(T + d)^2 = \Sigma x^2 - \frac{(\Sigma x)^2}{n}$$

To simplify this the following method may be used. The data may be set out in a table, the columns summed and the grand total found;

Results	Batch 1	Batch 2	..... Batch n
1	x_1	y_1	z_1
2	x_2	y_2	z_2
.	.	.	.
.	.	.	.
.	.	.	.
.	.	.	.
n	x_n	y_n	z_n
Totals	Σx_n	Σy_n	..... Σz_n
Grand Total =	Σx_n +	Σy_n +	..... Σz_n

Each observation may then be squared and these squares summed for each column. Let the total of these sums be A. The column totals may then be squared and each divided by the number of observations in each column. Let the sum of these be called B. Finally the grand total is squared and divided by the total number of observations. Let this be called D. A table of analysis of variance may then be set out:-

Source of variance	Sum of squares	Degrees of freedom	Mean squares
Between treatments	B - D	u - 1	
Residual	A - B	u(v-1)	
Total	A - D	uv-1	

Where u is the number of treatments and v is the number of replicates. The mean square is calculated by dividing the sums of squares by their degrees of freedom.

The variance ratio test was applied:-

$$F = \frac{\text{between treatments mean square}}{\text{residual mean square}}$$

In the table of variance ratios, (F), the tabulated value of F is found where n_1 is the number of degrees of freedom of the between treatments mean square and n_2 is the number of degrees of freedom of the residual mean square. If the calculated value of F exceeds this, the variance due to the effects of the treatment is significantly greater than the residual variance due to random error at that probability level.

APPENDIX III

Arcsin Transformation

To transform a proportion of value x an angle θ is found for which;

$$\text{Sin } \theta = \sqrt{x}$$

The transformed value θ is then used in the analysis instead of x.

BIBLIOGRAPHY

ALLEN T. (1975) Particle Size Measurement.
Chapman & Hall, London p.76

ASCHENBRENNER B.C.(1956) J. Sed. Petrol.26 pp 15-31

ASLANIAN S., KOSTOV I. (1972) Kristall und Technik.
7 (5), p 511

BARNES J.C. (1956) J.Sci.Instrum. 33 pp 494-495

BEDDOW J.K.,PHILIP G. (1975) Planseeber Pulvermetall.
23. p.1

BENNETT J.A.R., LEWIS J.B. (1958) Amer.Instn.
Chem. Engrs.J. 4 p.418

BERESFORD R.H. (1984) Royal Society of Chemistry -
P.S.A. Meeting: Image Analysis
13th June 1984. London House

BLIZNAKOV G., KIRKOVA E., NIKOLAEVA R. (1971)
Kristall and Technik. 5(3) P 387
and 6(1) p 33

BOISTELLE R. (1975) 6th Symposium on Industrial
Crystallisation. Usti, Czechoslovakia.
ed. Mullin J.W. pp 215 - 221.

BOURNE J.R., DAVEY R.J. (1976) J.Cryst.Growth 36. p 287

BRAVAIS A. (1866) Etudes Cristallographiques. Paris.

BUCKLEY H.E.(1951) Crystal Growth. John Wiley. New York.

BYTEVA I.M. (1966) in Crystallisation Processes. Consultants Bureau. New York p 99

CARLESS J.E., FOSTER A.A.(1966) J.Pharm. Pharmacol.18 pp 697 - 708

CARLESS J.E., FOSTER A.A.,JOLLIFFE G.O. (1966) J.Pharm. Pharmacol. pp 815 - 819

CLARK M.W. (1981) J.Int.Assoc.Math.Geol.13. pp 303 - 320

COX E.P. (1927) J.Palaeont. 1. pp179 - 183

CURIE P. (1885) Bull Soc. Franç. Mineral. 8.p 145

DONNAY J.D.H., HARKER D. (1937) Am.Mineral.22. p 446

ERIKSEN S.P., BIRD H.E. (1965) J.Pharm Sci. 54. pp 455 - 456

FLOOK A.G. (1978) Powder Technol.21 pp 295 - 298

FOX D., LABES M.M., WEISBERGER A. (1963)Physics and Chemistry of the Organic Solid State. Vol.I. Interscience Publishers. New York.

FRANK F.C.(1949) Disc. Farad. Soc. No.5. p 48

GIBBS J.W. (1929) Collected Works. London
Longmans Green.

GILMAN J.J., JOHNSON W.G.(1959) Dislocation and
Mechanical Properties of Crystals.
J.Wiley & Sons. New York. p 116

GILMAN J.J., JOHNSON W.G., SEARS G.W. (1958)
J.Appl. Phys. 29.p747

GOTOH K., FINNEY J.L. (1975) Powder Technol. 12. p. 125

HARTMAN P., PERDOK W.G. (1955) Acta. Cryst. 8 p49,
p 521 & 525

HAUSNER H.H.(1966) Planseeber Pulvermetall. 14
pp 75 - 84

HAUSNER H.H. (1967) Int. J. Powd. Metall. 3 pp 7-13

HEYWOOD H. (1933) Proc. Inst. Mech. Eng. 125. pp 383-459

HEYWOOD H. (1954) J.Imp. Coll. Chem. Engng. Soc. 8.
pp 25-33

HOUGARDY H.P. (1974) Microscope. 22.pp 5 - 26

HOUGARDY H.P. (1976) Microscope. 24. pp 7 - 23

KAWASHIMA Y., NAITO M., LIN S.Y., TAKENAKA H. (1983) Powder Technol. 34. pp 255 - 260

KAYE B.H. (1978) Powd. Technol. 21. pp 1 - 16

KAYE B.H. (1984) Paper to Nurnberg Laurentian University Conference. May 9th - 11th 1984. Sudbury, Ontario, Canada.

KERN R. (1953) Bull. Soc. Fr. Miner. Crist. 76. p 325

KHAMSKII E.V. (1975) 6th Symposium on Industrial Crystallisation. Usti, Czechoslovakia. ed. Mullin J.W. pp 215 - 221

KOSSEL W. (1934) Ann. Phys. 21. p 455

KOSTELNIK M.C., BEDDOW J.K. (1971) Advances in Powder Metallurgy. ed. Hausner H.H. Plenun. New York. pp 29 - 48

KRUMBEIN W.C. (1941) J.Sed.Petrol. 11. pp 94 - 97

LEES G. (1964) Sedimentology 3. pp 2 - 21

LOVELL G.H.B. (1967) Lab. Pract. 16. p 1122

MACKIE W. (1897) Trans. Edin. Geol. Soc. 7. pp 298-311

MANDELBROT B.B.(1977) Fractals: Form, Chance and Dimension. W.H.Freeman. San Francisco.

MEDALIA A.I. (1970/71) Powd. Technol. 4. pp 117 - 138

MELOY T.P. (1969) Screening A.I.M.E.Washington D.C.

MELOY T.P. (1971) Techniques for Multidimensional Particle Characterisation and Recognition. ENG Foundation Conference.

MELOY T.P. (1977) Powd. Technol. 16. pp 233 - 253

MULLIN J.W. (1972) Crystallisation. 2nd edition. Butterworths. London.

NERNST W. (1904) Z.Phys.Chem. 47. p 52

NOYES A.A., WHITNEY W.R. (1897) J.Amer.Chem.Soc.19. p.930

NYVLT J. (1973) Soc.Chem.Ind.Monograph No.28 ed. Smith A.L.Academic Press.London. pp 131-141

OXFORD ENGLISH DICTIONARY (1961) Clarendon Press, Oxford.

RIDGWAY K., RUPP R.(1969) J.Pharm.Pharmacol. 21.
pp 30S - 39S

RIDGWAY K., SCOTTON J.B. (1970) J.Pharm.Pharmacol. 22.
pp 24S - 28S

RILEY G.S., MANN G.R. (1972) Mat. Res. Bull. 7.
pp 163 - 170

RILEY N.A. (1941) J. Sed. Petrol. 11. pp 94 - 97

SCHWARCZ H.P., SHANE K.C. (1969) Sedimentology 13.
pp 213 - 231

SCHWARCZ H., EXNER H.E. (1980) Powder Technol. 27.
pp 207 - 213

SCOTT M.W., MIN C.Y., CAMPBELL W.A., ANDERSON C.M.
(1964) J.Pharm.Sci.53. pp 1133-1134

SKERRETT E.J. (1968) J.Sci.Instrum. (J.of Phys. E.)
Series 2. 1. pp1242 - 1244

STANIFORTH J.N., REES J.E. (1981) Powder Technol. 21
pp 1 - 16

SUTTON H.M. (1976) in Characterisation of Powder
Surfaces. ed. Parfitt G.D. and
Singh K.S.W. Chapter 3.
Academic Press. New York

TESTER A.C. (1931) J.Sed.Petrol.1. pp 3 - 11

VARNEY G. (1967) J.Pharm.Pharmacol.19.Suppl. pp 19S-23S

VOLMER M. (1929) Z.Electrochem. 35. p 555

VON LAUE M. (1943) Z. Krist. 105. p 124

WADELL H. (1932) J.Geol. 40. pp 443 - 451

WATSON D.H. (1954) Proc. Int. Conf. Electron Microscopes. 3. p 497

WELLS A.F. (1946) Phil. Mag. 37. pp 184, 217, 605

WELLS A.F. (1949) Disc. Farad. Soc. 5. pp 19 & 197

WENTWORTH C.K. (1919) J.Geol. 29. pp 507 - 521

WHALLEY W.B., ORFORD J.D. (1928) Scanning Electron Microscopy.SEM Incorporated.A.M.F. O-Hare Chicago, Illinois. 60666. U.S.A. pp 639 - 647

WHALLEY W.B.,ORFORD J.D. (1983) Sedimentology 30. pp 655 - 668

WULFF G. (1901) Z. Krist. 34. p 449

ZINGG T. (1935) Schweiz Mineral und Petrograph. Mitt. 15. pp 39 - 140

BANES D., RIGGLEMAN O.H. (1971) J.Assoc.Official
Analytical Chemists.54.pp 1195-1199

BERTHOUD A. (1912) J.Chim.Phys. 10. p 624

BICAN-FISTER T., KAJGANOVIC V.(1964) J.Chromatography.
16. pp 503-509

BRUNNER C.A. (1972) J.Assoc.Official Analytical
Chemists. 55. pp 194-196

BRUNNER C.A.(1973) J.Assoc.Official Analytical
Chemists. 56. pp 689-691

DUX J.P.,ROSENBLUN C. (1949) Analytical Chemistry. 21.
pp 1524-1527

POWDER DIFFRACTION FILE (1975) Philadelphia.American
Society for Testing Materials.

SADTLER STANDARD SPECTRA (1962) I.R.Spectra
Pharmaceuticals. Vol.2.
Philadelphia R 344-750

TANSEY (1969) M.Sc.Thesis.University of Bath.

VALETON J.J.P. (1923) Z.Kristallogr. 59. p.135 and
p 335

VALETON J.J.P. (1924) Z.Kristallogr. 60. p 1.